UNITED STATES DEPARTMENT OF THE INTERIOR
GEOLOGICAL SURVEY

Geology and Uranium Mineralization of the Florida Mountain Area, Needle Mountains, Southwestern Colorado

by
James D. Collier[1]

Open-File Report 84-336

1985

This report is preliminary and has not been reviewed for conformity with U.S. Geological Survey editorial standards and stratigraphic nomenclature.

[1]Department of Geology
Fort Lewis College
Durango, Colorado 81301

CONTENTS

	Page
Abstract	1
Acknowledgments	2
Introduction	2
Location, Physiography, and Access	4
Land Status	5
Previous Work	6
History of Mining and Exploration	6
Methods of Investigation	7
Nomenclature	11
Regional geologic setting	11
Proterozoic rocks	11
Electra Lake gabbro	11
Eolus batholith	11
Phanerozoic rocks	13
Regional structure	13
Proterozoic rocks of the study area	14
Descriptive petrology and petrography	14
Eolus granite	14
Trimble granite	16
Chemical composition of the granites	17
Major normative minerals	19
Major and minor oxides	19
Trace elements	23
Rare-earth elements	28
Petrogenesis	30
Source rocks	30
Tectonic framework	32
Speculative petrogenetic model	32
Uranium residence in the granites	34
Uranium in hornblende-bearing granite	35
Uranium in hornblende-free Eolus granite	35
Uranium in the Trimble granite	36
Mafic dikes	36
Chicago Basin stock	37
Older intrusive body	37
Younger intrusive body	40
Dikes of granite porphyry	40
Late dike	40
Uranium residence	41
Uranium in the older intrusive body	41
Uranium in dikes of granite porphyry	41
Uranium in the younger intrusive body	41
Local structure	43
Surficial geochemistry	47
Distribution of metals	47
Zoning	51
Discussion	52

CONTENTS--continued

	Page
Vein mineralization and alteration	57
Bullion and Trimble Faults and related structures	59
Cornucopia, UJC, and LJC Veins	60
Cornucopia vein	60
UJC and LJC veins	62
Quartz-sulfide Veins	63
Wall-rock alteration	64
Chemical changes with alteration	65
Uranium residence and mobilization in the alteration zones	65
Paragenesis	68
Fluid inclusion studies	70
Description	70
Discussion	73
Comparison with fluid inclusion studies of other hydrothermal uranium deposits	74
Summary - Genetic model for mineralization	76
Magmatic concentration of uranium	76
The role of structure	78
Hydrothermal Mobilization and Concentration	79
Uranium occurrences outside study area	80
Grizzly Gulch	80
Thunder Mountain	82
Other occurrences	82
Economic potential	83
References cited	84
Appendix. Trace-element analyses of granites	88

ILLUSTRATIONS

Plate I.	Map showing location of study area in relation to prominent geographic features of Needle Mountains region	in pocket
II.	Geologic map of the Florida Mountain area, Needle Mountains, southwestern Colorado	in pocket
Figure 1.	Index map of southwestern Colorado showing location of study area	3
2.	Location of study area in relation to Weminuche Wilderness area and to the claim block of Public Service Company of Oklahoma	5
3.	Location of major mines and prospects, Needle Mountains mining district	8

ILLUSTRATIONS--continued

Figure 4. Geologic map of the Precambrian rocks of the Needle Mountains..... 12

5. Ternary diagrams for granitic rocks of the Eolus batholith..... 20

6. Harker-type diagrams for granitic rocks of the Eolus batholith..... 21

7. Variation diagrams of P_2O_5, TiO_2, and Th vs. SiO_2 for granitic rocks of the Eolus batholith..... 22

8. Variation diagrams of K_2O and Sr vs. Ba..... 24

9. Variation diagrams of Sr and Rb vs. K_2O and SiO_2.... 25

10. Variation diagrams of Ba, Sr, TiO_2, and P_2O_5 vs. Rb..... 26

11. Distribution of chondrite-normalized rare-earth element patterns..... 29

12. Variation diagram of lanthanum versus cerium..... 31

13. Variation diagram of normative diopside and normative corundum versus SiO_2..... 33

14. Distribution of the strikes of vertical or near vertical joints..... 44

15. Areal distributions of anomalous Mo, Au, and Ba in surface rock samples..... 48

16. Areal distributions of anomalous Cu and As in surface rock samples..... 49

17. Areal distributions of anomalous Ag, Sn, and Bi in surface rock samples..... 50

18. Contour map of Zn/Pb in surface rock samples..... 53

19. Contour map of Pb/Sn in surface rock samples..... 54

20. Contour map of Ag/Au in surface rock samples..... 55

21. Distribution of uranium occurrences relative to Tertiary plutons..... 56

22. Locations of holes drilled by Public Service Company of Oklahoma..... 58

Geology and uranium mineralization of the Florida Mountain area Needle Mountains, southwestern Colorado

by

James D. Collier

ABSTRACT

The Florida Mountain area in the Needle Mountains mining district of southwestern Colorado is cut by numerous veins bearing uranium and base and precious metals. In addition to uranium, the area has anomalously high concentrations of a variety of metals, including gold, silver, and molybdenum. Uranium presents the greatest economic potential and was the major focus of this research.

The veins are hosted by two Precambrian granitic map units, the Eolus and Trimble granites. Trace-element interpretations suggest that there were at least three intrusive phases, and part of what has been mapped as Eolus Granite is actually a comagmatic and more primitive phase of the Trimble Granite. The Trimble Granite was the final stage of extensive fractionation of mafic igneous sources. The observed variation in plutonic rock types was the product of both melting and fractionation processes. More highly differentiated fractionation series were probably the result of remelting of products of earlier partial melting. Uranium and other incompatible elements were strongly enriched during both melting and differentiation.

Uranium in early intrusive rocks is present only in common accessory minerals such as zircon and allanite, but disseminated, uranium-rich minerals such as uraninite formed in the more felsic, highly differentiated units. These were later destroyed by hydrothermal alteration to liberate uranium for concentration in the vein systems.

The Chicago Basin stock, a composite hypabyssal body of granite and rhyolite porphyries, was emplaced during the late Tertiary. Geochemical evidence indicates that the stock is a cupola of a larger intrusion, another apophysis of which is inferred to occur nearby. Although these intrusions were sources of metals such as molybdenum, they are not likely to have been the sources of uranium. Instead, they established the convective circulation system by which uranium was leached from the Precambrian granite country rocks. They also helped open pre-existing fractures during intrusion. Leaching of uranium occurred principally along two large breccia zones, the Bullion and Trimble Faults.

Pitchblende was deposited from oxidizing, paragenetically early fluids at approximately 300°C. Later fluids were more reducing; a sulfide-dominant stage precipitated at about 250°C. Pitchblende-depositing fluids were rich in CO_2 and either boiled or effervesced CO_2. Uranium was precipitated as a result of increase in pH and/or reduction produced by boiling or effervescence. Uranium is believed to have been transported as the complex $UO_2F_3^-$.

The vein systems of the Florida Mountain area and its immediate surroundings possibly contain a resource of uranium that, although small by some world standards, is comparable in size to several hard rock uranium mines of the United States and larger than other known intragranitic deposits. Economic, political, and environmental factors seriously constrain the viability of the deposits.

ACKNOWLEDGMENTS

This study first appeared as part of doctorate thesis at the Colorado School of Mines. I therefore wish to thank the members of my thesis committee for their time and effort: Drs. Richard H. De Voto and Samuel B. Romberger, Co-chairmen; Drs. Gregory S. Holden, F. Edward Cecil, J. Thomas Nash (U.S. Geological Survey), and Wilmar Bernthal (University of Colorado), members. E. Craig Simmons of the Department of Chemistry and Geochemistry, Colorado School of Mines was of considerable help in interpreting trace-element data. R. A. Zielinski of the U.S. Geological Survey kindly assisted in preparation of fission-track radiographs. William Carlson, formerly of Public Service of Oklahoma, and others of P.S.O. were very cooperative in allowing use of their data, facilities, and drill core. Bendix Field Engineering Corporation provided funding for the first summer's field work.

INTRODUCTION

The Needle Mountains mining district of southwestern Colorado (fig. 1) contains abundant quartz-sulfide veins with local ore shoots of base and precious metals. The veins are spatially, if not genetically, related to a Tertiary hypabyssal stock and are hosted by Precambrian granites. Part of the district, including the area surrounding Florida Mountain (pl. I), also contains numerous uraniferous veins. The uranium deposits of the Florida Mountain area, as well as the associated base-metal veins, are the principal objects of this study.

There is a strong correlation between vein-type uranium deposits and anomalously uraniferous granitic rocks. According to Rich and others (1977), about 85 percent of all hydrothermal uranium deposits in the United States are associated with granitic rocks. There is also a strong possibility that many other types of uranium deposits, such as contact-metasomatic or even sandstone types, may have some association with granitic rocks. Understanding the characteristics that make granites potentially good source rocks, therefore, takes on considerable significance to exploration, particularly considering the numerous plutonic bodies in the United States with high uranium contents.

The uranium deposits of the Florida Mountain area are classified as intragranitic deposits because granites probably acted as both source rocks and hosts. Intragranitic uraniuum deposits have received extensive study in Europe, particularly in France, but are virtually unknown in the United States. The Florida Mountain uranium deposits have no known analogs in the United States and have little in common with deposits of France. The granites are very different in composition and origin, and the veins formed under conditions different from those in France. Thus, exploration models based on characteristics of French deposits are not universally applicable. Comparison of the deposits at Florida Mountain with those in Europe might help highlight the general conditions necessary for the formation of intragranitic uranium deposits.

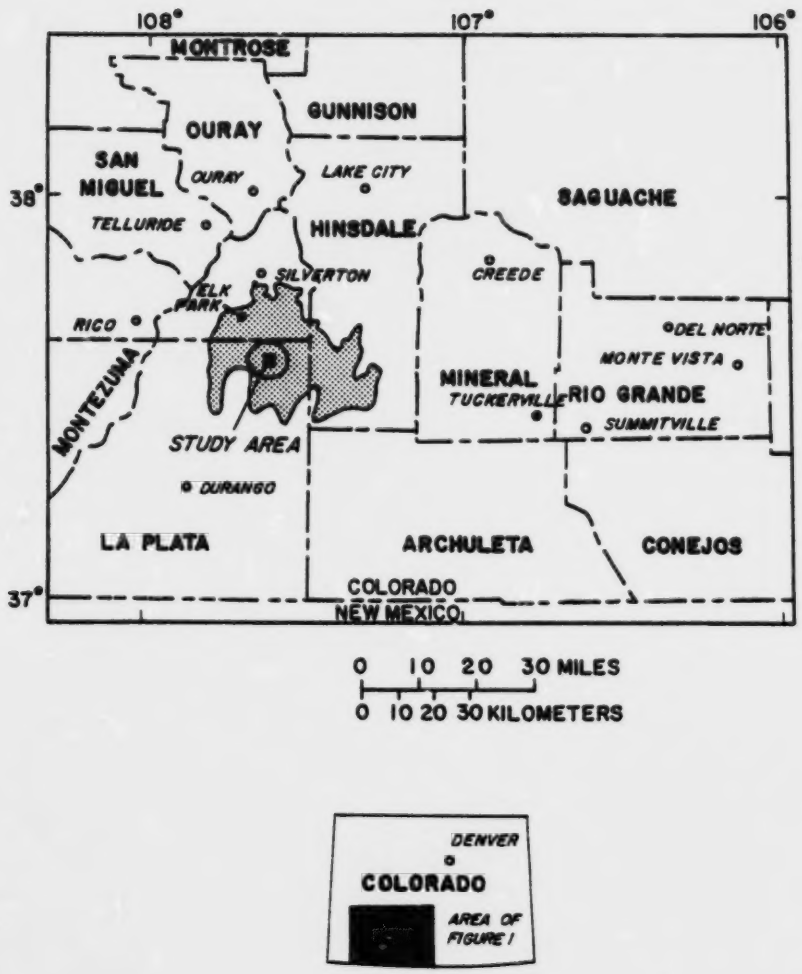

Figure 1. Index map of southwestern Colorado showing location of study area. The Needle Mountains correspond approximately to the area of outcrop of Precambrian rocks, which is shown by the stippled pattern. The circled region around the study area is the approximate area of the Needle Mountains mining district.

In addition to reviewing the physical and historical settings of the Needle Mountains, this study examines the surface and subsurface geology of the Florida Mountain area by a variety of methods, including defining field relationships through mapping, mineralogical associations by petrography, geochemical evidence for petrogenesis and metallogeny, fluid inclusion and thermodynamic evidence for conditions of vein formation, and radiographic evidence for the behavior of uranium. This information is then used to establish a framework by which concepts of genesis may be addressed.

Location, Physiography, and Access

The area of study is located in La Plata County, southwestern Colorado, approximately 25 km south of the town of Silverton and 16 km east of the Animas River (fig. 1 and pl. I). The study area is located within the central Needle Mountains, which make up part of the larger San Juan Mountains range. The area encompasses approximately 13 sq. km and can be subdivided into several physiographic regions (pl. II). Chicago Basin, in the northwestern part of the study area, is a composite cirque that forms part of the upper watershed of Needle Creek, draining to the west into the Animas River. Vallecito Basin, another cirque, is located in the east-central part of the area. Silver Mesa is a broad, south-sloping plateau dissected by Missouri Gulch and Crystal Valley. Lillie Lake (Durango City Reservoir No. 3) is a tarn at the head of Crystal Valley and is the headwaters of Florida River which flows to the south into Lemon Reservoir. One of the salient features of the area is Florida Mountain, for which the study area is named. Florida Mountain lies between Lillie Lake and Vallecito Basin. Plate I shows the location of the study area in relation to the major geographic features of the region.

The study area occurs within the quadrangle having the highest average elevation in the continental United States. Topography is extremely steep and rugged, with elevation ranging from 3379 to 4057 m. During years of normal precipitation, snow covers the area from mid-September to early- or mid-July, resulting in very short field seasons.

Most of the Needle Mountains have been incorporated into the Weminuche Wilderness Area, making the study area inaccessible to vehicles. Extended work requires the support of either helicopters or pack animals. Problems of access and topography not only make extended research in the area difficult and expensive, but also place serious constraints on the potential for economic development of the area. This problem will be addressed in a later section on economic potential.

Land Status

Nearly all of the central and western Needle Mountains are included in the Weminuche Wilderness Area, which includes a vast area from Emerald Lake to the west, Highland Mary Lakes to the north, and within a few kilometers of Vallecito Reservoir to the south (fig. 2). The study area lies within the heart of this region.

Within the vicinity of the study area, numerous patented claims preserve a potential for economic interest. An area from Florida Mountain in the north

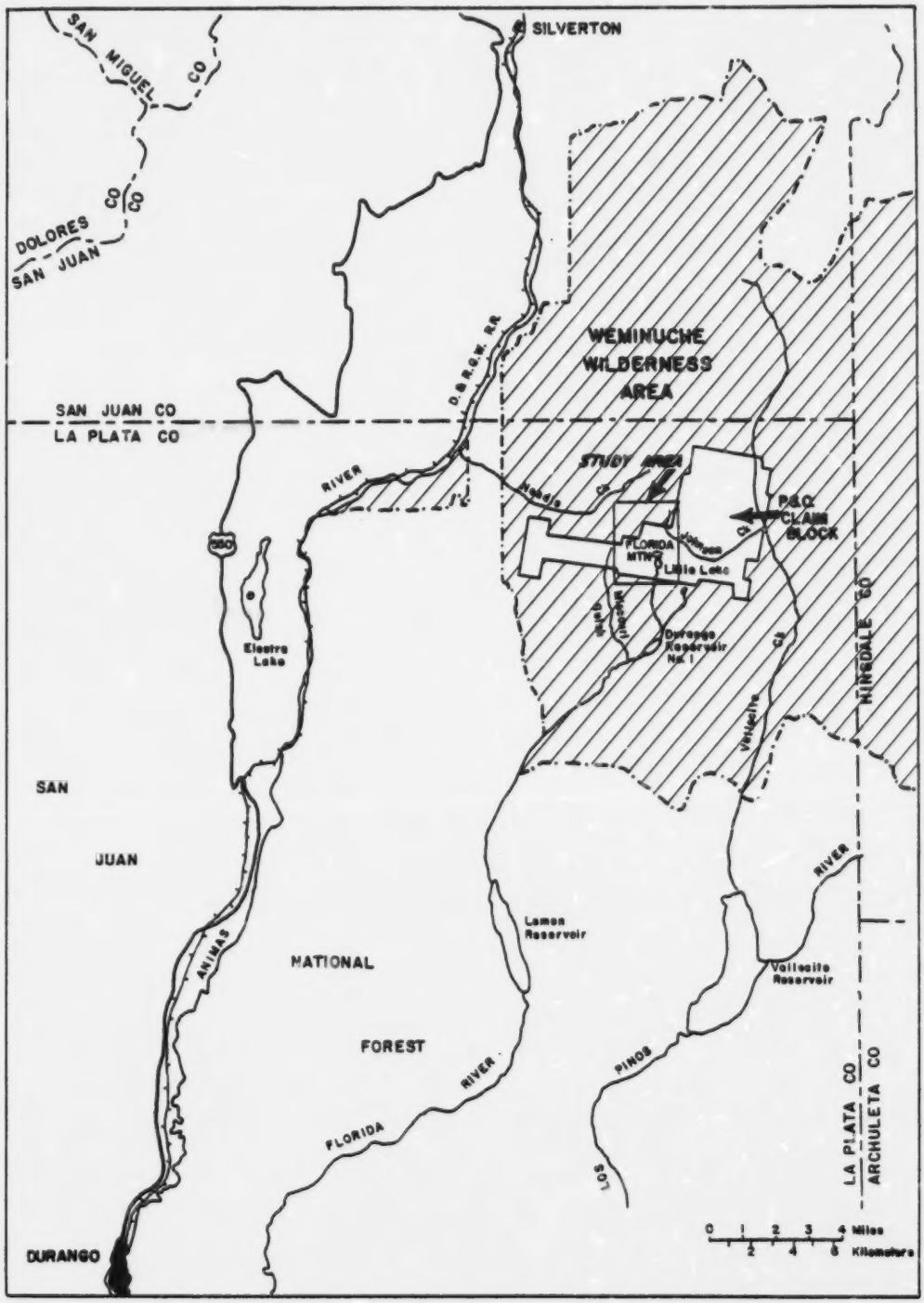

Figure 2. Location of the study area in relation to the Weminuche Wilderness Area and the claim block of Public Service Company of Oklahoma.

to Sheridan and Sheep mountains in the south remains outside the wilderness system. The city of Durango owns this area to preserve its reservoirs and sources of drinking water. Much of the study area is included within a claim block which, at the time of this writing, belongs to Public Service Company of Oklahoma (P.S.O.), whose exploration interests are represented by Central and South West Fuels, Inc. This block, which is shown on figure 2, consists of 469 unpatented and 41 patented claims, or about 40 sq. km. The unpatented claims are subject to withdrawal into the wilderness system should the claim leasees be unable to demonstrate sufficient mineral wealth within them.

Previous Work

The Precambrian rocks of the Needle Mountains were studied by numerous geologists prior to the turn of the century (Endlich, 1876; Comstock, 1883; Emmons, 1890). The first comprehensive discussion of the Needle Mountains quadrangle was published as a United States Geological Survey folio by Cross and others (1905). This and other work was later summarized by Cross and Larsen (1935), and Larsen and Cross (1956). Barker (1969) published an excellent summary paper on the Precambrian rocks of the Needle Mountains as part of the Durango 1° X 2° quadrangle. This work later appeared in a 1:250,000 geologic map (Steven and others, 1974).

The geology and mineral deposits of the Needle Mountains mining district, of which the study area is a part, were described briefly as part of an evaluation of the mineral potential of the San Juan Primitive Area (Steven and others, 1969). Field data from this investigation were later expanded upon and published separately (Schmitt and Raymond, 1977). This latter work concentrated principally on the Chicago Basin stock, a small composite Tertiary intrusion in the northern part of the study area. Uranium was omitted from their chemical analyses, and therefore the ubiquitous uranium mineralization in the area, which is the principal focus of this study, was not discovered.

A large amount of unpublished data has been accumulated by Public Service of Oklahoma during their involvement in the Needle Mountains. This work will be discussed in the following section.

History of Mining and Exploration

The study area encompasses most of the mines and prospects of what has been termed the Needle Mountains mining district. The area has numerous adits, shafts, and trenches, most of which are inaccessible due to flooding, caving, low oxygen levels, or perennial snowbanks. As a result, much of the information presented here is from that gathered by Steven and others (1969) during 1967 and 1968.

Mining activity began in the Needle Mountains district in 1881 and continued sporadically through 1917. The village of Logtown, of which only vestiges remain today, was established below Lake Marie (Durango City Reservoir No. 2) and had regular postal service, a testimony to the amount of interest and activity once shown in the area. Despite intense activity, it is doubtful whether returns from production ever equaled or exceeded costs of operations and transport. Mining was resumed briefly in 1934 when the price

of gold reached $35 per ounce, but production failed to match the costs of operating in such rugged terrain.

Based on very sketchy records of mineral output, Steven and others (1969) estimated total production to have been $12,500, of which the Eureka and Aetna mines each produced $5,000, the Pittsburgh Shaft accounted for $2,000, and the Aztec Mine contributed $500. Figure 3 shows the names and locations of the prominent mines and prospects of the study area.

Nearly all production revenues were derived from gold and silver. Because of difficulties in transportation, the early ores were probably hand-cobbed for the precious metals. Table 1 shows selected assay data from dump samples collected by Steven and others (1969). It is apparent that silver is the dominant economic metal, and that its distribution in paying quantities is limited and sporadic. Gold occurs in very low concentrations, except in isolated oxidized portions of the veins, where it may be locally upgraded.

In 1960, AMAX, Inc. drilled a 300 m hole in Chicago Basin on a geochemical molybdenum anomaly. According to Steven and others (1969), the hole averaged less than 0.01 percent MoS_2, which prompted AMAX to relinquish its claims. Several years later AMAX reacquired the property and drilled several more holes. Again insufficient molybdenum was discovered to warrant maintaining the claims and the property was abandoned.

In September of 1974, Public Service Company of Oklahoma, as represented by Central and South West Fuels, Inc., contracted an airborne radiometric survey of the region and discovered numerous radioactive anomalies. A preliminary field check in October, 1974 verified the presence of significant amounts of uranium. During 1975, P.S.O. began land acquisition and initiated a geological assessment of the area. As a result of the 1975 program, drilling was commenced in the summer of 1976. From 1976 through 1978, P.S.O. drilled over 12,000 m of core and amassed a considerable volume of geologic data. Early in 1979 and shortly after this writer initiated plans to study the area, P.S.O. withdrew all active participation in the project. Although the major difficulties of access, topography, and environmental opposition certainly influenced their decision, P.S.O.'s withdrawal was prompted largely by a combination of lack of a firm nuclear policy from Washington, a deterioration of the uranium market, and their inability as a utility company to use their product due to restrictive nuclear licensing regulations. At the time of this writing, no further involvement in the area on the part of industry is planned.

Methods of Investigation

Mapping and sampling were conducted during the summer of 1979, with additional sampling and map revision during 1980. General features were mapped on color photographs at a scale of 1:12,000, and more detailed features were mapped on color photographs enlarged to 1:4,800. This information was then transferred to a 1:4,800 topographic map, enlarged from a portion of the United States Geological Survey's Columbine Pass 7.5 minute quadrangle (pl. II). Sampling was guided by an attempt for as broad a coverage as possible but, because of the localized nature of important rock types, was more selective for variety than to be representative. Three general series of

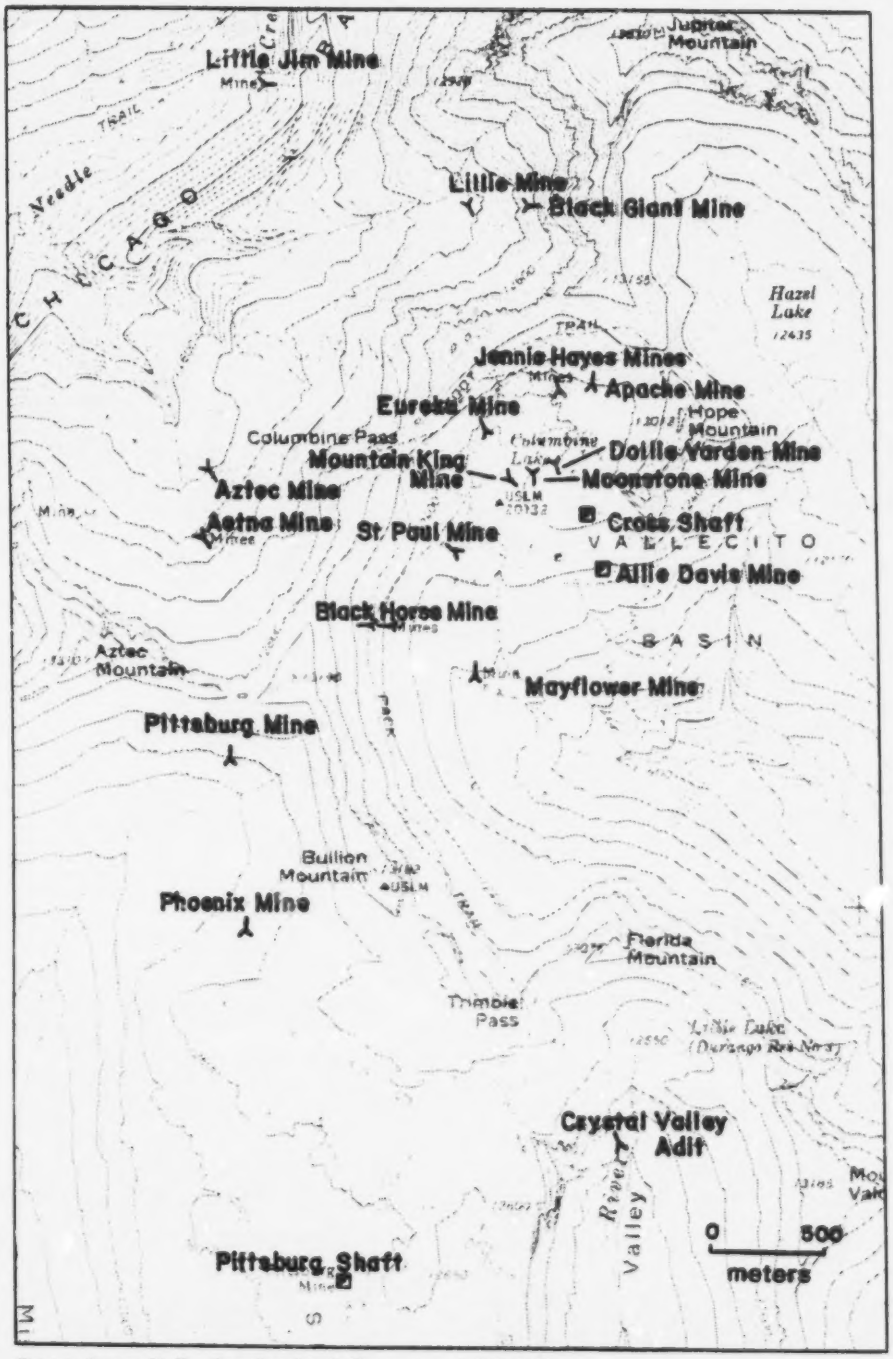

Base from U.S. Geological Survey, 1:24,000
Columbine Pass, 1973

Figure 3. Location of major mines and prospects, Needle Mountains mining district. The area of this fi ure is shown on figure 2.

Table 1.--Selected assay data from mine dump samples

(from Steven and others, 1969)

Mine	Au(oz/ton)	Ag(oz/ton)	Cu(%)	Pb(%)	Zn(%)
Aetna	.01	5.13	.56	1.84	5.96
Apache	tr	1.68	.15	.66	.65
Aztec	.02	4.28	.41	2.44	3.86
Black Giant	tr	1.40	.08	.56	.90
Black Horse	.02	2.98	.43	1.24	3.05
	.04	37.56	.20	.36	.65
Clipper	tr	.70	.16	.20	.56
Cross Shaft	tr	1.16	.10	tr	.15
Eureka	.01	1.40	1.04	3.40	5.98
Jennie Hayes	.02	25.48	1.23	4.95	5.94
Lillie	.01	.32	1.14	1.68	2.82
Mayflower	tr	2.68	.58	tr	.48
Moonstone	.03	5.57	.09	.48	.42
Neglected	.02	27.94	1.36	.90	tr
Pittsburgh	.02	6.84	1.08	1.20	2.36
Pittsburgh Shaft	.04	83.66	.18	.73	.12
Phoenix	.01	1.20	tr	.76	.24

samples were taken. Surface samples were obtained within the study area for general description of the host rocks and veins. These sample localities are shown on plate 2. Twenty-five samples were taken regionally to try to characterize the fractionation history of the Eolus batholith. These samples (EG-series) are shown on plate I. In addition, numerous drill core samples were used for assessing vein paragenesis and alteration and for fluid-inclusion studies.

Whole-rock analyses were obtained for 37 samples. All of these samples were analyzed for uranium and thorium. In addition, the 25 EG-series samples were analyzed for a wide variety of trace elements.

Over 300 thin sections were examined in the course of this study. Of these, about 150 were used in making radiographs. Sites of uranium residence were studied by a variety of methods. The location of uranium in vein samples was determined by an alpha-radioluxograph technique described by Dooley (1958). Thin sections were placed in a Polaroid MP-4 Land Camera back[1], and a phosphor screen, made by coating cellulose tape with a zinc-sulfide phosphor (DuPont Luminescent Chemical Type 1101), was placed between the samples and a high-speed Polaroid film (Type 47, equivalent ASA 3000). When struck by alpha particles, the phosphor screen emitted light and hence exposed the film. The technique was useful for identifying radioactive vein material for X-ray analysis, but lacked sufficient resolution to study nonmineralized samples.

Uranium residence in nonmineralized or low-grade rocks was studied principally by using fission-track radiographs. Thin sections were covered with a muscovite detector and bombarded for 4,000 KWH by a thermal neutron flux. Upon etching in HF, damage tracks from the fissioning of ^{235}U were observable in the muscovite. This technique provided the best resolution of any method used but, because of radioactive isotopes formed during bombardment, long periods of time (generally 6-8 weeks) elapsed before the samples could be handled.

Two types of natural alpha-track detectors were used. Cellulose nitrate film (Type CN85, supplied by Kodak-Pathe, Vincennes, France) and CR-39 plastic provided much better resolution than autoradioluxographs and were useful when results were needed in short periods of time (a few days-2 weeks). These detectors were particularly useful in scanning large areas of rock for widely scattered minerals such as uraninite, which might easily be missed in random thin sections. In general, CR-39 plastic proved to be less expensive, to have better resolution, and to have easier etching and handling characteristics than did cellulose nitrate. The relative merits of these two techniques, as well as other solid-state nuclear-track detectors, are discussed by Basham (1981). Uranium-bearing minerals located by radiography were identified either optically or by electron microprobe or scanning electron microscope.

---

[1]Trade names in this report are used for descriptive purposes only and do not reflect endorsement by the U.S. Geological Survey.

Fluid inclusions were studied on a Chaixmeca heating and freezing stage, modified after Cunningham and Corollo (1980). Doubly-polished plates were prepared from both surface and drill-core samples.

Nomenclature

Most of the rocks described in this paper are granitoids in both texture and mineralogy. Not the least of the many controversies involving granitoids is their classification. Although for generic usage the terms "granite" or "granitic" will appear throughout the text, when concerned with specific compositions the classification of Streckeisen (1976) will be used. This is an attempt at uniformity, and for plutonic rocks the classification of Streckeisen appears to be gaining, albeit reluctantly, a certain degree of acceptance.

REGIONAL GEOLOGIC SETTING

The Needle Mountains consist of an uplifted inlier of Proterozoic rocks, the general area of outcrop of which is shown on figure 1. The Proterozoic rocks are flanked on the north and northeast by Tertiary volcanic rocks of the San Juan volcanic field. Paleozoic sedimentary rocks border the Needle Mountains on the west, south, and southeast.

Proterozoic Rocks

Barker (1969) recognized two major Proterozoic tectonic events in southwestern Colorado, both of which involved deposition, folding, and plutonism. The first cycle occurred between approximately 1,800 and 1,700 m.y. (million years), and the second cycle between about 1,650 and 1,450 m.y. Rock sequences are described by Barker (1969) and summarized by Collier (1982), with recent modifications by Ellingson (1982) and Tewksbury (1982). Figure 4 is a sketch geologic map of the Proterozoic rocks of the Needle Mountains. Of concern to this study are the Proterozoic Y, anorogenic granitic rocks of the Eolus batholith and, to a lesser extent, the coeval and perhaps genetically related gabbros and diorites of the Electra Lake Gabbro.

Electra Lake gabbro.--Barker's (1969) second tectonic cycle was followed by the roughly concurrent intrusions of the Electra Lake Gabbro and the composite Eolus batholith. The Electra Lake Gabbro consists of small masses of gabbro, augite biotite diorite, and quartz diorite all in gradational contact. Compositionally the rocks show a complete range from olivine gabbro to biotite augite granodiorite, but the most abundant rock type is augite labradorite gabbro. Bickford and others (1968) obtained a Rb/Sr whole-rock age of 1,454 ± 50 m.y. for the Electra Lake Gabbro.

Eolus batholith.--Two bodies of granitic rocks, both of batholithic proportions, constitute the greatest volume of rocks in the Needle Mountains. These two bodies, which are collectively termed here the Eolus batholith, consist of the Eolus and Trimble granites and a small pluton called the Quartz Diorite of Pine River by Barker (1969). The genesis of these rocks is closely linked with that of the mineral deposits described later, therefore discussion of these rocks will be included with that of the local geology of the study area.

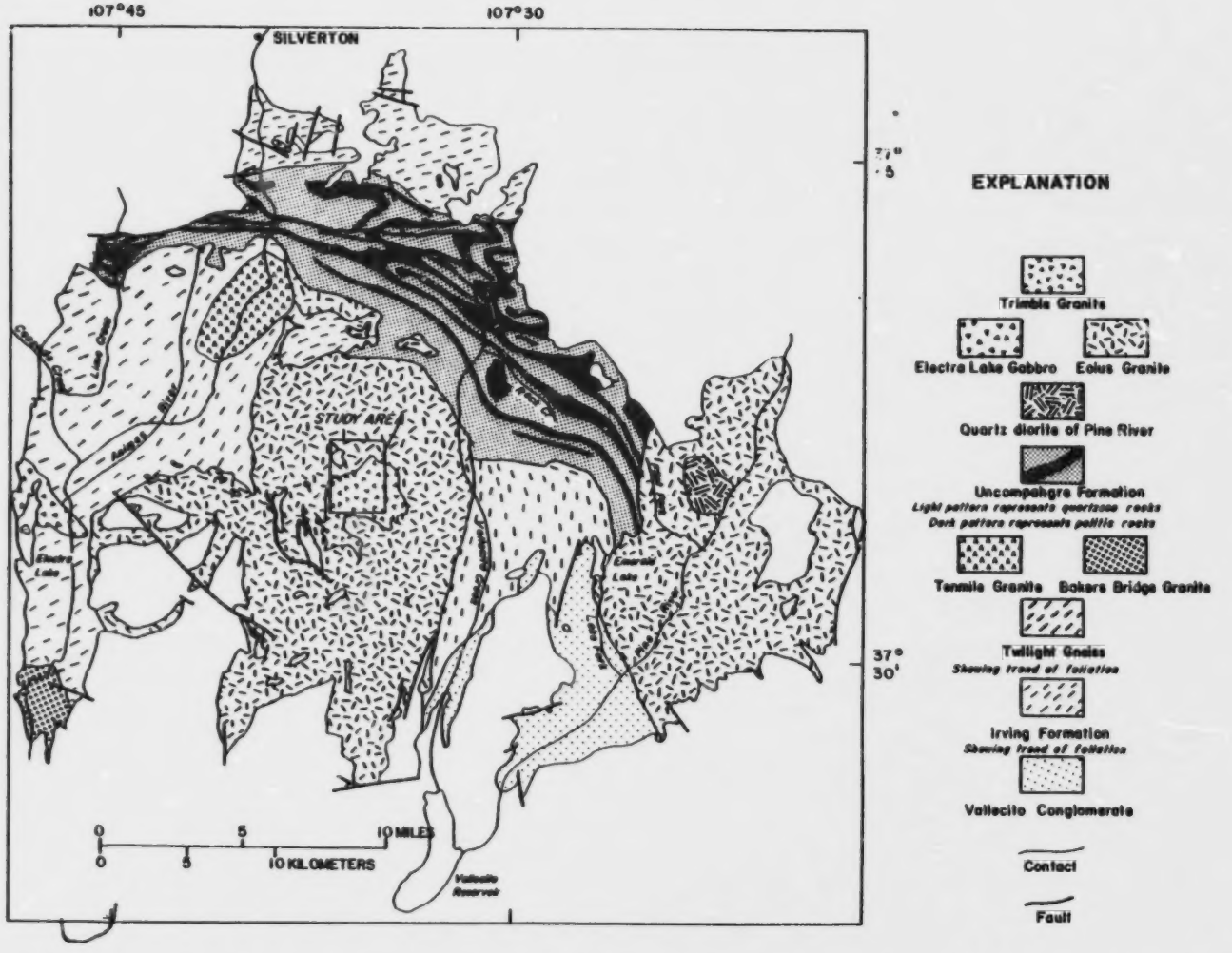

Figure 4. Geologic map of the Proterozoic rocks of the Needle Mountains (from Barker, 1969).

Phanerozoic Rocks

Although the Needle Mountains consist dominantly of Precambrian rocks, a brief discussion of younger sedimentary and volcanic rocks is necessary to review the entire geologic history of the region.

During the late Precambrian to early Cambrian, much of what is now the Needle Mountains was deeply eroded. During the late Cambrian, quartz sandstones and conglomerates of the Ignacio Quartzite were deposited. Upper Devonian shales, sandstones, and limestones of the Elbert and Ouray Formations were unconformably deposited on the Ignacio Quartzite. These in turn were unconformably overlain by carbonates of the lower Mississippian Leadville Limestone.

A major disconformity between Mississippian and Pennsylvanian rocks, and a change from marine carbonates to nonmarine red beds, marks the uplift of the Uncompahgre-San Luis highlands, a major element of the ancestral Rocky Mountains. The late Paleozoic to early Mesozoic Molas, Hermosa, Rico, and Cutler formations consist mostly of terrigenous red beds, with some locally thick marine limestone and shale sections in the Hermosa Formation.

A Jurassic erosion surface developed on the higher parts of the old Uncompahgre highlands, and most of the pre-Jurassic rocks were stripped off to expose the Precambrian basement. The time period from the Jurassic to the end of the Cretaceous was one of dominantly shoreline and marine sedimentation. A thick sequence of sedimentary rocks was deposited on the old highland area prior to the late Cretaceous to early Tertiary, when Laramide activity uplifted the old Uncompahgre-San Luis highlands, as well as the area of the present Needle Mountains. Erosion stripped much of the sedimentary cover and exposed Precambrian rocks in the area of the Needle Mountains.

Volcanism was the dominant geological process in the area during the mid-Tertiary. The volcanic succession in the San Juan area is reviewed by Steven and others (1969) and Lipman and others (1970). Of note, however, is that one of the latest events associated with volcanic activity in the San Juan Mountains region was intrusion of hypabyssal rocks in the study area.

By the Quaternary, the Needle Mountains were already high, with streams dissecting out rugged topography and removing any volcanic cover. The spectacular scenery present today is mainly a result of Pleistocene glaciation which dissected the steep-walled canyons and basins of the higher elevations.

Regional Structure

As discussed previously, folds and foliation are present within the metasedimentary rocks of the Needle Mountains. Faulting, however, is not a prominent characteristic of the region. Some faults with minor displacement were mapped by Larsen and Cross (1956). Barker (1969) reinterpreted many of these faults as intrusive contacts; his version is shown on figure 4. However, the difficulty in differentiating between faults and intrusive contacts may have been complicated by intrusion along faults, which is suggested by the several linear segments of the Eolus Granite contacts shown

on figure 4. Those faults in the region that have been confidently identified are mostly normal faults, tend to be tangential to the outline of the Needle Mountains, and usually postdate the Eolus Granite.

No shear zones similar to those found elsewhere in Precambrian terranes of the Rocky Mountain region are evident in the Needle Mountains. In fact there are very few structures available to aid in interpreting the tectonic history of the area. As a result, only the local structures of the study area will be treated in any detail, and these will be considered in a later section.

PROTEROZOIC ROCKS OF THE STUDY AREA

The study area lies entirely within what was termed the Pine River batholith by Larsen and Cross (1956). This batholith actually consists of two composite bodies. A western body, including the study area and the Eolus and Trimble granites, occupies approximately 260 sq km between Vallecito Creek and the east rim of the Animas River canyon (fig. 4). An eastern body, consisting of Eolus Granite and a small pluton called by Barker (1969) the Quartz Diorite of Pine River, underlies much of the drainage of Pine River. Barker (1969) referred to these intrusions as the eastern and western bodies of the Eolus Granite. The practice of Larsen and Cross (1956) of collectively referring to all intrusive varieties of the two bodies as a single batholith will be followed here using the name Eolus batholith. The Trimble and Eolus granites, first named by Cross and others (1905), are the principal map units and these terms will be continued. Barker's Quartz Diorite of Pine River will not be distinguished as a separate map unit but will included as part of the Eolus Granite. It will be shown later that the intrusive relationships within the Eolus batholith are more complex than the map names suggest.

Descriptive Petrology and Petrography

The study area is underlain by approximately equal areas of Eolus and Trimble granites. The very heterogeneous nature of the Eolus Granite prompted reconnaissance sampling outside the area since a compositional suite was considered necessary for adequate petrogenetic modelling. Sample localities outside of the study area are shown on plate I. Difficulties in access allowed only the western part of the Eolus batholith to be studied.

Eolus Granite.--The Eolus Granite was named for Mount Eolus (4296 m), which is located less than 1 km north of the study area. The Eolus Granite constitutes the greatest volume of plutonic rocks in the Needle Mountains. It actually consists of many small intrusions ranging in composition from monzodiorite to granite. Varieties include biotite-hornblende monzodiorite, biotite-hornblende granodiorite, biotite monzogranite, and biotite granite. Textures range from coarse-grained porphyritic to aplitic. Despite this wide variation, the rocks of the Eolus Granite may be crudely divided into three dominant textural and mineralogic variants. These include: 1) coarse-grained, dominantly porphyritic, hornblende-bearing rocks, 2) coarse-grained, commonly porphyritic, hornblende-free, biotite-bearing rocks, and 3) equigranular, fine- to medium-grained, biotite aplites.

The hornblende-bearing varieties range in composition from monzodiorite to monzogranite; the most common variety is granodiorite. Barker's (1969) Quartz Diorite of Pine River (monzodiorite) is included in this group. The rocks are mostly gray and inequigranular, consisting of scattered coarse- to very coarse-grained (1.5-5 cm) phenocrysts of microcline set in a medium- to coarse-grained groundmass of quartz, plagioclase (An_{40-45}), biotite, and hornblende. The phenocrysts are usually fresh, microperthitic, and show conspicuous Carlsbad twinning. Plagioclase occurs as irregular shaped grains and almost always shows some degree of sericitization, although rarely is it very strongly altered. Differential alteration, with sericitization often beginning in the centers of the grains, suggests that the cores of plagioclase are more calcic than the rims. Modal plagioclase ranges from 35 to 60 percent. Quartz ranges from 15 to 20 percent and only rarely shows undulatory extinction or other evidence of strain. Hornblende and biotite together may constitute as much as 35 percent of the rocks, with their relative proportions ranging from hornblende-dominant to biotite-dominant. Hornblende occurs as anhedral, pleochroic, green-brown, often poikilitic grains. In some of the more mafic rocks, hornblende occasionally contains cores of clinopyroxene. Biotite is generally quite fresh and only rarely shows evidence of chloritization. Accessory minerals include a few percent magnetite and ilmenite, apatite, and an occasional grain of sphene.

Another dominant group of textural and mineralogical varieties consists of generally inequigranular biotite monzogranites. Unlike the hornblende-bearing varieties, these rocks are commonly pink to brick-red in color. They are usually porphyritic and contain variable amounts of coarse- to very coarse grained phenocrysts of microcline microperthite in a medium- to coarse-grained groundmass of quartz, sodic andesine, and biotite. In addition to lack of hornblende, these rocks differ from the hornblende varieties in their accessory mineral assemblages. Sphene is generally absent and apatite is less abundant. Zircon and allanite are much more common than in the hornblende-bearing suite.

Although pegmatites are quite rare in the Eolus Granite, aplitic phases are fairly common. Equigranular, fine- to medium-grained, biotite monzogranite or granite aplites are scattered throughout the Eolus Granite and appear to have been intruded at several different times. The aplites are gray to pink in color and generally contain more than 20 percent quartz, less than 15 percent biotite, and variable percentages of plagioclase (An_{25-35}) and microcline.

This study only encountered unconformable contacts of the Eolus batholith with Paleozoic sediments; therefore nothing could be ascertained as to the nature of its emplacement. Cross and others (1905) mapped several of the contacts of the Eolus Granite with surrounding country rocks as faults, but Barker (1969) reinterpreted many of these as intrusive contacts. He described an extensive breccia zone along the eastern contact of the western body of the Eolus Granite with the Irving Formation. This suggests that the Eolus Granite may have been forcibly injected at shallow depth. Lineation of phenocrysts is common near the margins of the Eolus batholith.

Within the batholith relative ages of various intrusive phases were often

difficult to obtain. However, field relationships generally indicate that the more mafic, hornblende-bearing varieties were the earliest intrusions. This was particularly true near the western margin of the batholith where the most mafic samples were obtained. Silver and Barker (1968) obtained a U/Pb zircon age of 1,460 ± 20 m.y. for the Eolus Granite. Bickford and others (1968) established a compatible Rb/Sr whole-rock age of 1,466 ± 27 m.y., and obtained mineral isochrons of approximately 1,400 m.y. K/Ar determinations on hornblende of 1,460 ± 70 m.y. and on biotite of 1,390 ± 40 m.y. by R. E. Zartman (in Barker, 1969) suggested to Barker that part of the Eolus Granite may have suffered a thermal disturbance 60 or 70 m.y. after the rocks were intruded. It is not known which variety of the Eolus Granite was sampled for the age determinations; it may be that the thermal disturbance marks the intrusion of a textural and mineralogic variety not sampled for the age determinations.

Trimble Granite.--The Trimble Granite is a small pluton occurring roughly within the center of the western body of the Eolus batholith. The granite underlies part of Vallecito Basin, East Silver Mesa, Florida Mountain, and upper Crystal Valley. The rock was named for its exposure at Trimble Pass. Trimble Granite clearly intruded the Eolus Granite, and the contact between the two is generally sharp and without chill margins. It dips away from the Trimble Granite at approximately 20-30°, suggesting that the Trimble Granite may have a laccolith configuration.

The Trimble Granite is a fairly homogeneous body of fine- to medium-grained biotite monzogranite and granite. The rocks contain 20-30 percent quartz, 5-15 percent biotite, and variable percentages of microcline and plagioclase (An_{25-35}). Potassium feldspar is always present in greater amounts than plagioclase. Microcline is relatively fresh, whereas plagioclase nearly always shows evidence of sericitization. Even drill core samples taken from depths of more than 500 m showed intense sericitization, suggesting that plagioclase was probably deuterically altered. Biotite is also often partially or intensely chloritized. Fine-grained interstitial muscovite is present in minor amounts in many samples. The muscovite is generally intimately intergrown with biotite and appears to be a secondary replacement product, rather than being of primary origin. Other accessory minerals include zircon, ilmenite partially altered to leucoxene, magnetite partially altered to hematite, and metamict allanite.

Texturally the Trimble Granite ranges from crudely equigranular to inequigranular-seriate to porphyritic. Most of the rock is medium grained and equigranular. Both aplites and pegmatites, although not abundant, are present in the Trimble Granite. Pegmatites are generally quite small, occurring either as lenses (usually less than 1 sq. m in area) or as 1-3 cm wide growths in fractures. The aplites range from a few centimeters to a meter or more in width, and average less than 25 m in length. The number of aplites and pegmatites, as well as the ubiquitous deuteric alteration, suggest that a more substantial volatile phase developed during the crystallization of the Trimble Granite than for the Eolus Granite.

Bickford and others (1968) obtained a Rb/Sr whole-rock age of 1,350 ± 50 m.y. for the Trimble Granite. However, Bickford (oral commun., 1980) felt

that the Trimble age was perhaps the least reliable of any age determination from the Needle Mountains. It is possible that the actual age of the Trimble Granite is somewhat older, perhaps corresponding with the thermal disturbance of the Eolus Granite at 1,390 to 1,400 m.y.

Chemical Composition of the Granites

The rocks of the Eolus batholith constitute a geochemical province with an above-average content of uranium. Because the Eolus batholith, and in particular the Trimble Granite, probably acted as the source of uranium for the deposits of the study area, the genesis of these rocks is an important part of the history of uranium mineralization. Although incomplete data coupled with the general complexity and inadequacy of understanding of granitic systems preclude making any definitive statements on petrogenesis, the chemical and mineralogic compositions of the granites may be combined to construct a tentative genetic model. Such a model is a necessary framework in which to place later discussions of the mineral deposits hosted by the granites.

Granites can form from an almost infinite variety of primary magmas, which may be derived from crustal sediments, a variety of crustal igneous sources, and possibly from the mantle. Chappell and White (1974), White and Chappell (1977), Ishihara (1977), and White (1979), among others, have compiled mineralogic and geochemical parameters by which first-order identification of source rocks can be made. Granites derived from igneous sources (I-type granites of Chappell and White, 1974) should differ from those derived from sedimentary sources (S-type) primarily by chemical differences reflecting whether or not the source has been through a weathering cycle. I-type granites may also differ from S-types by a wider compositional variation and greater abundance of mafic cognate phases reflecting their differentiation from more mafic sources, by different trace-element behavior reflecting different chemical relations between melt and restite, and by greater initial abundances of characteristically "igneous" elements and minerals. Major and minor oxides, trace elements, and mineralogic evidence suggest that the granites of the Eolus batholith formed by partial melting of igneous sources. Trace-element evidence also suggests that several partial melting events occurred and that differentiation resulted in progressive enrichment of incompatible elements such as uranium and thorium.

In the following discussion, the chemical composition of the granites will be described and the chemical behavior of various elements will be used to characterize the differentiation history of the Eolus batholith. This information will then be combined with mineralogic evidence to briefly speculate on the source, tectonic setting, and general petrogenesis of the granites. A number of genetic models could be proposed; the one developed below is believed to be most consistent with available data.

Twenty samples of Eolus Granite and two samples of Trimble Granite were analyzed for major oxides and a variety of trace elements. X-ray fluorescence analyses for major and minor oxides were performed by the laboratories of the U.S. Geological Survey and are shown in table 2. CIPW norms calculated from these analyses are also shown in table 2. Trace elements (tabulated in the appendix) were analyzed by the Nuclear Division of Union Carbide

Table 2. Chemical analyses and CIPW norms for the Precambrian granitic rocks of the Eolus batholith.

[LOI-loss on ignition. Major oxide analyses by X-ray spectroscopy, USGS. Analysts: J.S. Wahlberg, J. Taggert, J. Baker. U and Th analyses by INAA, Nuclear Division, Union Carbide Corp.]

Field No...	EG-1	EG-2	EG-3	EG-4	EG-5	EG-6	EG-8	EG-9	EG-10	EG-11	EG-12	EG-14	EG-15	EG-16	EG-17	EG-18	EG-19	EG-20	EG-21	EG-22	EG-23	EG-25
CHEMICAL ANALYSES (wt. %, U & Th in ppm)																						
SiO_2	70.4	67.3	67.6	72.5	68.9	72.4	73.2	74.2	68.7	67.4	64.2	68.0	68.2	72.6	71.0	73.3	73.7	70.9	72.9	59.9	63.0	62.0
Al_2O_3	13.9	13.3	13.7	14.1	12.0	14.7	13.8	12.9	14.9	14.2	14.3	15.1	15.0	13.4	14.3	13.6	13.3	14.6	13.6	14.5	13.7	14.2
Fe_2O_3	3.32	6.80	5.58	1.63	6.02	2.33	1.20	2.44	3.21	5.51	7.55	3.39	2.81	2.41	2.22	2.46	1.93	2.51	1.89	10.5	8.79	9.40
MgO	0.70	1.23	1.07	0.54	1.22	0.41	0.24	0.46	0.74	1.00	1.28	0.96	0.75	0.55	0.63	0.52	0.42	0.70	0.46	1.87	1.64	1.79
CaO	1.00	2.63	2.41	0.73	2.14	0.02	0.40	0.47	1.15	1.84	3.02	1.32	1.71	0.60	0.60	0.79	0.99	1.40	0.72	4.25	2.97	3.68
Na_2O	3.24	3.27	3.40	3.54	2.80	0.37	3.26	3.14	3.32	3.17	3.55	3.60	3.70	3.24	3.24	3.24	3.61	3.74	3.24	3.58	3.15	3.52
K_2O	5.27	3.50	3.47	5.43	3.45	5.09	5.86	4.96	6.08	4.76	3.48	5.29	4.95	5.30	5.32	5.23	4.66	4.84	5.40	2.64	3.51	2.81
TiO_2	0.37	0.83	0.67	0.15	0.74	0.21	0.05	0.22	0.36	0.70	0.94	0.40	0.31	0.22	0.21	0.20	0.17	0.26	0.17	1.35	1.15	1.24
P_2O_5	0.11	0.20	0.17	<.05	0.19	<.05	<.05	<.05	0.08	0.16	0.25	0.13	0.10	0.07	0.07	0.08	0.06	0.08	0.06	0.34	0.28	0.32
MnO	0.04	0.10	0.08	<.02	0.09	0.04	<.02	0.03	0.03	0.08	0.11	0.03	0.04	0.02	<.02	0.03	0.03	0.04	0.03	0.16	0.12	0.14
U	6.1	3.6	2.6	8.7	3.4	5.2	11.0	7.0	3.4	2.8	3.5	3.7	5.2	7.7	8.2	15.0	11.0	8.5	16.9	3.4	3.5	3.0
Th	30	7.6	7.4	30	8.8	42	38	11.0	7.1	9.0	28	33	30	33	36	54	35	36	37	6.6	6.3	5.6
LOI	0.76	0.83	0.83	0.66	0.89	3.46	0.52	0.72	0.81	0.69	0.62	0.97	0.86	0.82	1.12	0.74	0.61	0.52	0.85	0.76	0.70	0.71
Total	99.10	99.99	98.78	99.35	98.44	99.08	98.60	99.59	99.38	99.51	99.30	99.19	98.43	99.24	98.73	100.3	99.48	99.59	99.32	99.85	99.01	99.81
CIPW NORMS (wt. %)																						
Quartz	27.31	25.49	26.40	28.44	31.75	49.66	30.63	34.56	21.69	23.86	19.95	21.81	22.49	30.83	29.26	31.31	31.67	26.03	30.78	14.80	20.15	17.98
Corundum	1.32	---	0.38	1.20	0.23	8.66	1.51	1.64	0.96	0.89	---	1.37	0.70	1.42	2.32	1.36	0.66	0.86	1.27	---	---	---
Orthoclase	31.39	20.68	20.72	32.30	20.71	30.36	35.12	29.43	36.15	28.27	20.71	31.51	29.72	31.56	31.84	30.85	27.68	28.75	32.13	15.62	20.95	16.64
Albite	27.64	27.67	29.07	30.15	24.07	3.16	27.98	26.68	28.27	26.87	30.25	30.71	31.81	27.63	27.77	27.36	30.71	31.81	27.60	30.34	26.92	29.84
Anortnite	4.28	11.28	10.96	3.32	9.52	---	1.68	2.01	5.21	8.12	12.90	5.75	7.95	2.54	2.55	3.39	4.54	6.46	3.20	15.72	13.01	14.67
Wollastonite	---	0.19	---	---	---	---	---	---	---	---	0.23	---	---	---	---	---	---	---	---	1.32	0.01	0.64
Enstatite	1.98	3.06	2.69	1.35	3.09	1.03	0.61	1.15	1.85	2.50	3.21	2.41	1.90	1.38	1.59	1.29	1.05	1.75	1.15	4.66	4.12	4.47
Ferrosilite	2.84	5.68	4.73	1.43	5.10	2.11	1.19	2.16	2.71	4.58	6.33	2.85	2.44	2.14	1.95	2.02	1.73	2.00	1.69	8.68	7.27	7.71
Magnetite	1.50	3.06	2.53	0.74	2.75	1.05	0.54	1.11	1.46	2.49	3.42	1.53	1.28	1.10	1.01	1.10	0.87	1.14	0.86	4.73	3.99	4.24
Ilmenite	0.71	1.58	1.29	0.29	1.43	0.40	0.10	0.42	0.69	1.34	1.80	0.77	0.60	0.42	0.40	0.38	0.32	0.50	0.32	2.57	2.21	2.36
Apatite	0.26	0.47	0.41	0.12	0.46	0.04	0.12	0.12	0.19	0.38	0.60	0.31	0.24	0.17	0.17	0.19	0.14	0.19	0.14	0.81	0.67	0.76
Total	99.24	99.18	99.17	99.34	99.11	96.47	99.48	99.28	99.19	99.32	99.39	99.03	99.13	99.18	98.87	99.27	99.39	99.48	99.15	99.26	99.31	99.31

Corporation. Both instrumental neutron activation and inductively coupled plasma spectrometry methods were used. Instrumental neutron activation is a technique that, although capable of great sensitivity and accuracy, requires a high level of competance on the part of the analyst. The reader should be forewarned that analyses of USGS standards BCR-1 (basalt) and G-2 (granite) suggest that the accuracy of the trace-element data is variable and may often be poor. Precision, which is the more important factor for the applications described below, was very carefully evaluated and considered to be good.

Major normative minerals.--Three ternary combinations of normative feldspars and quartz are shown on figure 5. In addition, the positions of the rocks relative to the alumina saturation classification of Shand (1927) are presented graphically. The ternary plot Q-Or-An+Ab corresponds to the Q-A-P classification scheme of Streckeisen (1976). Most of the hornblende-bearing rocks fall within the granodiorite field, whereas the biotite rocks would be classified as monzogranites. Exceptions are one hornblende-bearing rock with the lowest SiO_2 content (Sample EG-22) which by Streckeisen's classification would be called a monzodiorite, and one strongly altered aplite (Sample EG-6) which falls within the alkali granite field. The An-Ab-Or diagram shows a linear trend away from plagioclase towards the minimum-melting trough. A linear trend is also seen from metaluminous hornblende-bearing rocks to peraluminous hornblende-free rocks.

Major and minor oxides.--The behavior of major oxides as a function of SiO_2 is shown in standard Harker-type diagrams on figure 6. The patterns are consistent with silica and potassium enrichment from granodiorite to granite. The strong linearity of the trends is suggestive that there may be a genetic relationship between the various samples. The two samples of Trimble Granite are not very representative in that they have lower SiO_2 contents than most of the Trimble Granite. Additional major oxide analyses for samples of Trimble Granite are available (see table 5, p. 67). However, as no trace-element data, which will form the basis for much of the following discussion, were obtained for these samples, they were omitted from figure 6.

Variation diagrams illustrating the behavior of P_2O_5, TiO_2, and Th with increasing SiO_2 are shown on figure 7. Both P_2O_5 and TiO_2 decrease strongly with increasing SiO_2. White and Chappell (1977) suggest that steep linear trends in variation diagrams may represent progressive separation of residual material and melt. They believe that many granites consist of mixtures of residual source material (restite) and products of crystallization from melts. Restite is recognized petrographically by such features as pyroxene cores within anhedral hornblende or calcic cores in plagioclase (both observed in the Eolus Granite). According to White and Chappell (1977), elements such as phosphorus and titanium do not enter appreciably into minimum partial melts of sources containing quartz and feldspar. Hence, their content in a rock is controlled by the amount of restite present. During the ascent of a magma, restite may be progressively removed, resulting in increasingly greater proportions of melt and correspondingly lower contents of P_2O_5 and TiO_2. Pure minimum melts without restite , corresponding to about 76 percent SiO_2 (White, 1979), should contain no P_2O_5 or TiO_2. It is interesting to note that

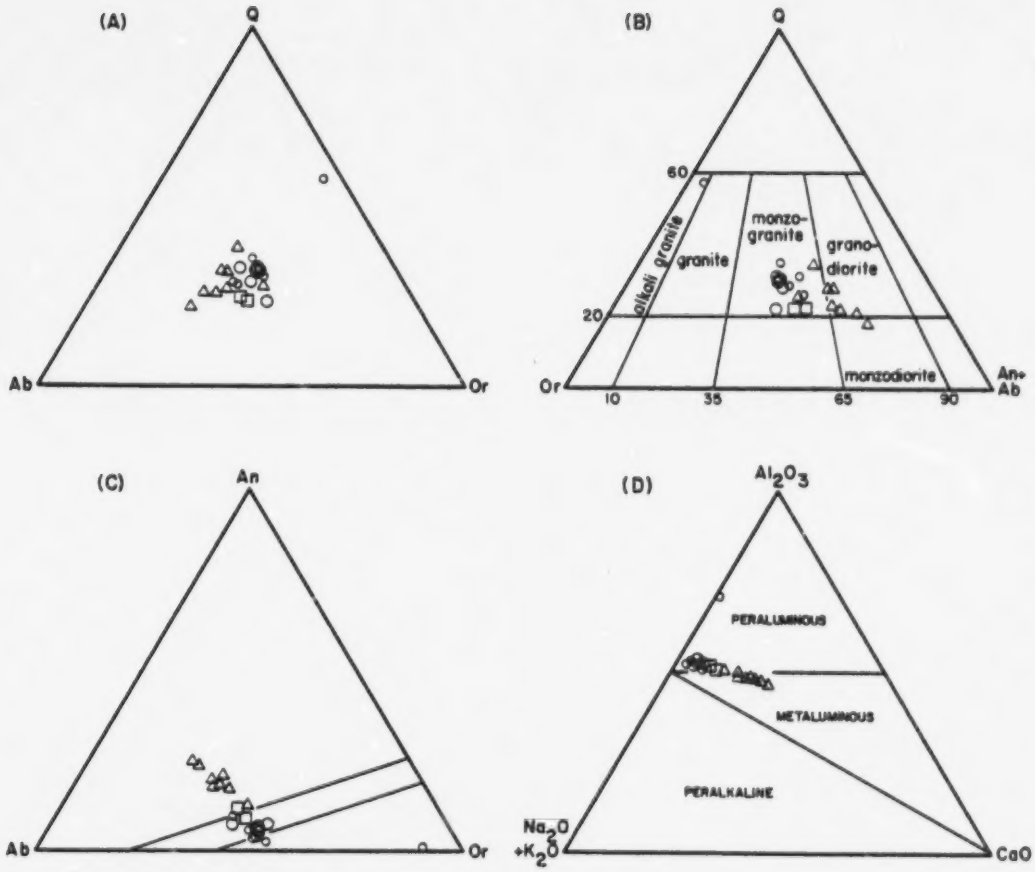

Figure 5. Ternary diagrams for granitic rocks of the Eolus batholith. Triangles represent hornblende-bearing Eolus Granite. Large circles represent coarse-grained, hornblende-free Eolus Granite. Small circles are samples of Eolus Granite aplites. Squares represent Trimble Granite. Figure 7B shows the classification fields of Streckeisen (1976). Figure 7C shows the minimum melting trough after Yoder and others (1957). Figure 7D shows the alumina saturation classification fields after Shand (1927). All norms and oxides in mole percent.

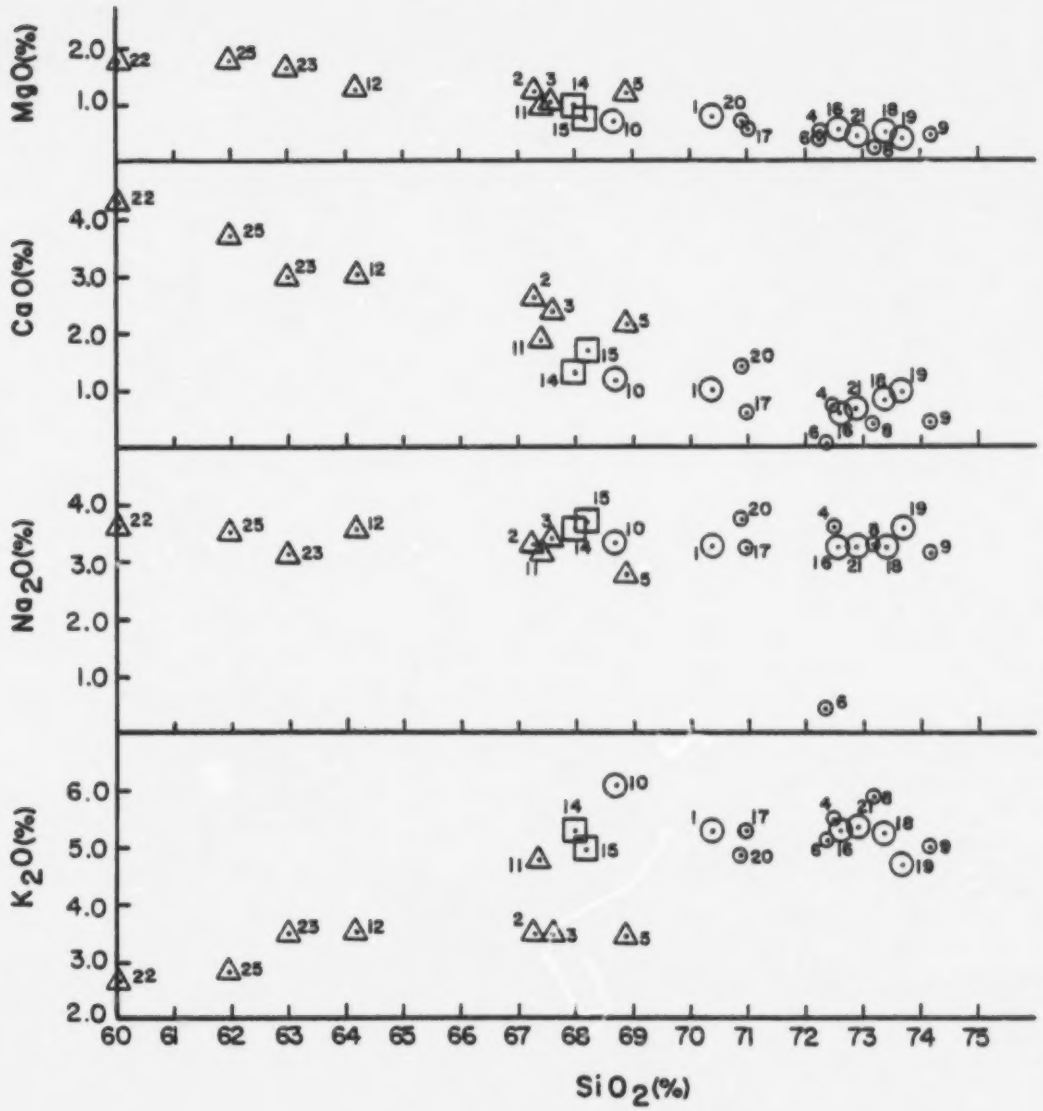

Figure 6. Harker-type diagrams, in weight percent, for granitic rocks of the Eolus batholith. Triangles - hornblende-bearing Eolus Granite, large circles - hornblende-free Eolus Granite, small circles - aplitic Eolus Granite, squares - Trimble Granite. Sample numbers correspond to those of table 2.

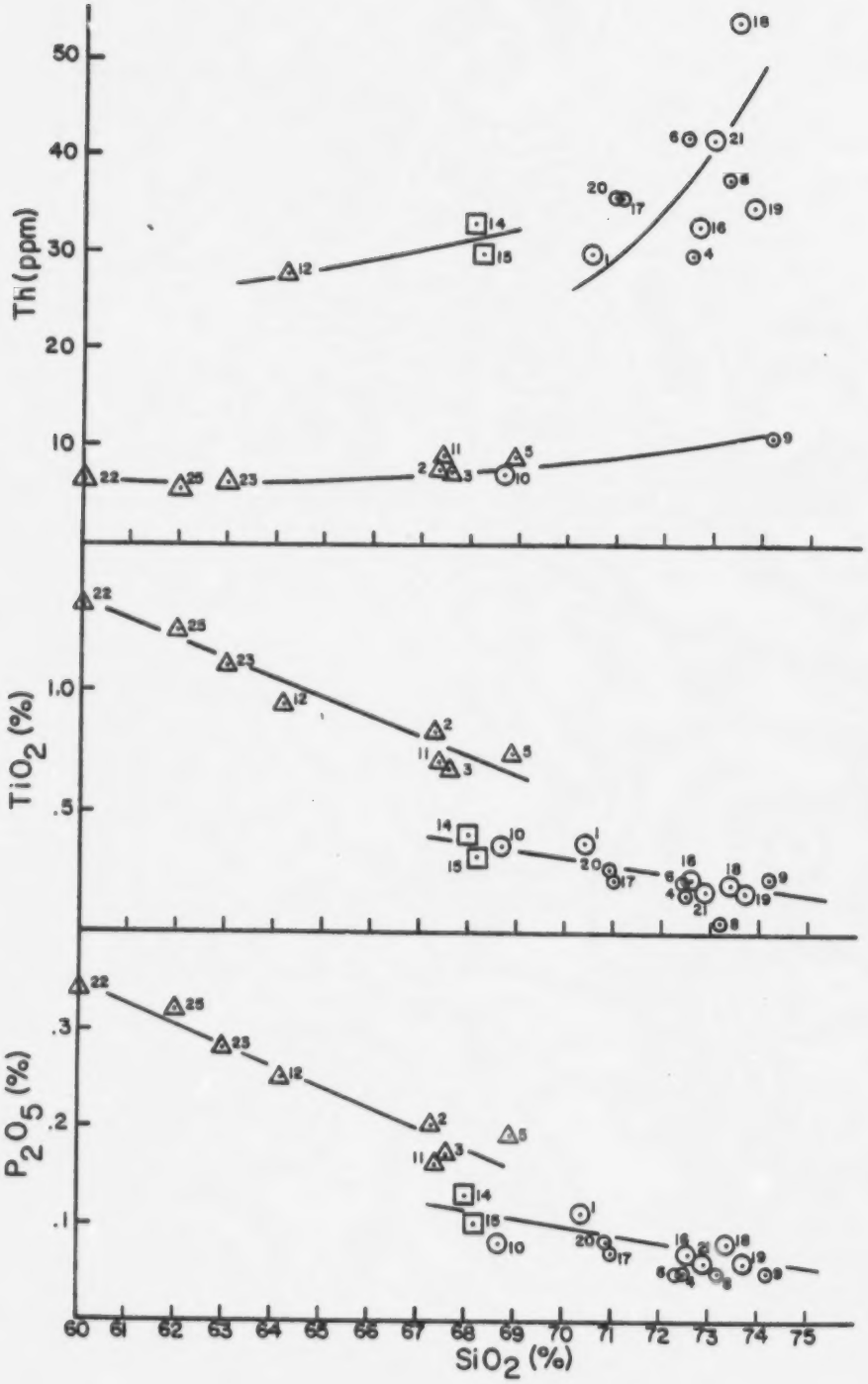

Figure 7. Variation diagrams of P_2O_5, TiO_2, and Th versus SiO_2 for granitic rocks of the Eolus batholith. Same symbols as preceding diagrams.

projections of the upper trends of P_2O_5 and TiO_2 vs. SiO_2 both intersect the SiO_2 axis at 76 percent. The breaks in the slopes of both diagrams are Papparently controlled by hornblende, but cannot easily be explained by simple application of the restite model. A number of possible causes which could not be determined, such as saturation of the melt with a higher SiO_2 phase or the initiation of volatile transfer, might explain the changes in slopes.

The plot of Th vs. SiO_2 is interesting in that it distinguishes three apparent trends. Sample EG-12 is mineralogically and texturally identical to the other hornblende-bearing rocks, yet contains considerably more thorium. A much greater density in fission-track radiographs of Sample EG-12 indicates that the discrepancy is not due to analytical error. It appears to lie on a possible trend with Trimble Granite samples, which also have relatively high thorium contents. There are insufficient samples to fully characterize the trends, but it is apparent that the relationships between samples are more complex than suggested by the behavior of major oxides.

Trace elements.--Strontium, rubidium, barium, and the rare-earth elements are the most useful elements for modelling magmatic processes because partition coefficients for these elements have been measured for a variety of minerals in various rock types (Arth, 1976). Figures 8, 9, and 10 are plots of Sr, Rb, and Ba versus each other and various oxides.

On figure 8, K_2O and Sr are plotted against Ba. In K_2O vs. Ba both elements increase together in the hornblende-bearing rocks. This indicates that neither were in equilibrium with a mineral having a high distribution coefficient (K_d) for these elements. A mineral/melt K_d is the measured weight fraction of a given trace element in a mineral divided by the measured weight fraction of that mineral in a coexisting melt. The only minerals relevant to this suite having high K_d's for Ba are potassium feldspar and biotite (Arth, 1976), indicating that they were not early fractionating phases. However the non-hornblende-bearing rocks show a strong decrease in Ba with relatively constant K_2O, suggesting that potassium feldspar was probably fractionating within this trend (progressive increases in Rb, for which biotite has a high K_d, on figures 9 and 10 suggest that biotite was not a major fractionating phase). Assuming a minimum-melt composition for a monzogranite of 35 percent orthoclase, 35 percent plagioclase, and 30 percent quartz (this is also the average normative composition of monzogranites from the Q-Or-An+Ab diagram in figure 5), and assuming about 15 percent K_2O in potassium feldspar (Deer and others, 1966), the average bulk composition for these rocks should be approximately 5.25 percent K_2O. This is in good agreement with the diagram.

Both Sr and Ba decrease in a crudely linear fashion in the upper diagram of figure 8. The liquids were thus in equilibrium with minerals having high K_d's for these elements. The bulk distribution coefficient (D_o) for each element can be expressed as

$$D_o = X_a K_d^a + X_b K_d^b + \ldots \qquad \text{(Arth, 1976)}$$

where D_o is the bulk distribution coefficient of the trace element, X_a and X_b are the initial weight fractions for relevant solid phases a and b, and K_d^a and K_d^b are mineral/melt distribution coefficients. Assuming the same average

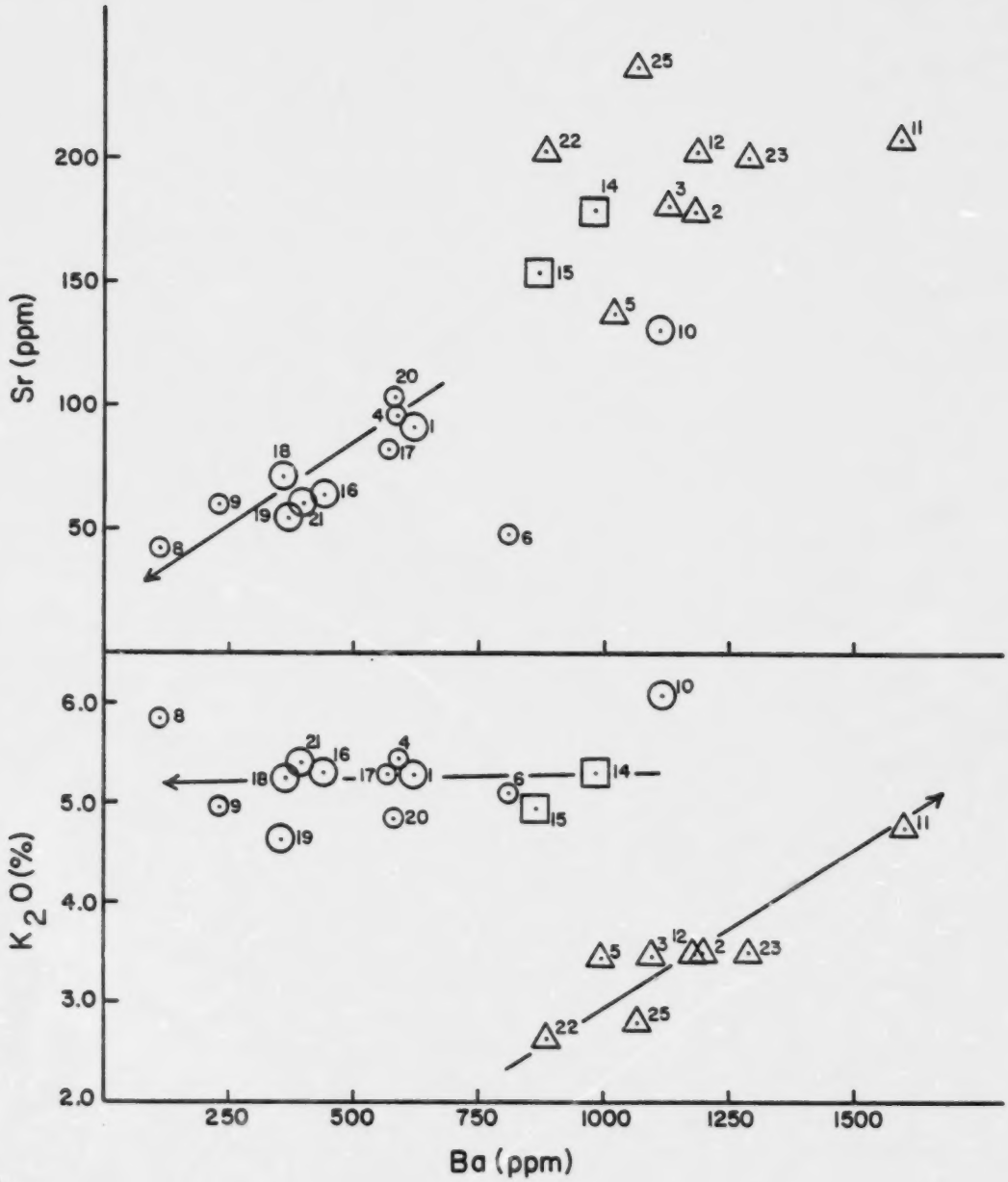

Figure 8. Variation diagrams of K_2O and Sr versus Ba. Triangles - hornblende-bearing Eolus Granite, large circles - coarse-grained hornblende-free Eolus Granite, small circles - Trimble Granite. Arrows point in direction of increasing differentiation.

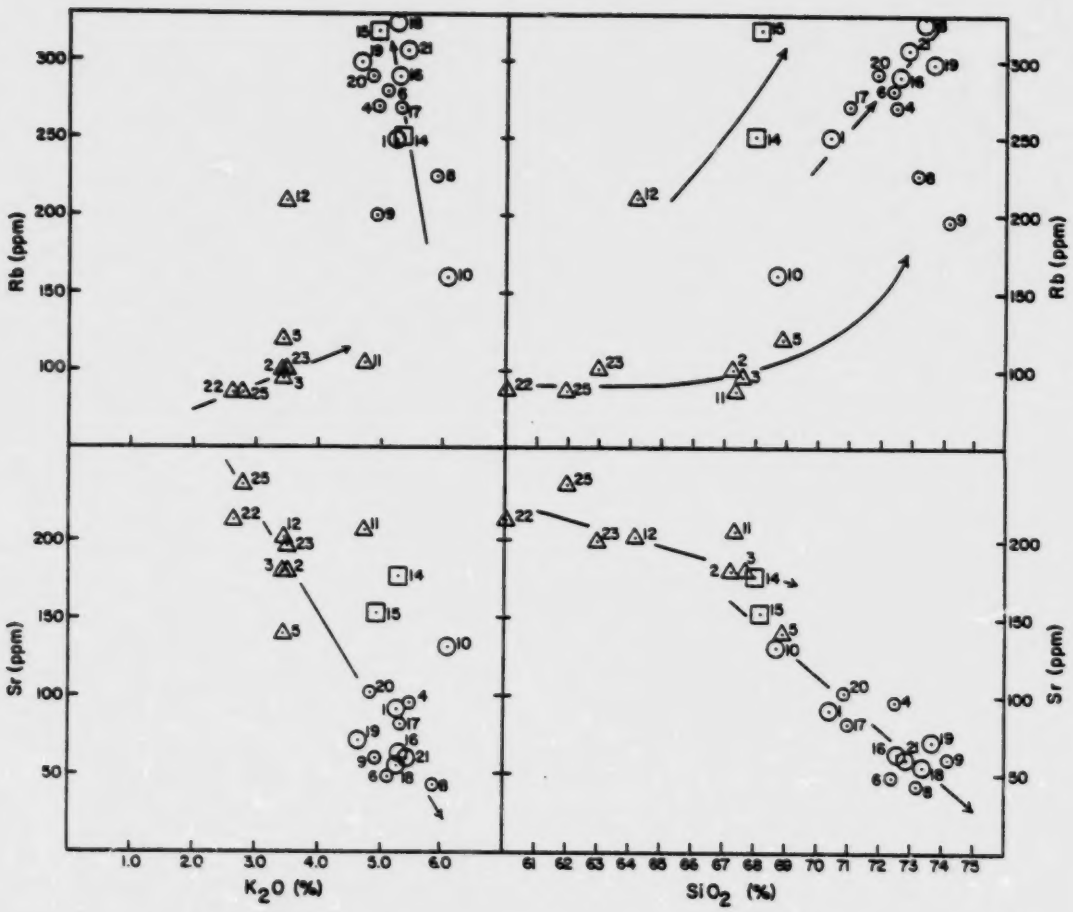

Figure 9. Variation diagrams of Sr and Rb vs. K_2O and SiO_2.

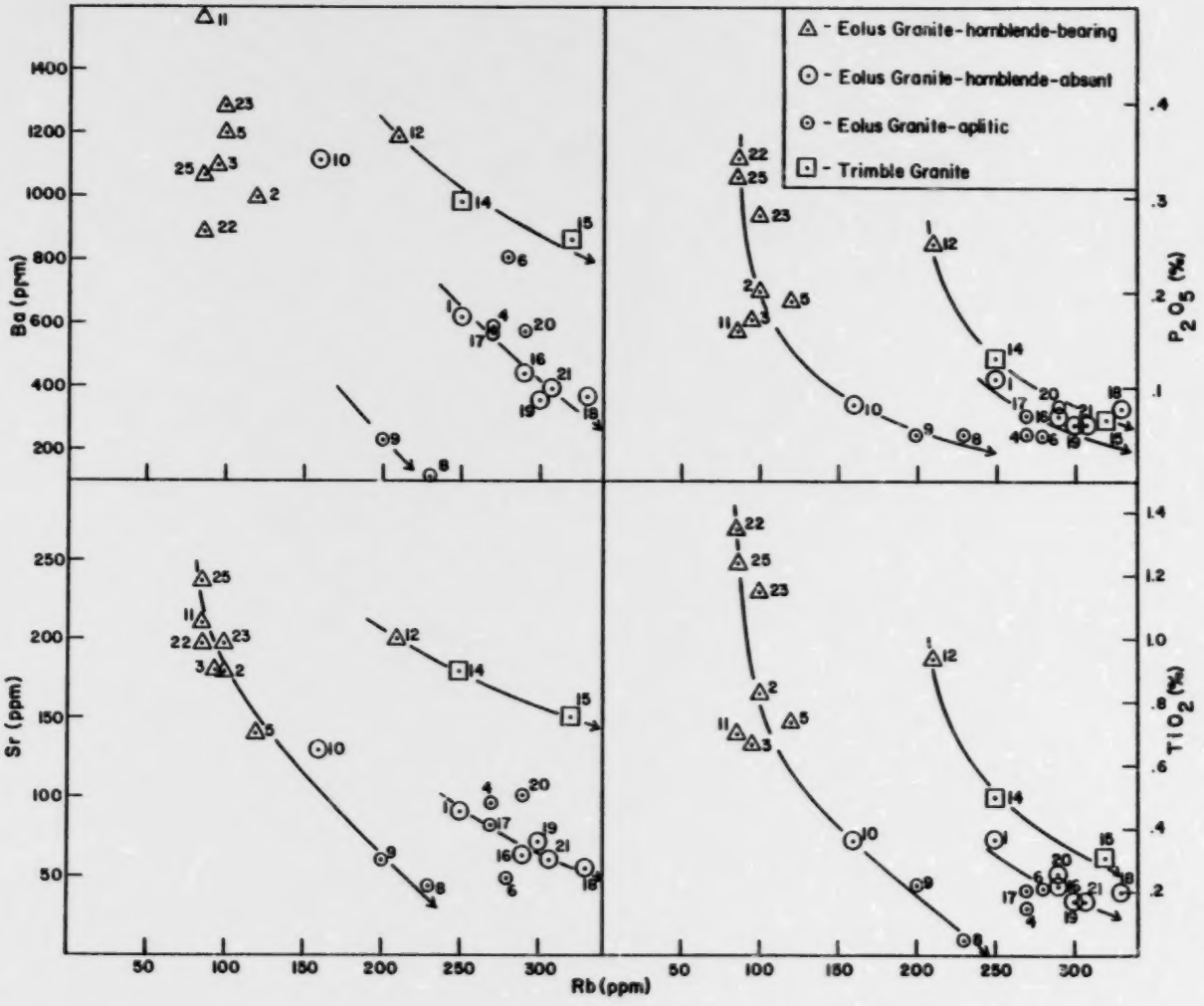

Figure 10. Variation diagrams of Ba, Sr, TiO_2, and P_2O_5 versus Rb.

mineral composition used above, the bulk distribution coefficients for Sr and Ba, using data from Arth (1976), are:

$$D_{o(Ba)} = (X_{K\text{-spar}})(K_d K\text{-spar}) = (.35)(6.12) = 2.1$$

$$D_{o(Sr)} = (X_{K\text{-spar}})(K_d K\text{-spar}) + (X_{plag})(K_d plag) =$$

$$(.35)(3.87) + (.35)(4.4) = 2.89 \quad .$$

The similar values explain the nearly 45° slope of the diagram. The wide scatter of points among the hornblende-bearing rocks is probably because K-feldspar was not fractionating Ba. The slope of the hornblende-free rocks cannot be explained solely by K-feldspar fractionation; it indicates that plagioclase was also a fractionating phase.

Somewhat more information may be gathered from the diagrams of figure 9. In the lower diagrams Sr decreases with increasing K_2O and SiO_2. Again the decrease is due to liquid in equilibrium with minerals having high K_d's for Sr. It has already been shown that K-feldspar did not control the hornblende-bearing trend, whereas both K-feldspar and plagioclase were important phases affecting the hornblende-free trend. The negative slope of hornblende rocks in Sr vs. SiO_2 suggests that plagioclase removal controlled the formation of that trend. The steeper slope shown by nonhornblende-bearing rocks suggests that both plagioclase and K-feldspar fractionation controlled the trend.

In the upper diagrams of figure 9, Rb is plotted against K_2O and SiO_2. The plot of Rb vs. K_2O is somewhat similar to K_2O vs. Ba (fig. 8) in that K-feldspar fractionation appears to hold K_2O constant, or actually decreases it slightly. However, Rb increases constantly regardless of the behavior of K_2O, indicating that there were no fractionating phases such as biotite having a high K_d for Rb. Thus Rb appears to be a largely incompatible element in this system, and the diagram Rb vs. SiO_2 is, in essence, the behavior of an incompatible element with differentiation. The three apparent trends are similar to those in Th vs. SiO_2 (fig. 7), suggesting that thorium is also an incompatible element in this system.

Rubidium is plotted against a number of elements on figure 10. The three trends break out consistently. Again the hornblende-bearing Sample EG-12 appears to fall on a trend with samples from the Trimble Granite. This trend has the highest relative Rb contents, suggesting that it is the most highly fractionated. One might infer from these diagrams that the three trends represent different partial melts, and that the rocks within each trend are related to each other by fractionation, most likely by crystal fractionation. Since the Trimble Granite is younger than the Eolus Granite, it is possible that the three trends represent differentiation of parent melts of different age. The diagrams also suggest that some of the hornblende-bearing granodiorites that have been mapped as Eolus Granite may actually be of the same age and comagmatic with the Trimble Granite.

To briefly summarize, trace elements indicate that, despite the linear behavior of major oxides, all the rocks of the Eolus batholith are probably not derived from the same parent. There appear to have been at least three different partial melts, of which the Trimble Granite and perhaps its more primitive cognates are the most highly enriched in incompatible elements. The rocks within each trend are probably related by fractionation. The sharp decrease of such elements as strontium with differentiation cannot be easily explained by partial melting. The modal melting equations of Shaw (1970) indicate that for bulk distribution coefficients such as that for strontium, there is little change in the ratio of trace-element concentrations between liquid and solid with different degrees of partial melting. In contrast, Rayleigh fractionation models for fractional crystallization, as in Hanson (1978), adequately explain such rapid decreases. Thus, the rocks within a given trend are probably related by fractional crystallization rather than by partial melt fractionation. The behavior of trace elements also indicates that plagioclase was the only feldspar to fractionate in forming the hornblende-bearing rocks, whereas both feldspars fractionated in the hornblende-free trends.

Rare-earth elements.--Another set of trace elements for which partition coefficient data are available are the rare-earth elements (REE). These can be used not only to help corroborate the relationships observed above, but to provide additional information on fractionation mechanisms and perhaps give some insight into the nature of the source rocks. Chondrite-normalized rare-earth element patterns are summarized on figure 11.

All the rocks show strong enrichment in the light REE, moderate depletion in the heavy REE, and moderate to strong negative europium anomalies. As illustrated on figure 11, most of the patterns fall within three general groups. Relative to other samples, the hornblende-bearing rocks on the average have lower light REE and less pronounced Eu anomalies. The wide spread in the heavy REE precludes comparison between samples. Hornblende-free Eolus granites and Trimble granites show progressively greater light REE enrichment and larger Eu anomalies.

REE patterns are consistent with the relationships inferred from the trace elements discussed earlier. The light REE have low mineral/melt K_d's and would be expected to become further enriched with increased differentiation. This is seen in the higher values for the Trimble Granite. Sample EG-12's REE pattern is very similar to those of the Trimble Granite and has much higher light REE values and a significantly larger Eu anomaly than the other hornblende granodiorites. This corresponds with the three trends seen in earlier diagrams.

All samples have negative Eu anomalies, indicating that feldspars were removed or were residual during melting. The hornblende-bearing rocks have significantly smaller Eu anomalies than do the other samples. This can be explained in part by the fact that only plagioclase was fractionating, whereas both K-feldspar and plagioclase, each with high K_d's for Eu, controlled differentiation in the other samples. However, K-feldspar has a much lower K_d for Eu than does plagioclase, and is unlikely to fully explain the difference in the size of the anomalies. The Eu anomalies of the hornblende-bearing

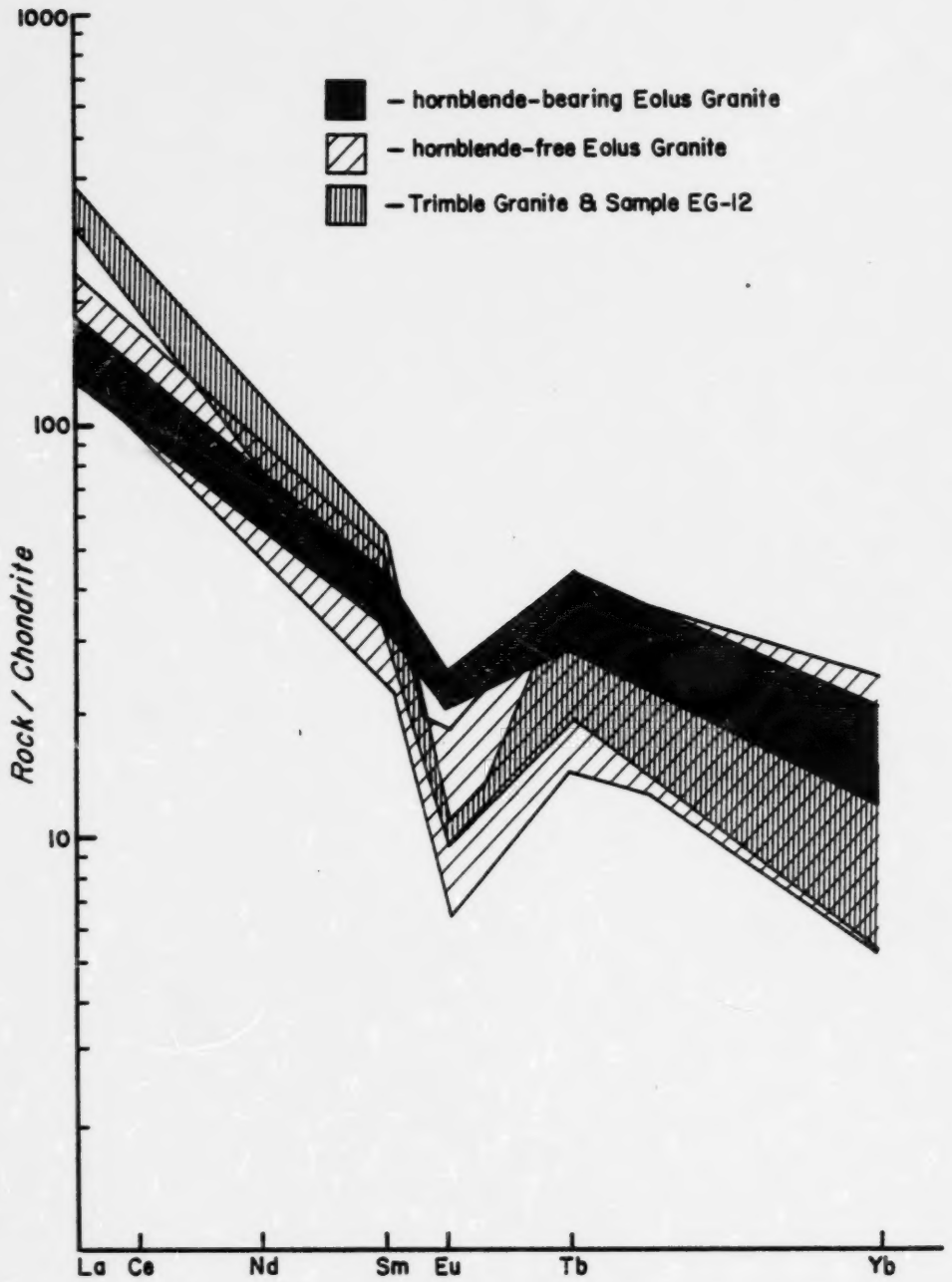

Figure 11. Distribution of chondrite-normalized rare-earth element patterns for samples of granitic rocks from the Eolus batholith. REE analyses from appendix.

rocks were probably buffered by the fractionation of minerals which tend to contribute to positive Eu anomalies. Minerals which might accomplish this include clinopyroxene, orthopyroxene, hornblende, and apatite (Hanson, 1978). The pyroxenes have much lower K_d's for Eu than hornblende and apatite and were, therefore, not likely a major factor. Apatite, if present in significant quantities, could easily buffer the Eu anomalies, but would probably also result in a significant depletion of the middle REE, a relationship not observed. Thus hornblende, and perhaps to a lesser extent apatite, were probably fractionating phases during formation of the hornblende-bearing rocks.

Figure 12 is a plot of lanthanum versus cerium. The samples define a very tight linear trend, indicating very little variation in La/Ce ratios. This suggests that the parent material for the samples had very similar bulk distribution coefficients for these elements. Rocks from different parents, and therefore different assemblages of melt and restite, would show a variety of La/Ce ratios. Although this diagram does not necessarily indicate the same parent for all the rocks, it strongly suggests very similar source material for the rocks and a probable genetic link between the parents.

Petrogenesis

Source rocks.--The behavior of incompatible elements such as Th and Rb suggests that the samples from the Eolus batholith represent at least three partial melts, and subsequent fractional crystallization of plagioclase and K-feldspar produced the observed compositional variation. The mineralogies and chemical compositions of the granites can now be used to suggest possible sources for these partial melts.

The high potassium and low nickel contents of the Eolus granites effectively rule out their direct derivation by partial melting of mantle material. Most other chemical and mineralogical properties, however, point to an igneous rather than sedimentary source.

The presence of both biotite and hornblende, and lack of muscovite, are generally considered indicative of an igneous source (White, 1979). Sphene and allanite, as opposed to monazite, also suggest igneous derivation. The K_2O/Na_2O ratio is relatively low in rocks of the Eolus batholith, an indication that Na_2O was not removed by weathering of the source. Calcium in the more mafic rocks is high, also suggesting that the source was not weathered. The high Th/U ratios for most of the Eolus granites is also characteristic of an igneous source.

The ratio $Al_2O_3/(Na_2O + K_2O + CaO)$ is often considered an indication of source weathering as the ratio should increase by the removal of Na_2O, K_2O, and CaO during weathering. Most S-type granites are therefore peraluminous and corundum-normative. The biotite monzogranites are mostly peraluminous, as shown on figure 5, and are corundum-normative, characteristics which are not typical of I-type granites. However, figure 13 indicates that the rocks change from diopside-normative to corundum-normative in a progressive fashion, suggesting that the relative alumina enrichment was a function of magmatic processes rather than of the composition of the source. A number of explanations have been proposed to explain trends from diopside to corundum

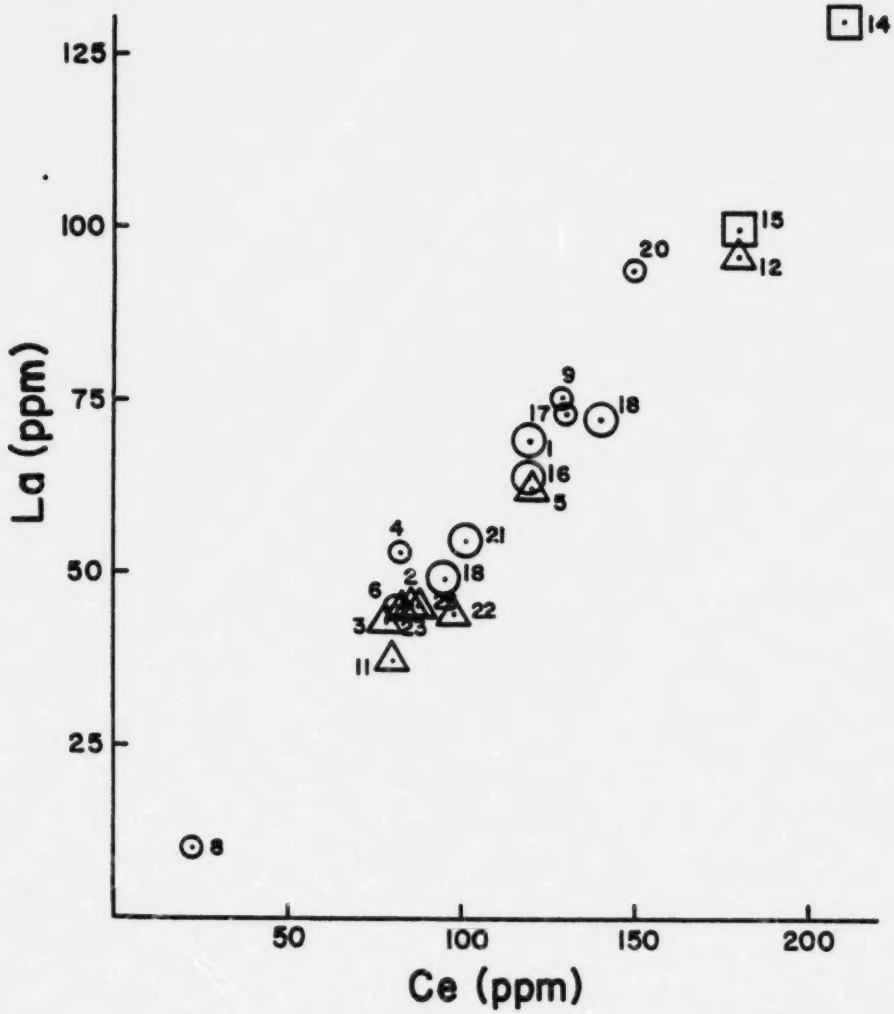

Figure 12. Variation diagram of lanthanum versus cerium for granitic rocks of the Eolus batholith. Symbols are the same as used in preceding diagrams.

norms. Possible mechanisms, summarized by Cawthorn and others (1976), include secondary alteration, vapor phase transfer, assimilation, crustal remelting, hydrous melting of upper mantle, and fractional crystallization of a variety of phases. Cawthorn and others (1976) favored hornblende fractionation as the most plausible mechanism. It was previously shown that hornblende was probably an early fractionating phase in the Eolus batholith.

All evidence points convincingly towards igneous sources for the granites, and trace elements suggest chemical similarities between the sources of the three different partial melts. It is only possible to speculate on what the actual compositions of the sources were. The compositionally expanded nature of the suite (particularly if the Electra Lake Gabbro is related to the Eolus Granite) and an intermediate average composition probably requires a mafic source. Calcic cores in plagioclase and clinopyroxene cores in hornblende may represent residual material from the source, and suggest that the source for the earliest partial melt consisted of hornblende + calcic plagioclase + clinopyroxene. Mafic amphibolite formed by melting of amphibolitized subducted oceanic basalt, as proposed by Burnham (1979), would provide the requisite mineralogy. Subsequent partial melting of this material in the lower crust, perhaps in a subduction zone, could produce an intermediate magma which, by fractionation, could produce granitic magmas.

Tectonic framework.--Very little direct evidence is preserved in the Needle Mountains to reconstruct the tectonic framework at the time of granite magmatism. However, comparison of the Eolus batholith with other batholiths formed in more conspicuous, well-studied orogenic belts may help to speculate on the tectonic setting. The general relationship between granite magmatism and tectonism has been discussed by many authors (e.g. Miyoshiro, 1961; Zwart, 1967, 1969; Pitcher, 1979a, 1979b). The two major generalized types of orogenies likely to result in extensive granite plutonism are the Hercynotype (Zwart, 1967) and the Andinotype (Pitcher, 1979a). Hercynotype orogenies are the result of intracratonic collision and are characterized by ductile, compressive tectonism. Magmas produced in such belts usually show little compositional variation, lack significant mafic cognates, and are the result of anatexis due to crustal shortening and thickening. Granitic rocks from this environment are dominantly S-type. The uranium-bearing two-mica granites of southwestern Europe are the classical products of such an orogen.

According to Pitcher (1979a), I-type batholiths with wide ranges in composition, such as the Eolus batholith, are most likely to occur in Cordilleran-type, ocean-continent, plate-edge orogens. It is likely that batholiths formed from such Andinotype orogenies would evolve over considerable lengths of time. Material derived from partial melting of oceanic crust and/or mantle which underplates the continental crust might be episodically remobilized during periods of extra rapid subduction. The different partial melts of the Eolus batholith might be expressions of this, and the Eolus batholith itself might be the expression of reactivation of a subduction process that began during earlier tectonism.

Speculative petrogenetic model.--The following model for the genesis of the Eolus batholith is largely speculative, but is the explanation most consistent with available data.

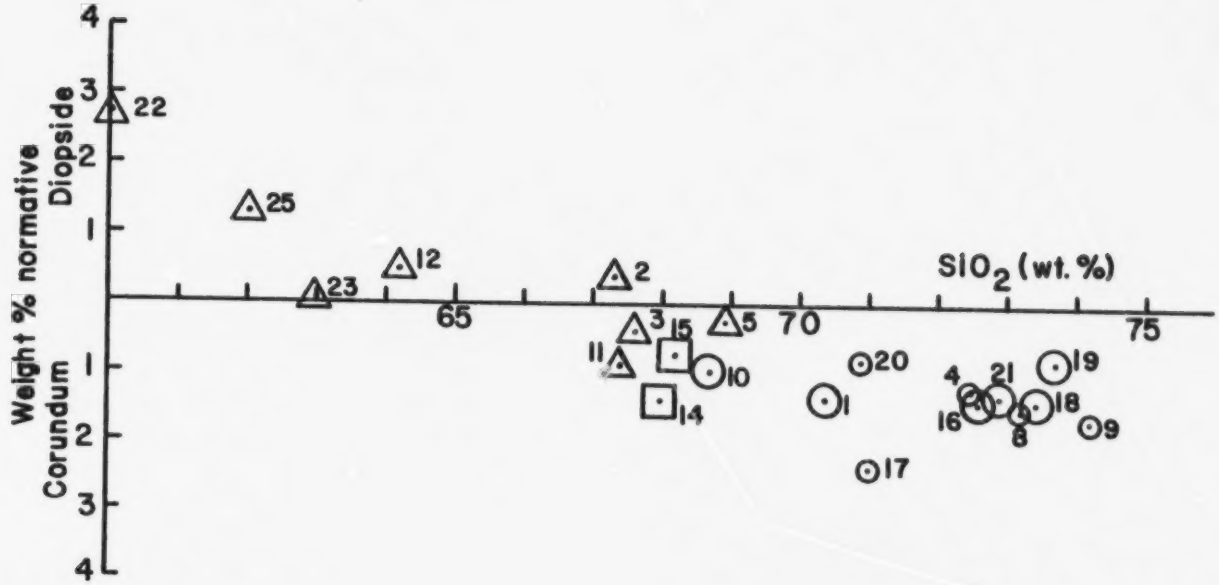

Figure 13. Variation diagram of normative diopside and normative corundum versus SiO_2. Triangles - hornblende-bearing Eolus Granite, large circules - coarse-grained hornblende-free Eolus Granite, small circles - aplitic Eolus Granite, squares - Trimble Granite.

In early Proterozoic time the area of the Needle Mountains was a plate margin between continental craton to the north and oceanic crust to the south. Episodic subduction along a Cordilleran-type margin resulted in underplating of the continental crust by igneous material. Burnham's (1979) model involving underplated mafic amphibolite derived by partial melting of amphibolitized subducted oceanic basalt appears to be a reasonable mechanism. Twenty percent partial melting would result in a mafic to intermediate calc-alkaline melt leaving a granulite residue comprised of clinopyroxene, calcic plagioclase, ilmenite, and magnetite. Melting of dehydrated, underplated crust is unlikely to occur without the introduction of heat and volatiles from elsewhere (Brown and Hennessey, 1978; Pitcher, 1979b; Burnham, 1979; Strong, 1980). Thus, melting of the initial source was likely triggered by hot mantle-derived material rising in a tensional environment, perhaps during periods of especially rapid subduction. Lamprophyre dikes found within the Eolus batholith, to be discussed later, are possible evidence of mantle involvement. The gabbros and monzodiorites of the Electra Lake Gabbro, of the same age as the Eolus Granite, may represent early products of such mantle-induced crustal melting. Some of the hornblende-bearing varieties of the Eolus Granite could be derived from this melt by crystal fractionation.

Trace elements indicate that all of the rocks of the Eolus batholith are not comagmatic, but may have been derived from sources that are in some way similar and perhaps genetically related. Successive magmas in the Eolus batholith become progressively more felsic and enriched in incompatible elements. This would require either progressively much larger degrees of partial melting of the same source, or remelting of derivatives of that source. Remelting of an earlier partial melt, perhaps such as the Electra Lake Gabbro, would result in an evolving trace-element chemistry consistent with that observed. It is possible that the Trimble Granite was derived from a basic cognate of the Eolus Granite.

The genesis of the Eolus batholith is of greatest importance in relation to the formation of the mineral deposits that it hosts. Uranium was deliberately ignored in the preceding discussions because of its high mobility and erratic behavior in chemical analyses. Uranium in the granites of the Eolus batholith will be discussed below.

Uranium Residence in the Granites

A major focus of this study was to investigate the possibility that granites of the Eolus batholith were source rocks for the uranium deposits which they host. Whether or not a granite may serve as a good source rock involves not only above normal uranium concentrations, but also the location of uranium within labile or readily leachable phases. The concept of granite fertility, first introduced by Marcel Moreau (Moreau and others, 1966), has a bearing not only on intragranitic deposits but on numerous other types of uranium deposits for which granites may have acted as sources. Detailed investigations have shown that granite fertility develops in the intragranitic deposits of France when uranium is redistributed during deuteric alteration from primary accessory minerals into labile phases such as uraninite (Cuney, 1978; Leroy, 1978). In the following section, the location or residence of uranium in unaltered rocks of the Eolus batholith will be discussed. In a later section the residence and remobilization of uranium (fertility) during alteration of the granites will be investigated.

Uranium in the hornblende-bearing granite.--Fission-track radiographs and, to a lesser extent, solid-state natural alpha-track detectors, were used to identify radioactive sources in the granites. Within the hornblende granodiorites, which contain an average of about 3.5 ppm uranium, tracks emanated almost exclusively from accessory minerals. Uranium occurs mostly within euhedral zircon grains and within small, anhedral grains of allanite. The allanite is commonly surrounded by anastomosing radiation fractures. Apatite grains, although often abundant, are only weakly radioactive. The few grains of sphene encountered were either nonradioactive or possessed only very low track densities. No uranium was associated with iron or titanium oxides, nor did any occur within microfractures.

I. R. Basham (Institute of Geological Sciences, oral commun., 1981) observed that widely scattered uraninite grains (which can contain more than 80 percent U) can account for most of the radioactivity in a granite. Such grains are unlikely to be encountered in random thin sections, but can be successfully located using rock slabs of about 100 sq cm or greater. However, radiographs of large surfaces of hornblende granodiorites failed to disclose any uranium phases other than those noted above. Whether or not the accessory minerals alone are sufficient to account for the total uranium content of the rocks can be tested by some simple mass balance equations, as shown by Basham and others (1979). Sample EG-2 contains 760 ppm zirconium, 0.47 percent normative apatite, and 3.6 ppm uranium. Assuming that zirconium comprises approximately one-half of a zircon (Deer and others, 1966), and assuming an average of 1,000 ppm uranium in zircon (Rogers and Adams, 1967), Sample EG-2 should contain approximately 0.15 percent zircon, accounting for 1.5 ppm uranium. Using an average content of 50 ppm uranium in apatite grains, as suggested by low-track densities, the apatite in the sample only accounts for about 0.24 ppm uranium, despite its greater abundance. It is not possible, without a quantitative analysis, to calculate the abundance of allanite due to its chemical complexity. However, allanite is somewhat less abundant by modal estimates than zircon, but is considerably larger in size and therefore probably constitutes as much or more of the volume of the rocks as zircon. Assuming 1,000 ppm uranium in allanite (an estimate based on fission-track density), allanite probably contributes as much or more to the overall radioactivity of the rocks as does zircon (1.5 ppm). Therefore the accessory minerals alone appear to be sufficient (although just barely) to account for the uranium content of the hornblende-bearing rocks of the Eolus batholith.

Uranium in hornblende-free Eolus Granite.--Uranium contents in the biotite monzogranites are much higher than the granodiorites, generally about 5-8 ppm for the samples analyzed, but ranging to as much as 16.9 ppm. Uranium detected in random thin sections of the monzogranites again occurs dominantly in zircon and allanite grains. In addition, some samples show weak tracks associated with iron oxides along cleavage planes in biotite, and several samples had minor uranium in magnetite, hematite, titanium oxides (altered sphene), and in microfractures. In general, however, the dominant uranium-bearing phases appeared to be the accessory minerals, and little evidence was seen for major uranium remobilization. One exception was Sample EG-21, an aplite, in which dense fission tracks were associated with oxidized margins and cleavage planes in biotite.

Quantitatively the biotite monzogranites contain less Zr and P_2O_5 than the granodiorites, which is expressed by lower abundances of zircon and apatite. Although the rocks contain somewhat more allanite, these minerals are not nearly sufficient to account for the higher uranium contents of the rocks. An approximately 125 cm^2 radiograph of Sample EG-18 using CR-39 plastic revealed four widely scattered uranium-rich minerals. Two of these were identified by SEM as uranothorites (up to 10 percent U according to Frondel and others, 1967), one was a high thorium uraninite, and the other may have been a grain of thorianite (up to about 45 percent U). In addition, a mineral in Sample EG-8 was tentatively identified by qualitative SEM spectroscopy as chevkinite ($(Ce,Y,Ca,U,Th)_2(Ti,Fe,Mg)_2(Si,Al)_2O_{11}$; U = 2.3 percent, Th = 18.4 percent). Despite their low abundances these minerals can easily account for the bulk of the radioactivity in the monzogranites.

Uranium in the Trimble Granite.--Uranium residence in the Trimble Granite is very similar in character to the monzogranites. Zircon grains are generally smaller and hence represent a lower total volume percentage, whereas allanites tend to be somewhat larger. Allanites are also commonly rimmed by nonradioactive epidote. Uranium occurs somewhat more commonly in hematitic margins of chloritized biotite than it does in Eolus monzogranites. Again, the major contributors to the overall uranium content of the Trimble Granite (approximately 15 ppm average) are widely scattered grains of uraninite and uranothorite. Uranium residence in the Trimble Granite will be discussed again in a later section on wall-rock alteration, where the questions of granite fertility and uranium mobility will be addressed.

MAFIC DIKES

There are several dark green lamprophyre dikes that intrude the Eolus Granite. One clearly cuts rocks of Late Tertiary age and will be discussed later. There are two other dikes of indeterminate age and of different composition than the Tertiary dike. One occurs on*the saddle below Jupiter Peak and the other is west of, and presumably extends under, Hazel Lake. These dikes consist of a few relict grains of potassium feldspar, biotite, and colorless diopside in an intensely altered matrix of chlorite, serpentine, and sericite. Numerous stringers of secondary calcite cut the rock. The dikes resemble the minette or vogesite dikes described by Cross and others (1905) which crop out throughout the Needle Mountains. These minette dikes are not known to transect rocks younger than Upper Cambrian. It is not known whether the lamprophyre dikes of the study area are genetically related but, if so, then they must be Middle Cambrian or older in age.

The association of lamprophyre dikes within (but later than) granitic plutons is not uncommon (Hyndman, 1972). The association between intragranitic uranium deposits and lamprophyres is also common, and in many districts in France there appears to be a direct correlation between presence of lamprophyres and grade of uranium mineralization (Moreau and Ranchin, 1973; Carrat, 1974). Lamprophyres are believed to be derived from alkaline olivine basalt (Hyndman, 1972), indicating upper mantle involvement. Assimilation of alkalis and volatiles from granitic or sedimentary rocks could account for the typically high alkali content and alteration of lamprophyres. Carrat (1975), in noting the lamprophyre dikes in the Morvan district of France, suggested

that mantle-depth late-orogenic fracturing allowed magmas of lamprophyre composition to ascend. Since CO_2 appears to have a strong control on uranium mineralization in at least one district in France (Poty and others, 1974), mantle degassing through these fractures may explain the proximity of lamprophyres to uranium mineralization. The lamprophyres in the study area may indicate mantle input; whether or not they are evidence of passageways for mantle-derived CO_2 is only speculative. The role of CO_2 will be discussed later.

CHICAGO BASIN STOCK

In Chicago Basin, in the northwestern part of the study area, there is a small hypabyssal composite stock which intrudes the Eolus Granite. The Tertiary Chicago Basin stock has been highly altered to bright shades of yellow, red, and brown, making it readily visible from the air and in the field. The stock is subcircular in outline and is approximately 1050 m in its east-west dimension, and 790 m from north to south. Parts of the eastern and southern contacts with the Eolus Granite are well exposed, sharp, and dip steeply inward toward the stock. However most of the stock is below timberline and often covered by vegetation, obscuring much of the contact. Three sharply dissected drainages provide most of the exposure.

Although alteration makes the original rock textures difficult to discern, the stock consists of two principal lithologies. There is an older body of highly altered granite porphyry, and a younger body of variably altered rhyolite porphyry which intrudes the central and southern part of the older body. The fission-track method yields ages of 9.0 ± 0.9 m.y. for the older body and 10 ± 1.1 m.y. for the younger body (Schmitt and Raymond, 1977). The relative ages of the two bodies are clearly established by field relationships; the discrepancy in absolute ages is well within the analytical error and is highly suggestive that the two intrusions were closely related temporally.

In addition to the stock itself, there are several small dikes outside the stock which are similar in composition to the granite porphyry. There is also a small dike of mafic composition within the stock.

Older Intrusive Body

The older intrusive body consists of several varieties of granite porphyry. These vary gradationally from an apparent chilled margin near the Eolus Granite contact, inward toward the interior of the stock. Near the margins the porphyry contains relatively few partially corroded quartz phenocrysts in a microcrystalline groundmass of mostly quartz and sericite. Flow structure is locally developed. Towards the interior of the stock, quartz phenocrysts become more abundant, and the grain size of the groundmass increases to a fine-grained mixture of quartz and sericite after feldspar. Possible relict feldspar phenocrysts are suggested by small pockets of sericite. Kaolinite and/or dickite were identified in a few localities. No flow structure was obvious near the interior of the older body. No mafic minerals were observed in any of the older rocks.

Alteration of the older body of the Chicago Basin stock was both pervasive and intense. Sericite is the dominant alteration mineral, although kaolinite and/or dickite are locally abundant, particularly in the western part of the older body. In a few localities the rock has been bleached and silicified. Disseminated pyrite is abundant throughout the intrusion.

Schmitt and Raymond (1977) identified 1Md, 1M, and 2M polytypes of sericite, which supposedly indicate increasing temperatures of alteration. The most abundant polytype is 1M, although in the western part of the body 2M sericite predominates and is associated with kaolinite, indicating more intense hydrothermal activity.

Near the eastern contact between the younger and older bodies there are several inclusions of older porphyry in the younger body. These inclusions are the least altered examples of the older porphyry, suggesting that alteration was less intense at depth, and also giving a better indication of the original texture and composition of the rock. These inclusions consist of medium- to coarse-grained, subhedral to euhedral, quartz and sanidine phenocrysts in a fine-grained groundmass of quartz and potassium feldspar. There are a few plagioclase grains which appear to be primary, although much of the minor plagioclase in the inclusions is interstitial or occurs in microveinlets, and is probably due to albitization.

Whole-rock analyses of representative samples are shown in table 3. The original rocks were apparently high in SiO_2 and K_2O, and relatively poor in Na_2O, MgO, and CaO. Although it is difficult to make inferences based on only a few samples, comparison of the least altered and most altered samples suggests that alteration caused slight enrichment in SiO_2 and K_2O, and strong depletion in Na_2O, CaO, and Al_2O_3. Such changes in composition are consistent with sericitization of feldspar.

Brecciation is common throughout the older intrusive body. In the northwestern part of the body, breccia fragments up to 3 cm in diameter, consisting of altered porphyry, suggest either shearing or the presence of a breccia pipe. In the southeastern part of the intrusion there are several fragments of quartzose conglomerate up to 1 m or more in diameter. These fragments, which consist mostly of very fine grained to cobble-size clasts of quartz and quartzite, were considered by Cross and others (1905) to be xenoliths of the Uncompahgre Formation. Schmitt and Raymond (1977) considered it unlikely that the Uncompahgre Formation should underlie the Eolus Granite in this area and also believed that the breccia fragments more closely resemble conglomerates of the Cambrian Ignacio Formation. Projecting from the nearest outcrops of Cambrian rocks on Mountain View Crest and Lime and Stag mesas, it is estimated that the current level of exposure is 700-800 m below the Cambrian erosion surface at the time the stock was emplaced. There is no way of accurately estimating what the thickness of Paleozoic or younger rocks was at that time, but because of considerable Laramide uplift and accompanying erosion it was probably fairly thin. This estimate of the depth of emplacement probably corresponds to the depth of mineralization in the area, and will be considered in more detail later.

Table 3.--Chemical analyses of the Chicago Basin stock

[Tiy- younger body, Tio - older body. Oxides in wt. percent. Mo, F, U, and Th in ppm.]

	CB-12 Tiy highly altered	CB-4 Tio- least altered	CB-13 Tio- most altered	VB-57 dike of Tio
SiO_2	88.2	74.0	77.8	74.9
Al_2O_3	7.55	14.3	12.4	13.0
Fe_2O_3	0.41	0.81	0.48	0.79
FeO	0.20	0.09	0.27	--
MgO	<0.1	0.2	0.4	0.63
CaO	<0.02	0.12	0.02	<0.02
Na_2O	<0.2	2.7	<0.2	0.33
K_2O	2.07	5.99	6.10	6.91
H_2O+	1.17	1.20	1.47	--
H_2O-	0.04	0.26	0.10	--
TiO_2	0.13	0.28	0.23	0.23
P_2O_5	<0.1	<0.1	<0.1	<0.05
MnO	<0.02	0.03	<0.02	<0.02
CO_2	<0.01	<0.01	<0.01	--
F	0.06	0.02	0.12	--
Mo	16	<5	<5	--
U	0.83	7.0	6.10	3.70†
Th	2.8	19.5	12.6	10.5†
Total	100.28	100.11	99.72	96.88

Analyses by USGS, Major oxides by x-ray spectroscopy, analysts: J. S. Wahlberg, J. Taggart, J. Baker. U and Th by delayed neutron activation, analysts: R. Bies, H. T. Millard, Jr., B. Keaten, M. Coughlin, S. Lasater. FeO, H_2O, CO_2 and F by wet chemistry, analysts: H. Neiman, F. Newman. Mo by optical spectroscopy, analysts: P. Briggs and D. Leland.

* Intrumental neutron activation analyses by Nuclear Division of Union Carbide Corporation, Oak Ridge, Tennessee.

Younger Intrusive Body

The younger intrusive body of the Chicago Basin stock is somewhat more resistant to erosion than the older body, and as a result stands out as an elliptical knoll mostly within the older body. The contact between the younger and older bodies dips inward towards the younger body at 75-80°. The relative ages of the two bodies is established by the inclusions as described earlier.

The younger body consists of a relatively homogeneous rhyolite porphyry. It contains medium- to coarse-grained subhedral phenocrysts of sanidine, oligoclase, partially corroded quartz, biotite, and relict sphene. The sphene is highly poikilitic and its presence is largely inferred by its relict form and alteration to leucoxene. The groundmass consists of quartz, variable amounts of incompletely altered biotite and feldspar, and the alteration products chlorite and sericite. Kaolinite or dickite are present locally in minor amounts. In most samples the groundmass displays flow structure.

The younger rocks are much less fractured than those of the older body, and alteration is generally considerably less intense. The principal alteration products are chlorite and sericite from biotite, and sericite or occasionally kaolinite from plagioclase. The sericite is mostly the 1Md variety, which indicates lower temperature alteration than do the 1M or 2M polytypes of the older body (Schmitt and Raymond, 1977). The fact that the younger body is less altered indicates that the alteration of the older body probably occurred before the emplacement of the rhyolite porphyry.

Dikes of Granite Porphyry

There are several dikes in both the Eolus and Trimble granites which appear to be localized along fractures radiating from the Chicago Basin stock. One small body occurs at the crest of Columbine Pass; another follows the Aztec vein; and one, which displays very conspicuous flow structure, occurs in Vallecito Basin along the Vallecito Fault. None of the dikes transect the stock on the surface.

Texturally and mineralogically the dikes resemble the older intrusive body of the Chicago Basin stock. Chemical analyses in table 3 show that the dikes (Sample VB-57) are compositionally very similar to the granite porphyries.

Late Dike

A small dike of dark-green porphyry, as much as 6 m in width, cuts both the older and younger bodies in the eastern part of the Chicago Basin stock. The dike consists of medium-grained subhedral to euhedral phenocrysts of quartz, sanidine, plagioclase, and pyroxene. The rock sustained weak propylitic alteration resulting in a minor amount of secondary chlorite and calcite.

The mafic character of the dike and its location suggest that it might be a less altered extension of the mafic dikes described earlier. However, not only do their mineralogies differ, but there are distinct differences in chemical composition as shown in table 4.

Uranium Residence

The Chicago Basin stock is a radiometric low, compared to surrounding granites, both in ground and airborne scintillometer surveys. A major question is whether this is due to low initial magmatic concentrations or due to depletion during alteration. If the low uranium contents are due to depletion, then the Chicago Basin stock may have been a possible source for the uranium deposits in the area. Radiographic investigations of uranium residence can provide evidence to help resolve this question.

Uranium in the older intrusive body.--Fission tracks from samples of the older body of the Chicago Basin stock are not, in contrast to the Precambrian granites, commonly derived from point sources. Zircon, allanite, and a few very small (<10μm) thorite grains are minor contributors; however, most of the uranium is fairly uniformly distributed throughout the rocks. It is very finely disseminated and no specific mineral host can be identified. In a few samples uranium appears to show a slight association with the phenocrysts. Track densities are similar to those produced by a 10 ppm glass standard, indicating that the disseminated uranium is easily sufficient to account for the total uranium content of the rocks. Despite the highly altered nature of the older intrusive body, there is little evidence to suggest uranium remobilization. Uranium shows no particular affinity for hematite-rich areas in the rocks, despite the fact that iron oxides will generally trap uranium during remobilization. Uranium also does not occur in microfractures, some evidence of which would be found if appreciable uranium mobilization had occurred. Thus, the older body of the Chicago Basin stock does not appear to have acted as a significant source of uranium.

Uranium in dikes of granite porphyry.--Dikes of similar composition to the older intrusive body show somewhat more evidence of uranium remobilization. Fission tracks of low-density emanate from uranium in microfractures, although much of the uranium is uniformly disseminated through the rocks, with slight differences in density with textural variations resulting from flow layering. Again the uranium shows little affinity for iron-rich areas, suggesting that remobilization was minor. It is quite possible that the uranium in the microfractures was derived by leaching from adjacent Eolus Granite.

Uranium in the younger intrusive body.--Uranium in the rhyolite porphyry does show considerable evidence of remobilization. There is a very minor association of uranium with zircon, epidote (not allanite), and sericite, but most uranium occurs within hematite in microfractures. The uranium content of the rhyolite porphyry is much lower than the granite porphyries, but since it is much less altered, this low content cannot be explained by depletion. The lower uranium concentrations could be explained by depleted volatile content, and perhaps by more rapid cooling of the rhyolite which would prevent incorporation of uranium into the fabric of the rock, causing it to accumulate in fractures.

Table 4.--Chemical analyses of mafic dikes

[Analyses of Tertiary late dike from Schmitt and Raymond (1977). Analysis of Sample VB-31 by USGS. Major oxides by X-ray spectroscopy, analysts: J. S. Wahlberg, J. Taggart, J. Baker. FeO, H_2O, and CO_2 by wet chemistry, analysts: H. Neiman, F. Newman]

	Tertiary late dike	Sample VB-31 (p€?)
SiO_2	54.4	46.0
Al_2O_3	12.3	14.1
Fe_2O_3	3.5	4.65
FeO	3.5	8.35
MgO	5.1	3.6
CaO	7.0	6.55
Na_2O	2.2	1.3
K_2O	3.2	4.12
H_2O+	2.7	3.73
H_2O-	0.98	0.30
TiO_2	1.4	3.18
P_2O_5	0.55	0.4
MnO	0.26	0.12
CO_2	2.8	4.31
Total	99.89	100.71

Despite the fact that uranium in both bodies of the Chicago Basin stock is not tied up in refractory minerals and should therefore be labile, it does not appear to have moved appreciably. When uranium did move, as perhaps in the rhyolite porphyry, it did not move in significant amounts. Although the Chicago Basin stock may have been a contributor to the uranium deposits of the area, it is highly unlikely that it was the principal source rock.

LOCAL STRUCTURE

There is very little vegetation covering the study area and, as a result the extensive jointing, fracturing, and faulting of the granites are well exposed. There are at least six prominent sets of structural trends. These vary in dominance from one part of the area to another, as can be seen by the strike frequency distribution diagrams on figure 14. Two sets of intersecting steeply dipping fractures dominate the area; one strikes roughly north south and the other approximately east west. This rectilinear joint pattern probably developed in response to cooling of the granites. On Silver Mesa a few granite pegmatites, generally less than 3 cm in width, were emplaced within fractures concordant with these trends, suggesting that the joints formed during or shortly after emplacement of the Precambrian granites.

Average strikes and strike frequencies of the two sets vary within the study area. In the Silver Mesa area, most joints strike approximately N. 5 W. and dip within 10° of vertical. The east-west fractures are subordinate, generally striking N. 70 W. with nearly vertical dips. Much of the large Trimble Fault discussed later follows this trend. In the northern part of the area, the east-west fractures predominate, with strikes closer to N. 90 W. The north-south joint set also varies somewhat from Silver Mesa, with strikes slightly east of north.

Many of the joints making up the rectilinear pattern show evidence of later fracturing or even faulting. Slickensides are present on many fractures, although displacement was probably minor. A pegmatite cut by a N. 5 W. structure on Bullion Mountain was displaced vertically less than 3 m, the east side downdropped relative to the west. In several fractures on East Silver Mesa, vertical slickensides were overprinted by horizontal slickensides, indicating at least two periods of movement.

In addition to rectilinear joints, there are a number of conjugate joint sets particularly visible in the southern part of Silver Mesa. Conjugate joints are believed to form in response to compression; those on Silver Mesa probably yielded to north-south compressional forces sometime after the formation of N.S.-E.W. cooling joints.

Another structural set, mostly restricted to North Silver Mesa and Florida Mountain, consists of the Bullion Fault and minor structures parallel to it (pl. 2). These features strike approximately N. 70 E. and have vertical to near-vertical dips.

Although most of the visible joints and fractures in the study area dip steeply, there are at least two sets of shallow-dipping structures. Near-horizontal to horizontal sheeting is common within the Trimble Granite. These

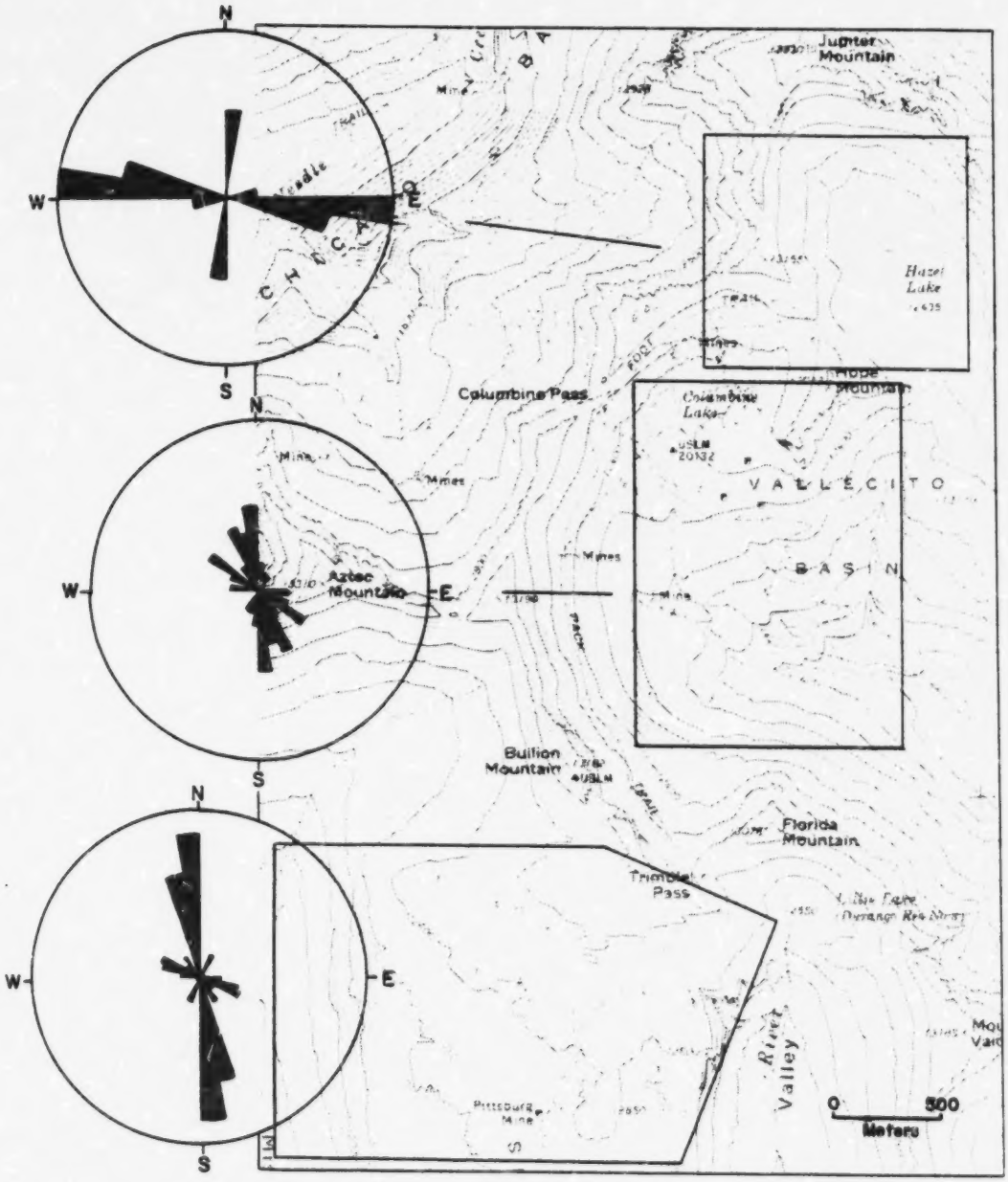

Figure 14. Distribution of the strikes of vertical or near vertical joints. Circumference of each circle represents 40 percent of total number of joints counted in outlines areas. Width of each ray is 10°; length of each ray represents percentage of joint strikes within 10° interval.

fractures are never the hosts of alteration or mineralization, show no evidence of movement, and therefore probably post-date all other structural features by a considerable length of time. They may be due to stress release during erosional unloading.

The largest structural features in the study area are the Trimble and Bullion faults (pl. 2). These are large breccia zones which dip vertically or steeply to the north. Despite widths often exceeding 30 m, there is little evidence for large displacement on these faults. Approximately 3 km west of the study area the Bullion-Trimble Fault system cuts through Paleozoic sediments. Projecting the offset of the basal Cambrian Ignacio Quartzite across the fault, there appears to have been 60-90 m of vertical movement. The northern block was the active downdropped block, making the structures normal faults. No evidence of vertical movement was seen within the granites themselves.

Left-lateral movement of approximately 6 m along the Bullion Fault is indicated by offset fractures and pegmatites of Trimble Granite. Although slickensides along the Trimble Fault east of Trimble Pass indicate horizontal movement, no direct evidence was seen for the amount of strike-slip displacement on the Trimble Fault. However, a N10W structure at Trimble Pass drags about 3-5 m to the east as it approaches the Trimble Fault from the north, indicating left-lateral movement on the Trimble Fault as well.

Perhaps the most important structural features of the study area in terms of hosting mineralization are a set of roughly parallel, moderately-dipping fractures which crop out on the north face of Florida Mountain (pl. 2). They strike roughly northwest and dip between 11 and 45° to the southwest. The Cornucopia, Upper Johnson Creek, and Lower Johnson Creek veins, discussed later, fill these fractures and contain most of the high-grade uranium in the area. Schmitt and Raymond (1977) believed these fractures to be exfoliation joints due either to regional uplift of the Needle Mountains, local upwarp caused by the emplacement of the Chicago Basin stock, or to erosional unloading. However, the fractures do not transect, and appear to originate at, the Bullion Fault and most likely formed by complex movement between the Bullion and Trimble Faults.

There are a number of fractures that are discordant with any regional trends. In Vallecito Basin, there are a number of short, discontinuous fractures with essentially random orientations. These may have been caused by the shallow intrusion of a cupola of an underlying pluton, further evidence of which is discussed in later sections. At least one fracture, the Vallecito Fault, appears to radiate directly from the Chicago Basin stock and was probably formed by its emplacement. The Aztec vein also appears to be localized along a fracture that radiates from the Chicago Basin stock. However, it is also concordant with the north-south fracture set, and is therefore of debatable origin.

It is most unlikely that all of the structures in the Needle Mountains district formed by the same mechanism. However, with the exception of the exfoliation sheets, all types of structures show some evidence of mineralization. Thus, despite a diverse structural history, all of the structural trends were probably opened or reopened at approximately the same times.

The earliest event was the formation of the N.S.-E.W. joint sets. Precambrian in age, these probably formed in response to cooling of the granites. Other joint sets on trend with the Trimble and Bullion Faults may have developed at this time and formed the original planes of weakness for later faulting. However, the area was tectonically quite stable after the intrusion of the Trimble Granite during the remainder of Precambrian time, and it is unlikely that deformational movement occurred during that time.

Two major tectonic events, widely spaced in time, affected the Needle Mountains. Either the Paleozoic uplift of the ancestral Uncompahgre highlands, or the early Tertiary Laramide orogeny could have caused the movement forming the Bullion, Trimble, and other faults. However, the tectonic styles of the two events were quite different. During the uplift of the Ancestral Rockies, the Needle Mountains were an integral part of the northwest-trending Uncompahgre highlands. During the Laramide, the Needle Mountains were centrally domed, with principal uplift occurring approximately 9-13 km north of the study area. Although during any tectonic event, adjustment and readjustment of structural blocks can cause diverse stress and strain orientations on a local scale, the principal north-south forces indicated by most of the structures in the study area are more consistent with Laramide activity than with the earlier event.

Although mineralization will be discussed in a later section, the deposits in the Needle Mountains district are structurally controlled and cannot be totally ignored here. Two observations in particular must be considered in the structural history: 1) most high-grade uranium occurs in a fault block between the Trimble and Bullion Faults, and 2) a considerable amount of open-space was present during mineralization.

The Cornucopia, Upper Johnson Creek, and Lower Johnson Creek veins, which host most of the higher grade uranium in the area, occur in shallow-dipping fractures in a wedge-shaped fault block between the Bullion and Trimble faults. Field evidence suggests greater displacement on the Bullion Fault than the Trimble Fault. Differential vertical movement, coupled with the slight northerly dips of the faults, could create secondary tension vectors. These might cause open gash fractures of the same orientation as the uranium veins.

As mentioned earlier, the abundance of fractures belonging to a particular joint set varies within the area. East-west fractures predominate over north-south fractures in the northwestern part of the area, whereas the converse is true in the southern part of the area. As can be seen on figure 14, the dominant trends intersect in the northwestern part of the area. This is where the Chicago Basin stock is located, and it is logical to assume that the stock was localized by the major intersection of joints.

Mineralization, presumably related to Tertiary intrusion, shows a distinct preference for north-south-trending fissures in the southern part of the area, and for east-west fractures in the northeastern part of the area. This might be explained by forceful injection of a Tertiary pluton, part of which is exposed as the Chicago Basin stock. Such an intrusion would cause radiating compression, closing east-west fractures south of the stock and opening them to the east.

A three-stage history is proposed for the structural preparation of the Needle Mountains district for mineralization. First, intersecting joint sets formed during Precambrian time creating planes of weakness for later fracturing and intrusion. Laramide deformation then enhanced previous lines of weakness, creating fluid passageways by faulting and perhaps, in the case of the Florida Mountain block, by creating new fractures. Some of this activity may have dated back to the late Paleozoic Uncompahgre uplift. Finally, forceful injection of a Tertiary pluton opened or further opened many of the fractures for mineralization.

SURFICIAL GEOCHEMISRY

During 1967 and 1968 Schmitt and Raymond (1977) collected approximately 200 outcrop samples of rocks from veins, wall rock, and fracture zones in the Needle Mountains district. These samples were analyzed for a number of metals by semiquantitative spectrographic and chemical methods. These analyses, which are tabulated in Steven and others (1969, table 10), will be used here to characterize some of the geochemical relationships of the study area.

A number of metals occur in locally anomalous amounts within the study area, including Ag, As, Au, Ba, Bi, Cd, Mo, Pb, Sb, Sn, U, W, and Zn. The areal distributions of metal anomalies are shown on figures 15-17. Anomalous values were selected by relative values and ranges of abundances within the Needle Mountains district; no attempt was made to statistically establish threshold values. Thus, concentrations considered anomalous might be low compared to other regions, and concentrations considered low within the study area might be anomalous in other regions. The distribution patterns are also influenced by the types of samples (e.g., vein vs. wall rock) as well as sample density. Sample locations, shown in Steven and others (1969, pl. 2) and Schmitt and Raymond (1977, pl. I), are more dense in Chicago Basin and are rather sparse in the southern part of the study area, influencing the relative accuracy of certain parts of the maps. Although the distribution patterns shown on figures 15-17 can only be considered approximations to the actual surface distribution of metals, together they are effective visualizations of the geochemical character of the area.

Distribution of Metals

Molybdenum occurs in anomalous quantities throughout most of the area. It occurs in highest concentrations within the Chicago Basin stock, where it can be found as megascopic flakes of molybdenite in the altered rhyolite and granite porphyries. Elsewhere in the study area it occurs in altered wall rock adjacent to quartz veins as well as an accessory mineral in pegmatites. Molybdenite was only rarely found associated with uranium mineralization and was never found directly associated with intense base-metal mineralization.

Lead and zinc also are very widely distributed. They occur in highest concentrations within Vallecito Basin. Lead and zinc will be discussed further below under zoning.

Silver, gold, copper, and antimony appear to constitute a suite of metals with similar distribution patterns. Silver and copper have nearly identical

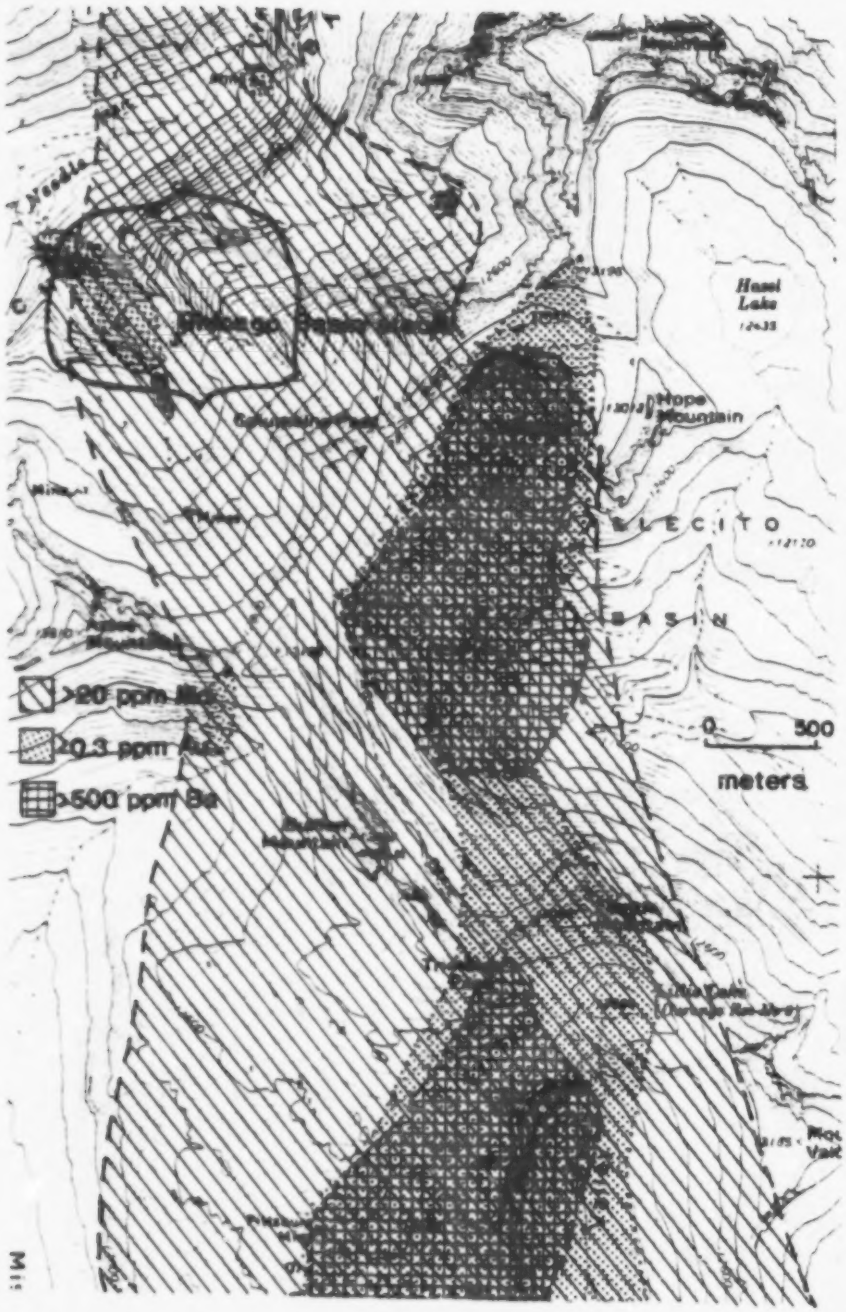

Figure 15. Areal distributions of anomalous Mo, Au, and Ba in surface rock samples. Data from Steven and others (1969).

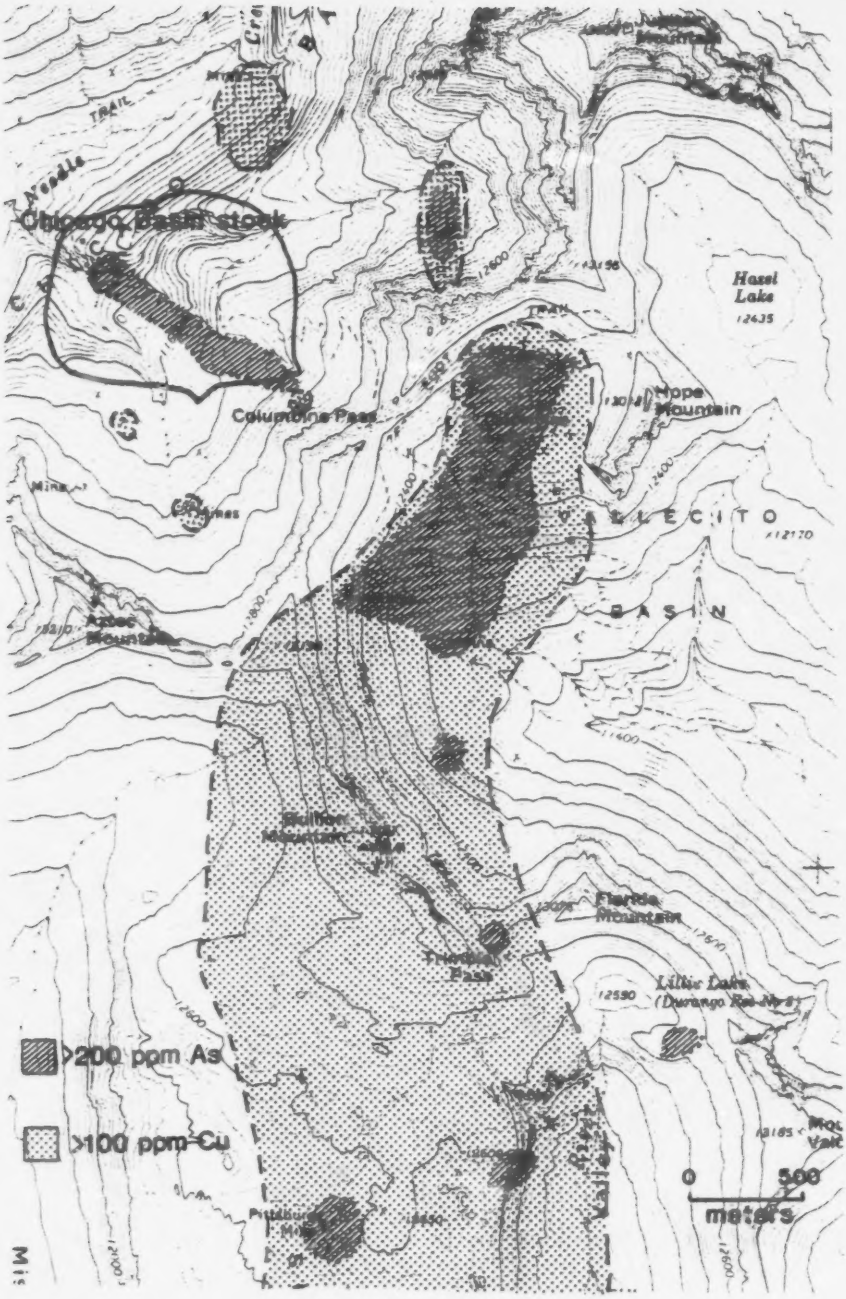

Figure 16. Areal distributions of anomalous Cu and As in surface rock samples. Data from Steven and others (1969).

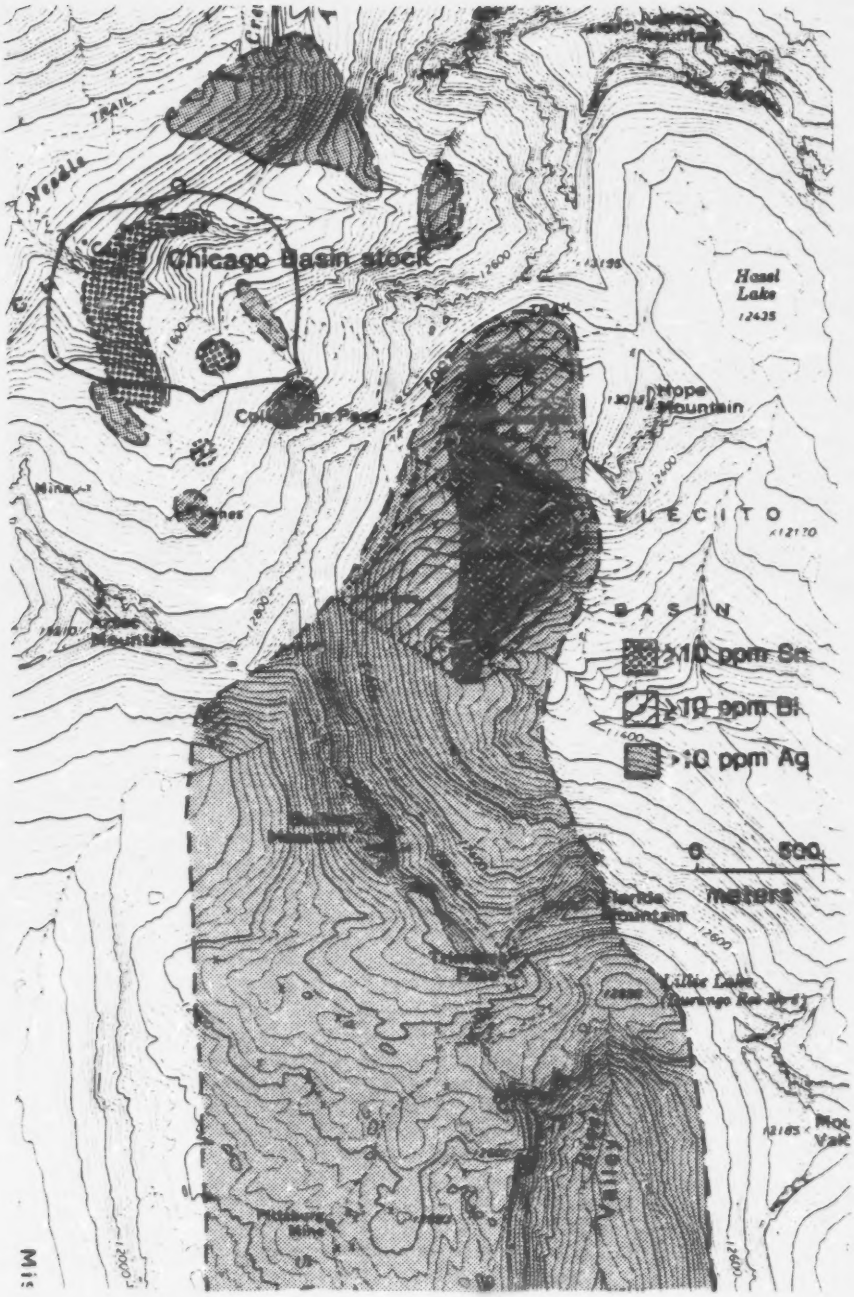

Figure 17. Areal distributions of anomalous Ag, Sn, and Bi in surface rock samples. Data from Steven and others (1969).

areal patterns. Both are broadly distributed, occurring mostly in a wide band from Vallecito Basin to south of the study area, as well as within a few scattered anomalous areas. Both metals occur in greatest quantities within Vallecito Basin. Copper occurs in chalcopyrite and tetrahedrite. No primary silver minerals were identified; it probably occurs in tetrahedrite or galena.

Gold is weakly anomalous over an area similar to that of silver and copper, although it is slightly more restricted in breadth. There is also a weak, but fairly broad gold anomaly within Chicago Basin.

Antimony occurs in greatest abundance in Vallecito Basin. The distribution of antimony, which is not shown in the figures, probably follows that of copper as both metals occur in tetrahedrite. Several very small fibers identified optically as jamesonite (or a mineral of similar habit) were found near Chicago Basin (Sample VB-6, pl. 2).

Anomalous barium roughly coincides with the distribution patterns of silver, gold, and copper; however, it is only weakly anomalous in Vallecito Basin. The strongest barium anomalies occur in the southern part of the area, where in several localities, particularly Crystal Valley, barite is a dominant gangue mineral. Most barium in Vallecito Basin occurs in psilomelane, which is quite abundant there.

Arsenic, bismuth, and tin constitute what might be considered another suite of metals in that they have similar and more restricted areal distributions. Anomalous arsenic is limited mostly to Vallecito Basin and Chicago Basin; however, the high detection limit of emission spectrography (200 ppm) may mask a broader distribution. Primary arsenic usually occurs within either arsenopyrite or tetrahedrite. Since no arsenopyrite was identified in the study area and because tetrahedrite is more widely distributed than the margins of the arsenic anomalies, it is likely that either arsenic was restricted in its mobility or is in fact more widely distributed than its pattern suggests. Enargite, a copper sulfarsenide, occurs in sparse quantities in Vallecito Basin.

High bismuth concentrations are restricted almost exclusively to Vallecito Basin. Samples containing high bismuth generally contain galena, in which bismuth probably occurs as inclusions of schapbachite ($AgBiS_2$) or native bismuth. However, anomalous bismuth is much more restricted than is lead, indicating limited mobility.

Anomalous tin occurs essentially only within part of Vallecito Basin and within the borders of the Chicago Basin stock. In Vallecito Basin, anomalous tin occurs in samples rich in chalcopyrite and tetrahedrite. In Sample VB-24 (same locality as CB-225 in Steven and others, 1969), the mineral stannite (Cu_2FeSnS_4) was identified by X-ray diffraction. However, in most samples no tin mineral was identified.

Zoning

In an ideal hydrothermal environment, changes in physicochemical conditions may cause the sequential deposition of metals, both in time and

space, in concentric zones about an igneous center. In the Needle Mountains district, there is no ostensible pattern of zonation about the obvious intrusive center, the Chicago Basin stock. However, the anomaly maps of figures 15-17 do not show relative strengths of anomalies, nor do they discriminate between types of samples (e.g, vein vs. wall rock). These biases can be partially removed by contouring metal ratios.

The ratios of Zn/Pb, Pb/Sn, and Ag/Au are shown on figures 18-20. Lead appears to increase relative to zinc outward from three apparent principal centers--Chicago Basin, Vallecito Basin, and slightly north of Vallecito Basin. This relationship is substantiated in the field by relative proportions of galena to sphalerite.

The contours for silver and gold are rather broad and diffuse, partly because of a bias toward silver due to its greater range and variability of concentration. However, again zoning appears to center about both Chicago and Vallecito Basins.

The closest approximation to the centers of zonation would be expected by plotting a more mobile metal (Pb) versus the most restricted metal (Sn). The Pb/Sn contours on figure 19 again point to centers of zonation within the two basins.

The surface outcrops of anomalous uranium within and just outside the study area are shown on figure 21. The distribution of uranium appears to form an arcuate band, suggesting that uranium is also zoned relative to an intrusive center. However, the anomalies are too few to indicate, if zoned, whether they are concentric about the Chicago Basin stock, as suggested by the solid lines of figure 21, or about Vallecito Basin, indicated by the dashed lines, or some combination of both.

Discussion

The ratios of Zn/Pb, Ag/Au, and Pb/Sn, as well as the distribution of anomalous concentrations of Sn, Bi, and U suggest a sequence of zones centered principally in Vallecito Basin and, to a lesser extent, in Chicago Basin. The zones, from the centers outwards, are:

Mo and Sn
Bi and As
Cu, Au, Sb
U
Zn and Cd
Pb and Ag

The zones are not strongly defined and overlap considerably, but appear to represent the surface intercepts of regions where particular metals are concentrated relative to other metals. The sequence represents only a spatial relationship and is not a paragenetic time sequence. This can be explained in part by varying mobilities, but might also be a function of different sources. For example Sn, Bi, and Mo are probably of magmatic origin and appear to eminate from within the centers of the zones. Uranium and lead, which may well be derived from the country rock, occur in outer zones.

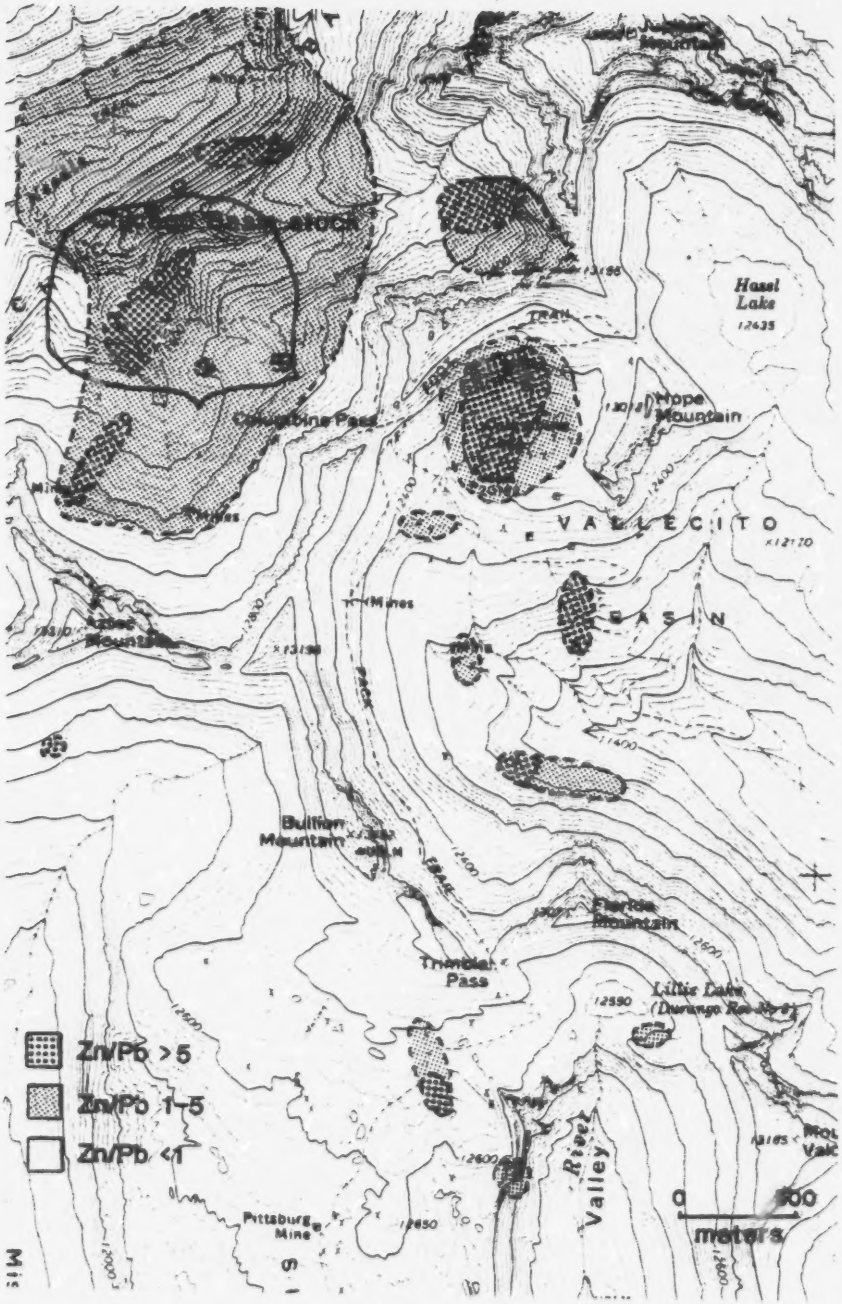

Figure 18. Contour map of Zn/Pb in surface rock samples. Data from Steven and others (1969).

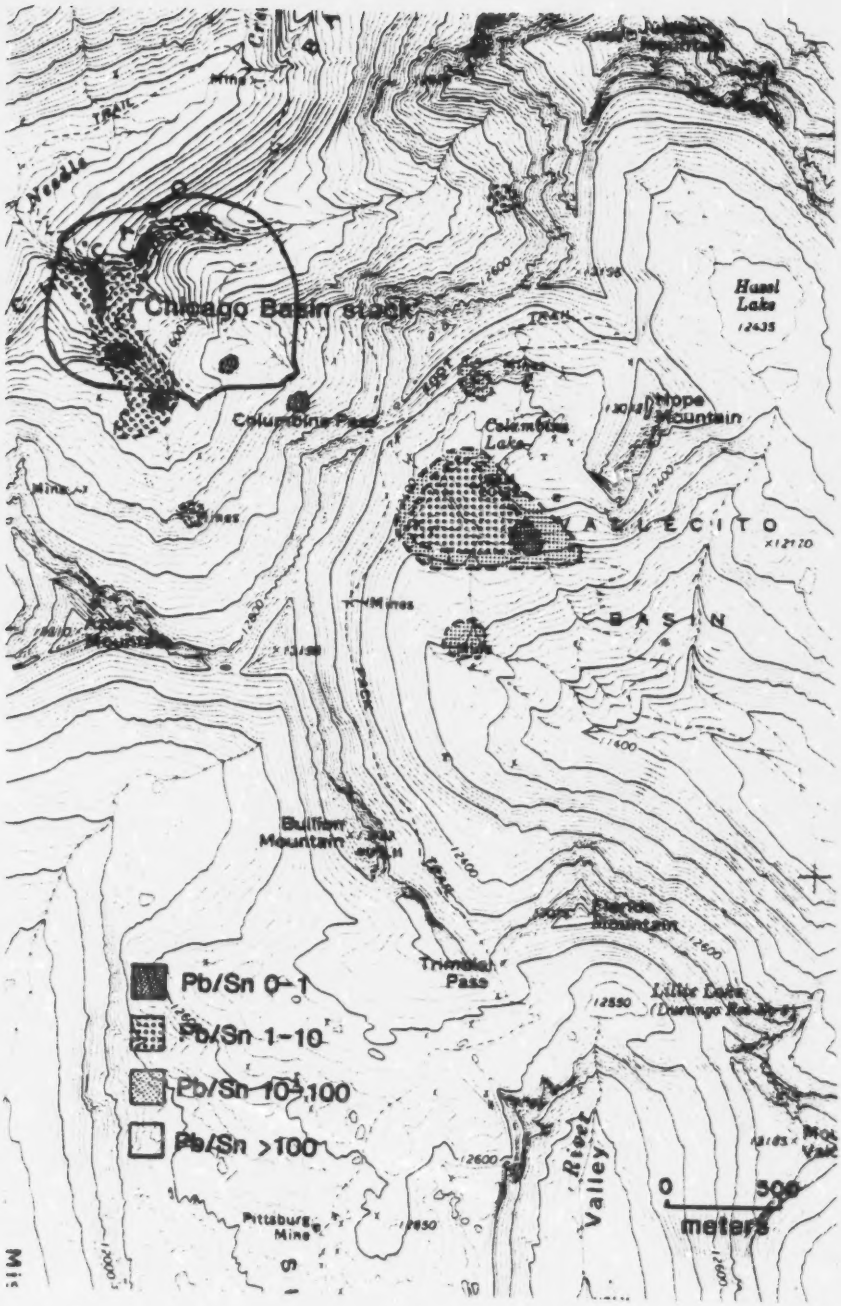

Figure 19. Contour map of Pb/Sn in surface rock samples. Data from Steven and others (1969).

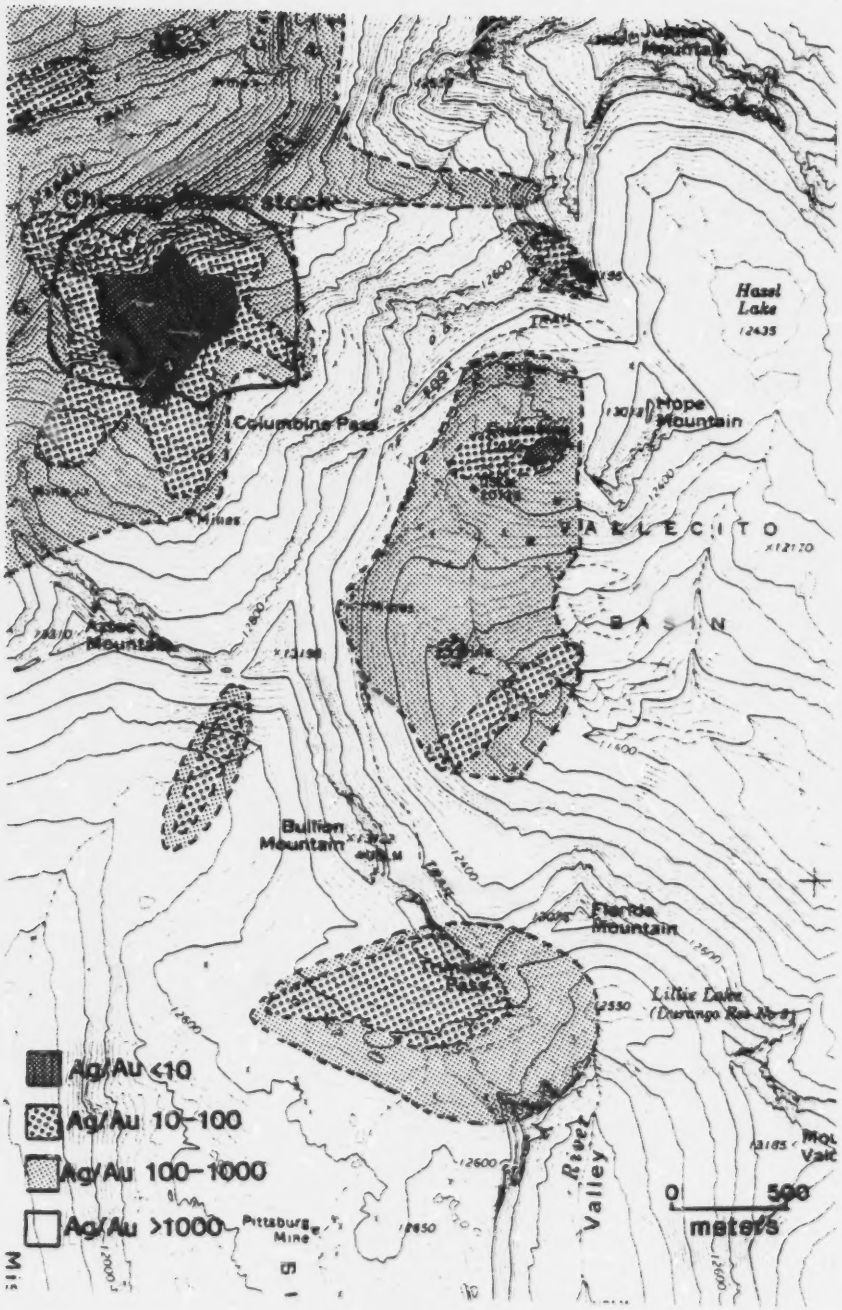

Figure 20. Contour map of Ag/Au in surface rock samples. Data from Steven and others (1969).

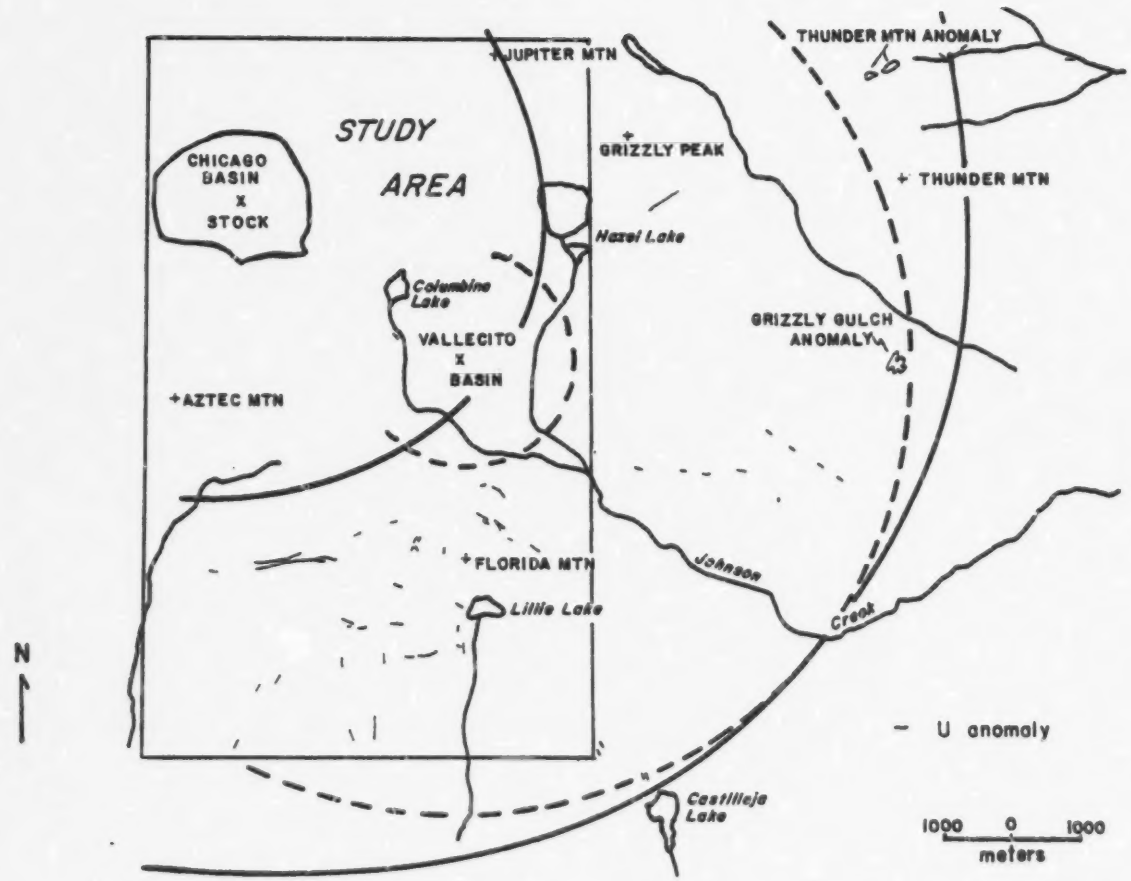

Figure 21. Distribution of uranium occurrences relative to exposed Tertiary pluton in Chicago Basin (solid arcs) and covered pluton in Vallecito Basin (dashed arcs).

The geochemical patterns in Vallecito Basin closely resemble those of the exposed Chicago Basin stock. This is a strong inference that the Chicago Basin stock is merely a cupola of a larger intrusive body, which also has an apophysis below Vallecito Basin. The fact that anomalous tin does not occur more than a hundred meters or so outside the margins of the Chicago Basin stock, yet is present in Vallecito Basin, suggests that the buried pluton may be quite shallow below Vallecito Basin.

The possibility of uranium zonation is potentially of great importance. Not only does it delineate an area where uranium mineralization is likely to occur, but it is supportive evidence, albeit far from conclusive, for a Tertiary age of principal uranium concentration. If uranium is zoned about the Chicago Basin - Vallecito Basin intrusive body, it is possible, given favorable structures, that there is more uranium mineralization north and west of the study area.

VEIN MINERALIZATION AND ALTERATION

Perhaps, the most salient geological characteristic of the Florida Mountain area is a profusion of veins which reticulate the host granites. Most of the veins contain only quartz and minor sulfides, but local pods or shoots of rich sulfide mineralization may contain ore-grade quantities of silver or gold. The ore shoots prompted intense mining activity in the late 1800's, but the mineralization proved to be too spotty and of too small volume to be profitable.

In 1974, it was discovered that the area also contains a considerable amount of uranium, which occurs in faults and fractures scattered over more than 31 sq km. The greatest quantities and grades appear to occur within the study area.

Vein mineralization in the study area generally is of three different types, including: 1) generally low-grade uranium-bearing jasperoid stockworks, 2) higher grade uranium-bearing jasperoid breccia or fracture fillings, and 3) uranium-barren quartz-sulfide fracture fillings. A given area may contain all three types of mineralization and in places the distinctions between types may be subtle. For convenience, however, the following discussion will be organized by separately describing: 1) the Bullion and Trimble Faults, which are dominated by the low-grade stockwork-type mineralization, 2) the Cornucopia and related veins which host the higher grade jasperoid-type mineralization, and 3) the quartz-sulfide veins which occur throughout the study area.

The following discussion is based largely on megascopic and microscopic examination of drill core. Between 1976 and 1978, Public Service Company of Oklahoma drilled 38 core holes in the study area totalling over 12,000 m of core. The locations of these holes are shown on figure 22. All uranium grades and reserve calculations mentioned below were derived from unpublished reports by P.S.O. (Metzger, 1977, 1978).

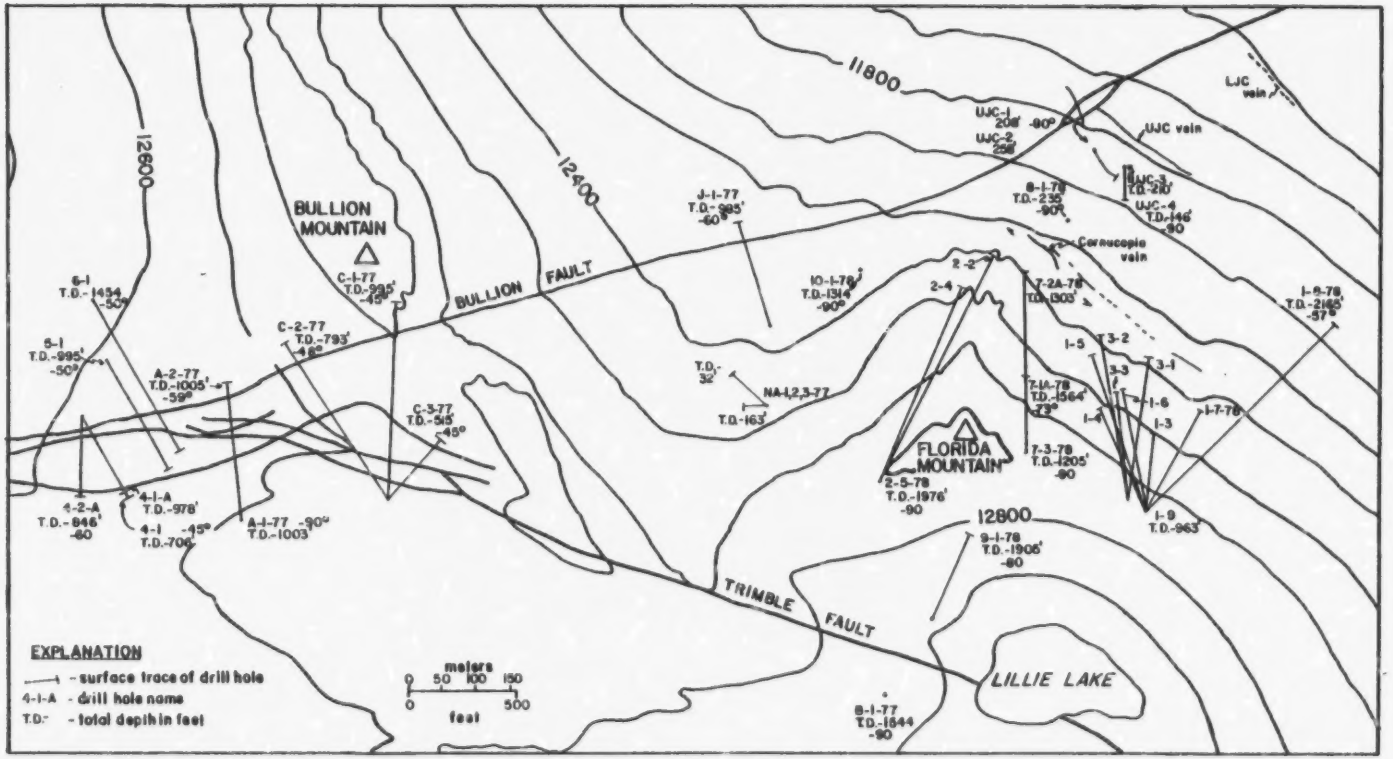

Figure 22. Location of holes drilled by Public Service Company of Oklahoma (from unpublished location maps of P.S.O.).

The Bullion and Trimble Faults and Related Structures

The Bullion and Trimble Faults are large zones of fractured and brecciated granite. On the surface they may vary in width from 5 to 50 m. The zones are characterized by argillic alteration over their entire lengths, and over much of their outcrop they contain a strongly silicified central core of a meter to about 15 m in width. The silicified zones are more resistant than surrounding rocks, making them readily traceable from the air. Because of their erosional resistance they may legitimately be termed breccia reefs.

A typical cross section through either the Trimble or Bullion Faults consists of a central zone of massive fine-grained quartz, surrounded by a zone of silicified breccia. The breccia zones contain intensely microfractured quartz and potassium feldspar fragments supported by a mylonitic matrix of microcrystalline quartz and sericite. The silicified zone grades abruptly outward to wide margins of argillically altered granite, generally followed in turn by a meter or two of propylitic and chloritic alteration. Although disseminated pyrite is common in silicified zones, the faults generally do not contain significant sulfide mineralization.

In the northern part of Silver Mesa the two faults converge to within 30 m of each other, and probably intersect at depth. Both faults thin near the convergence and the Trimble Fault splits into many segments, creating an area of complex smaller fractures and breccia zones.

Although barren of sulfide mineralization, there are widely scattered radiometric anomalies along the entire lengths of the Bullion and Trimble Faults within the study area. However, the most numerous and intense radiometric anomalies occur near where the two faults converge. The host Trimble Granite is nearly totally altered in the area of convergence, and the silicified zones there are almost always anomalous. The richest mineralization contains up to 0.33 percent U_3O_8, although in most places the mineralization is quite low grade, averaging about 250 ppm uranium. Uranium occurs in stockworks of reddish-brown jasperoid lacing the fault zones, or as minor fracture coatings of autunite, meta-autunite, uranophane, and gummite. Surface samples commonly were not in radioactive equilibrium, with radioactivity nearly always in excess of chemical uranium.

Ten holes drilled by P.S.O. in 1976 indicate considerable variation in the width and degree of alteration along the Bullion and Trimble Faults. Uranium mineralization in the subsurface is erratic, showing an apparent association with wider zones of alteration. However, whenever significant uranium-rich zones were intercepted, they showed fairly consistent mineralogic styles. Most major ore intercepts encountered uranium-bearing, dark-gray to red-brown, wholly silicified breccia zones centered in thick (generally more than 30 m) zones of argillically altered granite. The silicified zones, ranging from a meter to over 6 m in thickness, consist mostly of fine-grained quartz, but may be laced with drusy quartz or coarse-grained massive quartz. Disseminated pyrite cubes are not uncommon in the massive silicified zones. Fission-track radiographs showed that in lower grade material (e.g. less than 0.1 percent U_3O_8), uranium generally occurs as very fine grained disseminations in quartz or adsorbed on hematite, whereas very fine grained disseminated uraninite or pitchblende is common in higher grade material.

The central silicified zones are usually surrounded by 5-15 m-wide stockworks of dark-gray to brown siliceous fracture fillings. The stockworks consist of randomly oriented veinlets, generally about a centimeter thick, that range in density from many veinlets per meter to one veinlet per several meters. The veinlets consist mostly of reddish-brown jasperoid, which in thin section are a mixture of microcrystalline quartz or chalcedony, crystalline hematite, sericite, and often minute fragments of minerals from the host granite. Uranium rarely occurs as scattered fine-grained uraninite; most commonly it occurs as very fine-grained disseminations.

The stockworks are generally flanked by 15 m or more of argillic alteration. These altered zones often contain minor fracture fillings of purple fluorite, pyrite, barite, and calcite.

The mineralized zones are of very low tenor, usually averaging about 5-15 m of 0.03 percent U_3O_8. Local intervals may reach 0.25 percent over a few centimeters. Unlike surface samples, uranium in the core is generally in equilibrium with its daughter products. Drilling indicates significant anomalies at least 200 m below the surface in the Bullion Fault, 150 m in the Trimble Fault, and closely spaced anomalies on the surface occur more than 550 m from the convergence. Thus, the area of the Bullion-Trimble convergence represents an area with a relatively large volume, albeit very low grade, of uranium. The actual intersection of the two faults, which does not occur on the surface but is inferred to be 460-490 m below the surface based on fault attitudes encountered in drilling, is yet untested by drilling and may contain an even greater volume of perhaps higher grade material.

There are scattered uranium anomalies elsewhere along the Bullion and Trimble Faults outside the area of their convergence. Along the Trimble Fault east of Trimble Pass several prospect pits exhibit 3-4 times background radiation. The pits, dug at intersections of the fault with north-south-trending structures, show no visible uranium minerals. Several small, scattered uranium anomalies occur along the Bullion Fault within thin red-brown jasperoid veinlets filling widely spaced fractures in massive quartz. The anomalies are too small and scattered to be of economic significance.

Cornucopia, UJC, and Lower Johnson Creek Veins

Three shallow-dipping structures constituted the principal uranium targets of P.S.O. and were named the Cornucopia, Upper Johnson Creek (UJC), and Lower Johnson Creek (LJC) veins (pl. 2). The structures crop out at fairly evenly spaced intervals on the precipitous north face of Florida Mountain. The three vein systems are similar in structural style and mineralogy, but have somewhat different characteristics than mineralized structures elsewhere in the study area.

Cornucopia vein.--The Cornucopia Vein strikes appoximately N. 55 W. and dips an average of 30° to the southwest. Subsurface dips locally flatten to as low as 12°, and increase to as much as 45°. However, most dips fall within a range of 20-35°. At the surface the Cornucopia vein has slightly over 300 m of strike length. The central portion of the vein is covered by talus, as is

its west end where it presumably intersects the Bullion Fault. The Cornucopia vein is apparently truncated at its eastern end by a zone of steeply dipping north-south-trending fissures.

The Cornucopia vein is not a single vein but rather a tabular zone or system of mineralized fractures. The term "vein" is used to refer collectively to numerous veinlets and associated alteration, all related to a relatively thin, tabular structural zone. The Cornucopia vein ranges in thickness from a few centimeters to several meters, averaging less than 1 m. The intensity of fracturing along the Cornucopia vein clearly influences the amount of mineralization. The Cornucopia vein thins and swells, separates many times, and is generally inconsistently mineralized. The thickness of mineralization seems to be controlled by the extent and thickness of argillic alteration, which in turn appears to be a function of the amount of fracturing of the host granite.

In general, uranium mineralization occurs in completely healed, red-brown to gray or black siliceous fracture fillings. No open-space is preserved in the mineralized zones, and with the exception of surface outcrops, distinguishable oxidation is generally not present. Two basic styles of veining are encountered in drill core. Most commonly, anomalous intervals consist of stockworks of thin (0.5-2 c) jasperoid fracture fillings. The veinlets are similar to those found in the Bullion and Trimble Faults; the jasperoid consists of chalcedony or microcrystalline quartz, sericite, crystalline hematite, and microbreccia fragments of wall-rock material. The jasperoid may contain disseminated pyrite, but is usually devoid of other gangue minerals. Uranium occurs both as scattered uraninite or as very fine grained disseminations. Grades are generally higher than those encountered at the Bullion-Trimble Fault convergence, but are still quite low.

A second type of jasperoid mineralization occurs as breccia fillings up to several centimeters thick, surrounded by closely spaced, generally parallel fracture fillings. Light- to dark-gray, black, or red-brown chalcedony or microcrystalline quartz fills fractures and intergranular spaces, or replaces sericite in argillically altered granite. Pitchblende occurs as discrete lenses parallel to silica veinlets or is disseminated and often intimately intergrown with fresh pyrite cubes. Uranium mineralization is nearly always associated with the red-brown, hematite-colored chalcedony.

Barite commonly is found as discrete, coarse, subhedral grains within the silica, as are occasional flakes of molybdenite. The silica veinlets are usually flanked by various combinations of purple fluorite, pyrite, calcite, and massive barite. The abundance of gangue minerals other than quartz distinguishes these jasperoids from the stockwork type. In addition they are generally of higher grade, often more than 0.10 percent U_3O_8 over widths of a meter or more, and several intercepts exceed 1.0 percent.

The highest grades of uranium are found on the surface. One grab sample assayed at 4.16 percent U_3O_8. The surface samples are partly oxidized and contain massive pitchblende with yellow and orange secondary minerals. The pitchblende forms microcrystalline masses that often show concentric banding and botryoidal textures. Later quartz often fills shrinkage cracks and spaces

between layers. X-ray diffraction patterns of pitchblende from surface samples yielded relatively broad but well-defined peaks with d(111) values of 3.156 A and 3.095 A. These indicate two different varieties with lattice constants of about 5.47 A and 5.38 A, respectively. The a_o value of 5.47 A is relatively large for hydrothermal pitchblende (Heinrich, 1958) and is about the same as the unit-cell edge dimensions for synthetic $UO_{2.0}$ of 5.47 (Frondel, 1958). The smaller value of 5.38 A suggests oxidation with partial conversion of U^{4+} to U^{6+} without destruction of the crystal structure. The unit cell edge of UO_2 decreases with increasing oxidation due to the relatively smaller size of the U^{6+} ion. The value of 5.38 A is close to the estimated unit cell edge for $UO_{2.6}$ (5.39 according to Frondel, 1958).

Pitchblende on the surface is commonly replaced by a bright-orange material consisting of two lead uranium oxides, fourmareirite and vandendriesscheite. These are very common weathering products of pitchblende and are major constituents of what is traditionally called gummite. The gummite is in turn partially replaced by uranophane. Both lead uranium oxides and uranophane commonly form pseudomorphs after colloidal pitchblende, often preserving layers and shrinkage cracks. Supergene oxidation was apparently an active process and the occurrence of the highest uranium grades at the surface suggests that enrichment may have occurred. However, the excess of radioactivity to chemical uranium at the surface is actually more suggestive of uranium leaching, and implies that mineralization at the surface consists of oxidation products of hypogene pitchblende. Secondary minerals are not present below the surface, and intercepts with grades in excess of 1.0 percent U_3O_8 (drill hole 3-1, fig. 22) have been encountered several hundred meters below the surface with no indication of oxidation present.

The thickness and amount of alteration along the ore-bearing Cornucopia vein decrease downward. Uranium grades appear to generally decrease with depth, although one hole (1-9-78, fig. 22) intercepted moderately high-grade material (0.8 m of 0.207 percent) approximately 250 m downdip from the surface. A thin zone of alteration with accompanying silicification, believed to be the Cornucopia vein, was encountered about 300 m downdip. The intercept contained no uranium, suggesting that uranium mineralization probably pinches out at depth.

UJC and LJC veins.--The Upper Johnson Creek (UJC) and Lower Johnson Creek (LJC) veins are very similar in structural and mineralogical characteristics to the Cornucopia vein system. The UJC vein crops out for nearly 500 m, strikes N. 45 W., and dips 20-30° to the southwest. Both the strike and dip of the UJC vein vary considerably, as does its thickness, which ranges from 0.3 to 4 m. The surface expression of the LJC vein is commonly concealed by vegetation and talus, but is assumed to intersect the Bullion Fault, as does the UJC Vein, and therefore probably has about the same length as the UJC vein. The LJC vein ranges in thickness from a few centimeters to about 1 m on the surface; because it was not drilled no subsurface data are available.

Mineralization along the UJC and LJC veins is nearly identical to that of the Cornucopia vein. They consist of stockworks of usually red jasperoid within argillically altered Trimble Granite. Individual veinlets range in thickness from less than a centimeter to about 0.3 m. The jasperoid can

easily be scratched by a knife, suggesting a significant content of hematite, sericite, and breccia fragments. The jasperoid is also commonly associated with pyrite, purple fluorite, and rarely molybdenite. Yellow secondary uranium minerals occur in a few surface locations as coatings of fracture surfaces.

Grades as high as 1.5 percent U_3O_8 have been found in surface samples from the UJC vein and up to 0.69 percent in the LJC vein. In contrast to the Cornucopia vein, the high-grade surface material is generally in equilibrium with its daughter products. However, lower-grade samples also from the surface (< 0.1 percent) are often out of equilibrium, with radioactivity in excess of chemical uranium. Little is known about the nature of uranium below the surface. The LJC vein was not tested by drilling, and only one hole (UJC-4-78, fig. 22) intercepted the UJC vein. Mineralization encountered in that one hole, 25 m downdip from its surface outcrop, consisted of 2.5 m of 0.083 percent U_3O_8 with smaller intervals as high as 0.4 percent. The uranium is in equilibrium with its daughter products.

Quartz-Sulfide Veins

Early prospecting concentrated on the dominantly north-south trending fractures of Silver Mesa, the almost randomly oriented fractures of Vallecito Basin, and similar structures throughout the Needle Mountains mining district. These veins, which are by far the most abundant mineralized structures in the area, differ from the veins discussed above in that they are nearly always steeply dipping, are usually barren of uranium, and often contain rich sulfide mineralization.

The quartz sulfide veins are relatively consistent in their style of mineralization, although the particular suite of sulfide and gangue minerals present in any one vein is quite variable. Over much of their lengths, which generally range between 300-1500 m, the veins consist simply of massive quartz. However shoots of sulfide mineralization, exposed in numerous prospect pits in the area, are scattered throughout the veins. When sulfide mineralization is encountered, a typical sequence includes a central vug (1 cm-30 cm wide by a few centimeters to several meters long) lined with free-standing euhedra of drusy quartz and less commonly with fluorite, calcite, or cryolite (Na_3AlF_6). Comb quartz encrusting euhedral fluorite occurs within some open spaces. The open zone is then surrounded by parallel veins or lenses of fine- to coarse-grained quartz, white chalcedony or microcrystalline quartz, calcite, green fluorite, rhodochrosite, or rarely barite. Base-metal sulfides occur within the finer grained quartz or chalcedony, and include pyrite, galena, sphalerite, tetrahedrite, or chalcopyrite. The sulfide-rich zone is then flanked by a thin (1-10 cm) zone of silicified granite, often containing disseminated pyrite and occasional flakes of molybdenite. The silicification grades into argillically altered rock, which in turn grades into propylitic and chloritic alteration. The entire vein, including the alteration zones, rarely exceeds 3 m in width.

The number and types of sulfide and gangue minerals commonly found in the veins varies from one part of the study area to another. The copper minerals

and sphalerite are generally restricted to Vallecito Basin. Green fluorite, although occurring sporadically throughout the area, is also most abundant in Vallecito Basin. One 30 cm-wide vein (Sample VB-50) consists almost entirely of massive, coarse-grained fluorite. Calcite appears to be more prevalent in the southern part of the area.

Oxidation of the veins is readily recognized by surface staining of limonite and manganese oxides. Limonite is largely the result of oxidation of pyrite. Manganese oxides are often seen developing from rhodochrosite, but rhodochrosite does not appear to be a sufficiently abundant mineral to account for the extent of manganese staining. Due to the topographic relief and different degrees of open space or permeability in the veins, the depth of oxidation is highly variable. Pyrite can be seen altering to limonite in drill core from more than 50 m below the surface. However, in many prospect pits and mine dumps pyrite appears fresh and unaltered.

Quartz-sulfide mineralization, particularly within north-south trending fissures, commonly intersects the jasperoid mineralization described previously. It is of considerable importance to note that uranium in the Cornucopia and UJC veins decreases in grade near intersections with north-south structures. In several intercepts of the Cornucopia vein, uranium anomalies terminate against north-south fissures, even though the host structure can usually be traced across them. There are several possible explanations for these phenomena. Either a late uranium-bearing fluid encountered less favorable depositional sites at the greater structural complexity of the intersections, or uranium was remobilized and leached from the intersections by younger fluids travelling within the north-south structures. Paragenetic relationships and fluid inclusion evidence discussed later indicate the latter process to be more likely and suggest that the Cornucopia-type structures were not open at the time of quartz-sulfide mineralization.

In general, whenever particularly intense sulfide mineralization occurs, uranium is absent. However, not all quartz-sulfide veins are totally barren of uranium. Small radiometric anomalies of generally under 15 times background are not uncommon. However, the anomalies are very isolated and limited in extent, and do not appear to hold any economic significance.

Wall-Rock Alteration

Nearly all mineralized structures, as well as many unmineralized fractures, have alteration haloes. The style of alteration is relatively consistent throughout the study area, although local variations in sequence, thickness, and intensity are common. A typical alteration pattern consists of a thin (generally less than 1 m) central quartz-sericite zone with or without veining. This grades outward into a zone of argillic alteration, which in turn grades into a propylitic zone. The argillic and propylitic zones are generally quite variable in thickness, and in many localities one or the other is totally missing.

The central quartz-sericite zone consists of scattered quartz and potassium feldspar fragments "floating" in a matrix of microcrystalline to

fine-grained quartz and sericite. Disseminated fine-grained pyrite often accompanies the quartz.

The intensity of alteration varies in argillic zones, which are easily recognized by gray-brown color in hand specimen. In some instances all feldspars are strongly altered to sericite and kaolinite, and biotite is generally absent. Elsewhere potassium feldspar remains relatively fresh, whereas plagioclase is moderately to strongly sericitized and biotite is generally totally altered to chlorite. X-ray diffraction patterns of sericite indicate a 2M1 muscovite. Kaolinite is usually present with sericite, but generally in subordinant amounts.

Feldspars within propylitically altered granite consist of relatively fresh microcline and weakly to moderately altered plagioclase. Biotite is either partly or totally altered to chlorite. Interstitial chlorite, often accompanied by secondary muscovite, is abundant and gives the rock a greenish color. Interstitial calcite and calcite veinlets are common.

The propylitic zones grade into "fresh" granite. The distinction is not always readily apparent, because although not hydrothermally altered, "fresh" Trimble Granite is nearly always deuterically altered. Biotite is usually partly chloritized and plagioclase partly sericitized. The most noticeable difference from propylitic rock is a lack of interstitial chlorite and green color.

Chemical changes with alteration.--A deep vertical drill hole (drill hole 2-5-78, fig. 22) collared on the western rim of Florida Mountain was selectively sampled to study variations in chemistry and uranium residence of the different types of alteration. Chemical analyses of eight fresh and altered samples of Trimble Granite are shown in table 5. Silica content apparently was unaffected by alteration, except of course within quartz-sericite zones which were not analyzed. Alumina also remained relatively constant, with perhaps a slight depletion in Sample 308, which was the most strongly altered rock. Relative to fresh rock, K_2O appears to have been slightly enriched in the altered granite, whereas CaO and Na_2O where moderately to strongly depleted. Iron is highest in Sample 277, which contains the most chlorite, but shows no consistent variation in the other samples. MgO appears to be enriched in the propylitic zones, indicating diffusion away from the veins and into the wall rocks.

Thorium contents are relatively constant and show little indication of mobilization. The one notable exception is Sample 1330, a strongly argillized rock taken from within a zone of uranium mineralization. No logical explanation for the very low thorium analysis can be given other than that the value is unusual or unreliable.

Uranium residence and mobilization in the alteration zones.--Uranium in unaltered Trimble Granite occurs dominantly in high-uranium minerals such as uranothorite and thorium-rich uraninite. Kinetic studies of uraninite dissolution by Grandstaff (1976) indicate that the high thorium contents may severely limit the solubilities of these minerals under surface oxidation conditions. Whether or not uranium was mobile under hydrothermal conditions can be investigated by textural evidence from fission-track radiographs of altered zones.

Table 5. Chemical analyses of fresh and altered Trimble Granite. Sample #'s represent depth in feet in hole 2-5-78. Major oxides in percent: U and Th in ppm.

	increasing alteration ---->							
Sample	173	235	930	167	277	495	1330	308
SiO2	71.1	70.8	73.3	73.4	71.6	72.2	73.5	74.2
Al2O3	14.4	14.4	14.0	13.9	13.9	13.7	13.7	12.8
Fe2O3	1.45	0.81	0.33	0.39	1.14	1.50	0.42	1.79
FeO	0.90	1.85	1.12	0.95	2.25	0.16	0.68	0.95
MgO	0.60	0.76	0.40	0.30	0.96	0.40	0.40	0.72
CaO	1.37	1.33	0.72	0.79	0.23	0.72	0.76	0.19
Na2O	3.0	3.2	3.2	3.0	0.8	1.8	2.2	<0.2
K2O	4.98	5.28	5.37	5.66	6.26	6.40	5.79	6.25
H2O-	<.01	<.01	0.06	<.01	0.15	0.15	0.11	0.15
H2O+	0.88	0.68	0.66	0.60	1.72	0.85	0.84	1.55
TiO2	0.28	0.31	0.13	0.11	0.30	0.13	0.08	0.29
P2O5	<0.1	0.1	<0.1	<0.1	<0.1	<0.1	<0.1	<0.1
MnO	<.03	0.03	0.02	0.02	0.03	0.22	0.02	<.02
CO2	0.29	0.18	0.28	0.23	0.04	0.56	0.47	0.03
F	0.17	0.14	0.09	0.10	0.14	0.10	0.06	0.14
U	12.7	10.7	16.6	26.8	4.96	23.3	55.4	29.0
Th	31.7	36.7	36.8	32.2	32.9	41.4	<12	32.7
Total	99.56	99.88	99.78	99.95	99.62	98.99	99.13	99.38
Th/U	2.50	3.43	2.22	1.20	6.63	1.78	0.22	1.13

Sample 173 - fresh, Sample 235 - fresh, Sample 930 - fresh to weakly propylitic, Sample 167 - slightly argillic, Sample 277 - strongly propylitic, Sample 495 - argillic, Sample 1330 - argillic and mineralized, Sample 308 - strongly argillic.

Analyses by USGS, Major oxides by X-ray spectroscopy; analysts: J. S. Wahlberg, J. Taggart. J. Baker. U and Th by delayed neutron activation; analysts: R. Bies, H. T. Millard, Jr., B. Keaten, M. Coughlin, S. Lasater. FeO, H2O, CO2, and F by wet chemistry; analysts: H. Neiman, F. Newman.

The uranium content of propylitically altered granite is quite variable, largely because certain samples represent zones of depletion whereas others are weakly mineralized. In general, the propylitic zones appear to have been at least initially depleted in uranium. Both zircons and allanites were stable during propylitic alteration, but no evidence is found for any primary high-uranium phases such as uraninite. Some samples are considerably depleted in uranium (Sample 278, 4.96 ppm U, table 5), as indicated by very low fission-track densities. Others contain moderate amounts of uranium tied up in minute uraninite grains in chlorite. No thorium is detectable in these uraninites by SEM, nor are more coarse disseminated grains found in any samples. It is believed that the uraninite in chlorite represents breakdown of primary phases and reprecipitation of free uranium by the iron in chlorite. Since the less soluble thorium should not have been transported with uranium, the uraninite in chlorite should be considerably more leachable than the primary phases.

Uranium behavior in argillically altered granite is also variable, and again probably because different samples represent various degrees of depletion or concentration. Strongly depleted samples show very low overall fission-track densities. Zircons are still fresh and showed no evidence of loss of uranium, whereas the allanites are partially destroyed and leached of some of their uranium. No evidence is found of primary igneous high-uranium phases. Some argillically altered samples appear to have localized some introduced uranium, particularly in iron and titanium oxides. Other samples contain concentrations of uranium as abundant disseminated uraninite and uraninite rims about pyrite. Thorium is not detectable in the uraninite and no primary accessory minerals other than zircon are preserved in the rocks.

The apparent general sequence of uranium remobilization from fresh rocks through increasing degrees of alteration can now be summarized. Uranium in relatively fresh rocks is located in common accessory minerals and to a greater extent in uranium- and thorium-rich minerals such as uranothorite and uraninite. Some uranium may have been redistributed by late-magmatic or early postmagmatic deuteric alteration as evidenced by weak radioactivity associated with oxidized margins of biotite, but such redistribution was probably not a significant factor according to fission-track densities. During early propylitic alteration, primary uranium-rich phases were at least partially destroyed and uranium either leached from the rocks or redistributed and trapped by iron oxides. It is difficult to state what factors controlled the solubilities of these minerals; the high thorium contents suggest that their solubilities should have been low (Grandstaff, 1976). Perhaps the age of the granites and the fact that the thorites were largely metamict helped contribute to their solubility; uraninite does not become metamict but will still suffer internal radiation damage that probably increases its solubility. In any event, the textural evidence indicates that the minerals were destroyed. Zircon and allanite were stable during propylitic alteration, but allanite was eventually destroyed during argillic alteration. As alteration progressed, uranium in grains of uraninite in chlorite was liberated and either reconcentrated as free uraninite or uraninite with pyrite, or removed from the rocks to end up in the vein deposits.

Paragenesis

The general paragenetic sequence of major vein minerals is shown on figure 23. The sequence is a compilation from many samples taken throughout the area both from the surface and from drill core. A single sample will not contain all the minerals shown, and deviations from the general sequence are possible on a local scale.

The earliest vein fillings (Stage I, fig. 23) involved fine- to coarse-grained massive white quartz. Minor disseminated, fine-grained, euhedral, pyrite occasionally accompanied the quartz. This stage was more or less restricted to the Bullion and Trimble Faults.

Stage I quartz deposition was followed by fracturing and the stage of principal uranium mineralization. White fine-grained quartz and chalcedony deposition was followed by jasperoid consisting of the coprecipitation of chalcedony or quartz, pitchblende, hematite, white barite, and pyrite. Minor galena and rare flakes of molybdenite occasionally formed in the jasperoid. Purple fluorite and calcite formed during or slightly after jasperoid mineralization. In a few localities, massive, euhedral, yellow barite formed late in Stage II.

Stage III was nearly a repetition of Stage I, with the deposition of massive, generally fine grained to microcrystalline quartz and very fine grained, disseminated euhedral pyrite. This quartz-pyrite stage often grades laterally into quartz-sericite wall-rock alteration, where small flakes of molybdenite are occasionally found.

Stage III quartz deposition was followed by fracturing and introduction of a complex quartz-sulfide stage. This was the principal event which filled most of the steeply dipping fractures in the area. Base-metal sulfides precipitated during this interval include galena, sphalerite, pyrite, chalcopyrite, and tetrahedrite. Pyrite and galena were generally most abundant, although sphalerite was locally abundant and in many localities predominated.

In many samples, sphalerite was the earliest Stage IV sulfide to form, often being replaced by later galena. However, sphalerite and galena often appear to have grown simultaneously. Galena, pyrite, and chalcopyrite generally precipitated at the same time, although in a few samples galena and pyrite preceded chalcopyrite. Stage IV pyrite was generally much coarser and less euhedral than preceding stages. Locally it was partially replaced by chalcopyrite. Gold and silver were probably introduced along with Stage IV sulfides, although their mineral associations could not be determined.

Quartz and chalcedony paragenesis during the base-metal stage was rather complex and varied between localities. There were at least three or four episodes of fracturing and annealing by microcrystalline quartz during Stage IV, but there are insufficient cross-cutting relations to fully characterize these events. Generally quartz paragenesis during Stage IV involved an early stage which preceded or accompanied the introduction of pyrite, chalcopyrite, galena, and tetrahedrite. A late phase of quartz was accompanied only by local fluorite and cryolite deposition.

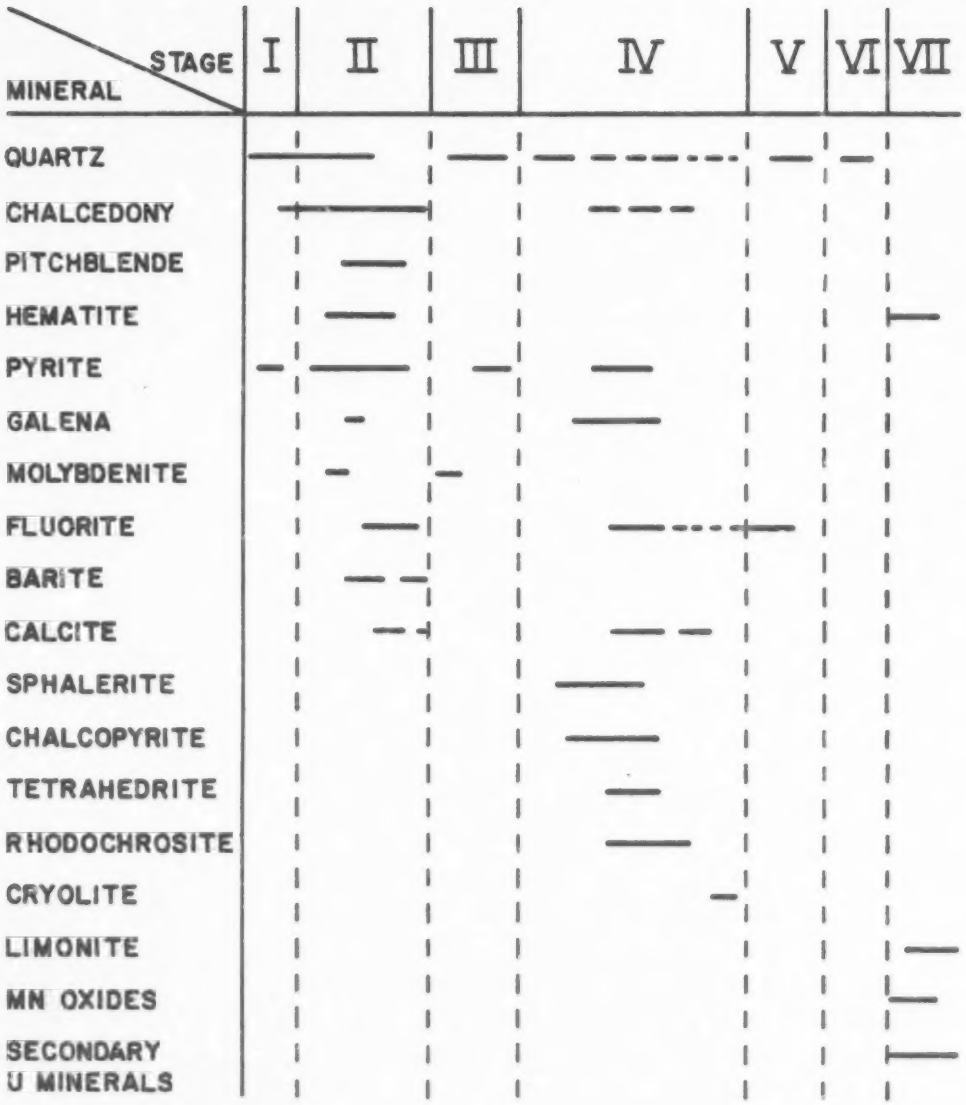

Figure 23. General paragenetic sequence of major vein minerals.

Gangue minerals other than quartz include rhodochrosite and calcite with minor barite and cryolite. White, green, and purple fluorite vary in abundance.

Euhedral fluorite also precipitated during Stage V, where it is usually encrusted with comb quartz. Stage V mineralization is mostly restricted to Vallecito Basin and was a relatively minor event, as was Stage VI. Stage VI consists of very minor fine-grained quartz. The quartz is indistinguishable from earlier phases; Stage VI was simply inferred from fluid-inclusion temperatures.

The final mineralizing event was probably not hypogene but involved supergene deposition of secondary uranium minerals, limonite, and manganese oxides.

Fluid Inclusion Studies

Description.--Fluid inclusions from all of the hypogene paragenetic stages were investigated using a Chaixmeca heating/freezing stage, described by Poty and others (1976) and modified for greater optical resolution and precision after Cunningham and Carollo (1980). Most of the samples were not particularly well-suited for inclusion studies. Many samples contained only a very few visible inclusions, and most inclusions were so small as to be scarcely resolvable when observed on the heating/freezing stage, the optics of which are not nearly as good as a conventional petrographic microscope. However, a sufficient number of homogenization temperatures were obtained to make reasonable estimates of fluid temperatures. Homogenization temperatures for 270 inclusions are shown on figure 24. Freezing determinations require much higher optical resolution than do homogenization tests, and only a limited number of results were obtained due to optical limitations. These data are also shown on figure 24.

Only one sample containing Stage I inclusions was studied. Inclusions in medium-grained comb quartz from the Trimble Fault, cut by uranium-bearing jasperoid, averaged less than 1 μm in diameter (Sample SM-30). However, a number of isolated inclusions ranged up to 25 μm, and were inferred to be of primary origin. These were simple two-phase inclusions without daughter products. The volumes of the gas phase showed considerable variation, and in several instances constituted the bulk of the inclusion. Homogenization temperatures for Stage I ranged from 195° to 378°C. Several inclusions with relatively large vapor fractions homogenized to a gas phase by disappearance of the liquid. No inclusions were found with temperatures in the range of 270° to 300°C. This gap, as evident on figure 24, suggests that the lower temperatures may be from secondary inclusions. However, comparison with Stage II temperatures suggests the gap could be due to limited data.

Freezing temperatures for Stage I inclusions clustered near zero. The largest freezing point depression, -0.3°, corresponds to approximately 0.5 weight percent equivalent NaCl (Potter and others, 1978). Ice in several liquids melted at slightly positive temperatures, due either to metastability of the ice or to a thermal gradient within the instrument. A small bubble separated from most liquids on cooling and is believed to be the carbon dioxide hydrate CO_2 5 3/4 H_2O.

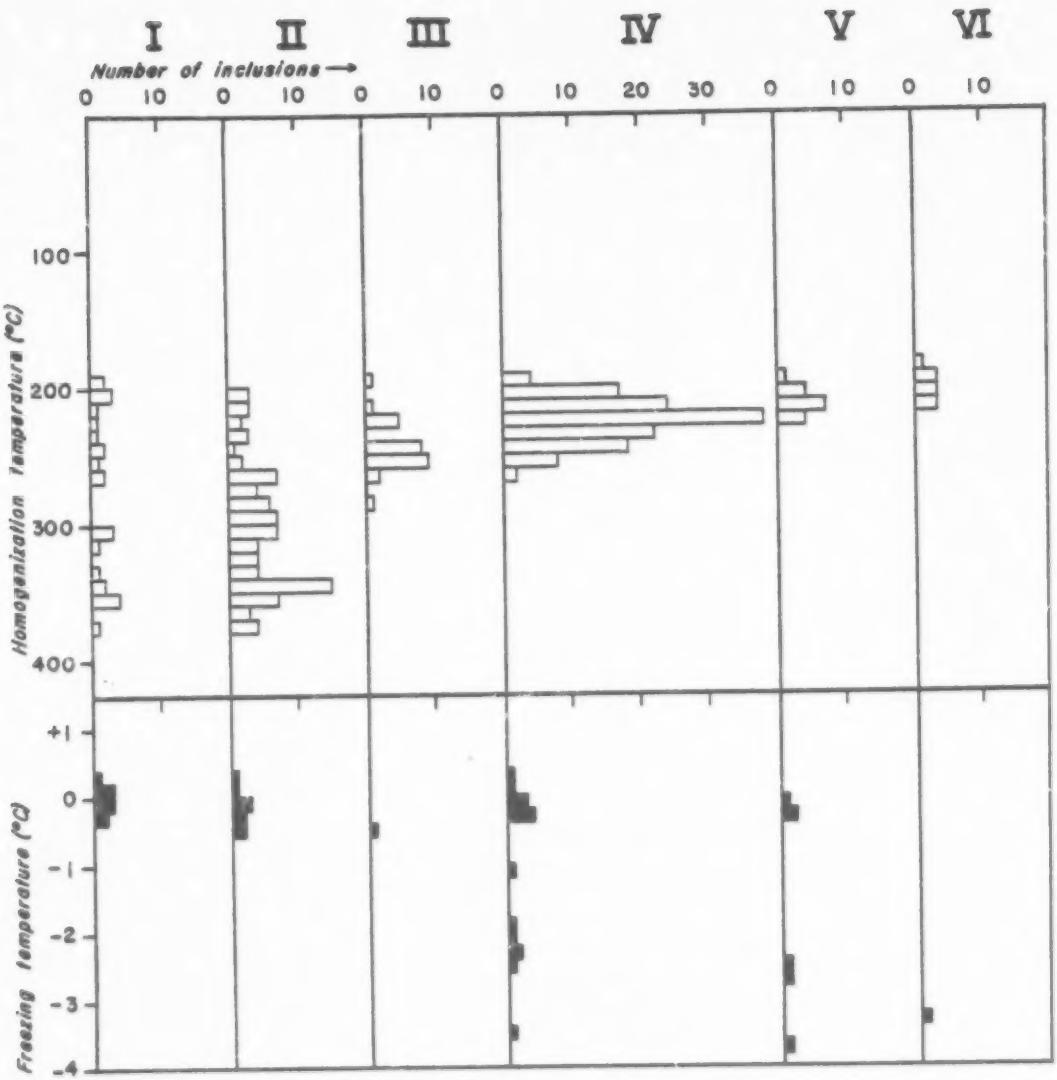

Figure 24. Fluid inclusion homogenization and freezing temperatures for six hypogene paragenetic stages.

Fluid inclusion data for Stage II were obtained from quartz, barite, fluorite, and calcite. A few primary inclusions are even found as minute vug fillings in chalcedony. Barite yielded the largest inclusions, often as large as 30 μm; however, the samples tended to disintegrate on heating, making homogenization temperatures difficult to obtain. Inclusions in Stage II fluorite, unlike later stages, are generally small and widely scattered. Those in quartz and calcite are generally isolated and very minute (<5 μm). The small size and isolation of many inclusions precluded distinguishing between primary and secondary origins. Most are simple two phase inclusions, although one rather large inclusion in barite may have contained a liquid CO_2 phase. Daughter products are generally absent, although some opaque specks within the very small inclusions, interpreted to be solid inclusions, may instead have been oxide or sulfide daughters. Vapor-phase fractions were generally difficult to estimate due to small size; larger inclusions in barite showed large variations in the relative fraction of vapor bubbles.

Stage II homogenization temperatures show a distribution similar to Stage I, ranging from 200° to 380°C. Temperature frequencies show a minor peak between 340° and 350°, but in general are fairly evenly distributed over the entire range. Freezing temperatures also are similar to Stage I, with maximum depressions of -0.5°C corresponding to 0.9 weight percent equivalent sodium chloride (eNaCl) or 0.15 molal eNaCl. Most inclusions yielded small quantities of CO_2 hydrate on cooling.

Inclusions were found in fine-grained quartz of Stage III. Most visible inclusions ranged in size from 5 to 10 μm, although one inclusion found was nearly 25 μm in diameter. No daughter products were apparent in the inclusions.

Homogenization temperatures in Stage III were more restricted in range than either of the previous stages, averaging about 250°C. The temperatures below 230° shown on figure 24 are interpreted to be from secondary inclusions, but without sufficient certainty to exclude them from the diagram. Only one inclusion was found that was sufficiently large to observe melting in freezing tests. It yielded a temperature of -0.5°C. No CO_2 hydrate was observed to separate on freezing.

Minerals from Stage IV were the most suitable for study as fluid inclusions were often much lar.er than in the preceding stages. Approximately equal numbers from quartz and fluorite were studied. Inclusions in quartz generally ranged from 5 to 15 μm in size; inclusions in fluorite were much larger, averaging 50 μm and being as much as 150 μm in diameter. Relative volumes of vapor phases were fairly consistent. They appeared to average approximately 20 percent of the total volume of the inclusions, although Roedder (1979) clearly pointed out that visual estimates can be very misleading. No daughter products were seen in these inclusions.

Despite the large number of inclusions studied, and the use of many samples from widely spaced localities and different mineral hosts, homogenization temperatures for Stage IV show a relatively narrow spread and a distinct peak at 220°-230°C. In contrast, freezing temperatures varied considerably, ranging from slightly positive values to a maximum depression of -3.6°. This corresponds to salinities of zero to approximately 5.8 weight

percent eNaCl (0 to 1.06 molal). No CO_2 hydrate was observed to separate on freezing.

Fluorite and accompanying encrustations of quartz provided fluid inclusion data for Stage V. The inclusions were similar in size and character to those of Stage IV. Homogenization temperatures again were fairly consistent, averaging at slightly lower temperatures (210°-220°C) than Stage IV. Only a limited number of freezing values were obtained; they also appear to be roughly similar to Stage IV.

The occurrence of a sixth paragenetic stage was inferred solely on the basis of fluid inclusion data, as the quartz of Stage VI is indistinguishable from that of earlier stages. Homogenization temperatures from inclusions of distinctly primary origin averaged slightly over 200°C, which corresponds to temperatures frequently encountered in secondary inclusions from earlier stages. Only one freezing temperature was obtained at -3.3°C.

Discussion.--Fluid inclusions from stages I and II showed large differences in homogenization temperatures, whereas inclusions from the later stages appear to define fairly narrow temperature ranges. A number of processes could explain the spreads shown in stages I and II. These include: 1) postcrystallization processes such as necking-down and coalescence, leakage, etc. (Roedder, 1979), 2) volatile effervescence due to pressure release, and 3) boiling (Roedder, 1970; Nash, 1972; Poty and others, 1974; among others). Natural temperature variations due to the use of samples from various locations and of different mineralogies are probably not a major factor, as Stage I temperatures, showing a wide spread, came from a single sample, and Stage IV temperatures, with a narrow range, came from many samples of different mineralogy.

Necking-down almost unquestionably accounts for some of the spread, but should not in itself explain the different temperature distributions between stages I and II and the later stages. The variable gas/liquid ratios in stages I and II, and the presence of inclusions with relatively large vapor phases which homogenize by disappearance of the liquid into the vapor, suggest that trapping of both liquid and "steam" inclusions ocurred. Thus effervescence of dissolved volatiles such as CO_2 or boiling of the aqueous fluid itself is a likely explanation for the wide range of homogenization temperatures for stages I and II.

The separation of CO_2 hydrate during cooling indicates a relatively high proportion of CO_2 in the early fluids. Takenouchi and Kennedy (1964) showed that at pressures over 200 atmospheres, CO_2 and H_2O display considerable miscibility, with the solubility of CO_2 being inversely dependent on temperature and generally independent of pressure. However, at pressures below approximately 200 atmospheres, CO_2 solubility at a given temperature is very sensitive to pressure changes. The depth below the paleosurface of the current exposure of the Chicago Basin stock, most likely equivalent to the depth of mineralization, was estimated earlier to have been 700-800 m. Hydrostatic pressure at this depth would be less than 100 bars (Haas, 1971), indicating that local decrease in pressure could easily cause immiscibility between CO_2 and H_2O. Thus, CO_2 effervescence was a plausible, if not likely, process during Stage I and Stage II deposition.

General boiling of the fluids can be postulated based on the theoretical thermal gradient for the pressures, temperatures, and densities involved. Figure 25 shows the boiling-point curves for H_2O liquid and for NaCl brines (from Haas, 1971). The freezing temperatures for inclusions from stages I and II suggest compositions close to pure H_2O. Assuming hydrostatic pressure, a depth between 700 and 800 m, and a salinity between zero and 5 weight percent, boiling would occur between 275° and 285°C. The highest average temperature for a nonboiling fluid (Stage III) was about 250°, which is not inconsistent with possible boiling at 280°. It appears that H_2O boiling is as equally plausible as is CO_2 effervescence for the mineralizing fluids of stages I and II. Rather elaborate tests, such as crushing of inclusions in oil or analysis of their vapor phases by gas chromatography would be necessary to determine what the dominant process was.

The later paragenetic stages all show fairly restricted ranges in homogenization temperatures. Average temperatures appear to be approximately 250°, 225°, 215°, and 205°C for stages III, IV, V, and VI, respectively. Data from Potter (1977) indicate that pressure corrections for 1 to 5 percent NaCl solutions are virtually negligible for the low pressures (<100 bars) believed to have been involved in mineralization in the Needle Mountains district. Thus, the homogenization temperatures are fair approximations (probably plus or minus 20°C) to the actual formation temperatures.

Although freezing temperatures seem to indicate a slight increase in salinities in the later stages, the salinities of inclusions from all stages are very low, the maximum value corresponding to about 1 molal NaCl. This suggests that chloride was not a major factor in the transport of metals.

Comparison with fluid inclusion studies of other hydrothermal uranium deposits.--Fluid-inclusion studies of other vein-type uranium deposits have been reported by several authors (Leroy and Poty, 1969; Tugarinov and Naumov, 1969; Naumov and others, 1971; Poty and others, 1974; Cuney, 1978; and Leroy, 1978). A number of other studies, summarized by Rich and others (1977), are not sufficiently complete to allow comparison with the Needle Mountains district. Those deposits for which data are available generally contained inclusions initially high in CO_2, and showed progressive decline of CO_2 content in later paragenetic stages. With one exception, temperatures of pitchblende deposition were less than 190°C. Formation pressures listed by Rich and others (1977) ranged from 300 to 900 bars. Boiling was demonstrated to have occurred in the Forez district of France by Poty and others (1974) and Cuney (1978). However, boiling was not associated with pitchblende deposition, which occurred in an earlier stage. Only within the episyenites of the La Crouzille (Limousin) district of France was there evidence of boiling during uranium mineralization (Leroy and Poty, 1969; Leroy, 1978). This occurred at formation temperatures of 340°-350°C and pressures of 700-800 bars.

Comparison with these other studies indicates that the Florida Mountain mineralization is fairly unique, in terms of conditions of formation, among hydrothermal uranium deposits. The La Crouzille district contains the only other deposits showing evidence of boiling during uranium deposition and temperatures in excess of 190°. Assuming a temperature of about 280° and low salinities for pitchblende deposition in the Florida Mountain area, corresponding hydrostatic pressure would have been between 60 and 70 bars

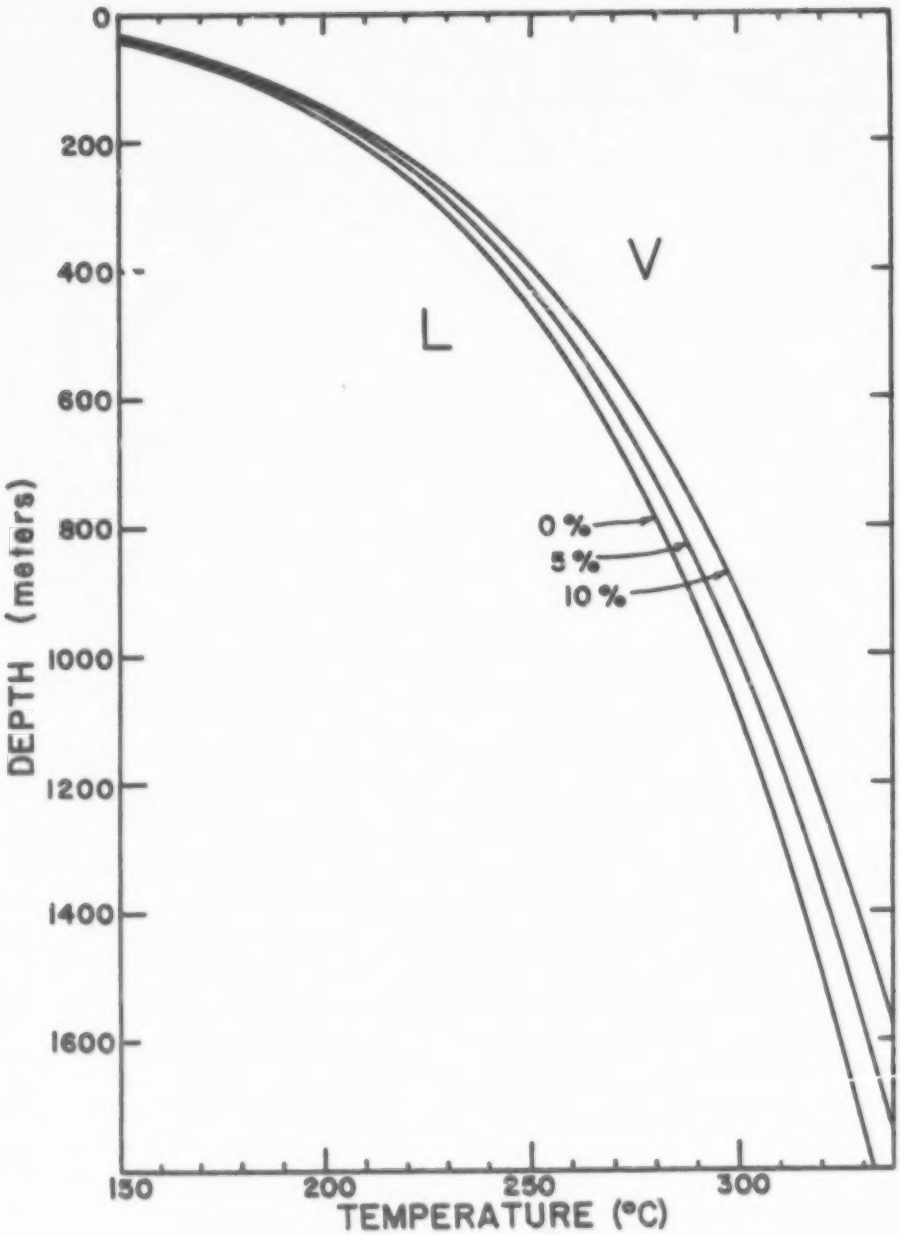

Figure 25. Boiling-point curves for H_2O liquid (0 wt. percent NaCl) and for brines of 5 and 10 wt. prcent NaCl (from Haas, 1971).

(Haas, 1971). This is considerably lower than any other reported formation pressure (all 300 bars or greater). The only major feature apparently shared by the Florida Mountain deposits and most other deposits is the probable initial high content of CO_2.

SUMMARY--GENETIC MODEL FOR MINERALIZATION

The discussions on the preceding pages indicate that a variety of factors played important roles in the formation of the uranium and base-metal veins. The following factors seem important in the formation of the uranium deposits: 1) Precambrian magmatic concentration and initial residence of uranium, 2) structural preparation, 3) uranium remobilization, and 4) precipitation during a complex Tertiary subvolcanic event. The data presented here may now be condensed into a single, albeit tentative, genetic model.

Because the Florida Mountain deposits have no known analogs in the United States, the following discussion might be reviewed in a better perspective if compared to the "classic" intragranitic uranium deposits of France. Table 6 displays some of the major characteristics of Florida Mountain and two important districts in France. The two districts from France (Limousin and Forez) are probably the most carefully studied examples of intragranitic vein deposits, but other variants are known and not all geologists accept the hypotheses proposed for these deposits. The Florida Mountain deposits are similar to the French deposits in vein mineralogy, but important differences are age, tectonic setting, and type of granite. Because veins in all three examples appear to have formed a significantly long time after crystallization of the host granite, it is not clear how important the differences in granite petrology and emplacement are to genesis of the deposits.

Magmatic Concentration of Uranium

The concept of granite fertility and the ability of a granite to act as good source rock require both initially above-normal uranium concentrations and the location of that uranium in labile phases (Moreau and others, 1966). Both aspects of granite fertility in the Needle Mountains were functions of magmatic processes.

Granitic magmas form by partial melting of a variety of sources under varying conditions of pressure, temperature, and water content. The conditions under which a particular granitic melt is generated often have a strong influence on the types of mineral deposits it might host. For example, melts producing hornblende granites, because of their low water contents and the negative slope of the water-saturated granite solidus, can rise to relatively shallow depths where they may induce meteoric convection systems and form such metal concentrations as porphyry copper deposits. In contrast, muscovite granite melts typically contain high-water contents, either from hydrous melting or from water concentration during fractionation, and therefore generally crystallize at greater depths. Perhaps because of the availability of magmatic hydrous fluids, these granites of I0 contain important concentrations of lithophile elements (Strong, 1980). The association of anomalous uranium and tin with the Hercynian two-mica granites of Europe is an example. Biotite granites such as those of the Eolus batholith, are intermediate between these end members and typically do not

Table 6.--Summary of general characteristics of the Florida Mountain intragranitic uranium deposits with those of two major districts of France

	Limousin*	Forez†	Florida Mountain
Principal host rocks	2-mica granite episyenite	2-mica granite	biotite granite
Age of host rocks	350-360 m.y.	335 m.y.	1350 m.y.
Source of host rocks	sedimentary	sedimentary	igneous
Orogenic belt setting	Hercynotype	Hercynotype	Andinotype
Orogenic timing	syntectonic	syntectonic	posttectonic
U content of host rocks	15-20 ppm	15-20 ppm	15 ppm
U released from host rock by:	deuteric alteration	deuteric alteration	hydrothermal alteration
Age of mineralization	275 m.y.	270 m.y.	<10 m.y.
Major U ore mineral	pitchblende	pitchblende	pitchblende
Major gangue mineral	quartz	quartz	quartz
Other gangue minerals	pyrite,hematite	pyrite,hematite, fluorite,calcite, barite	pyrite,hematite, fluorite,calcite, barite
Formation temperatures	345 °C	77-100 °C	280°C
Formation pressures	700-800 bars	300 bars	<100 bars
CO_2 in U-fluids	>3 molal	3 molal	2 molal(?)
Proposed U transport	$UO_2(CO_3)_2^{2-}$	$(UO_2CO_3)^\circ$	$UO_2F_3^-$
U fluids boiled or effervesced	yes	no	yes
Proposed heat source for hydrothermal mobilization	lamprophyres	late granite or radioactive decay	Chicago Basin stock

*from Leroy (1978) and Poty and others (1974)
†from Cuney (1978)

crystallize at shallow enough depths or generate enough mineralizing hydrous fluid to form economicly important concentrations of metals. The Trimble Granite is clearly an exception with its high uranium contents (average 15 ppm). The trace-element data presented earlier indicate that the Trimble Granite probably represents the final product of a long and extensive differentiation process involving both repeated remelting and fractional crystallization. Incompatible elements such as thorium and rubidium were significantly enriched during this process and it may be assumed that uranium behaved in a similar fashion. Thus, one criterion of a fertile granite, a greater than normal abundance of uranium, was produced by uranium enrichment during the extensive fractionation required to produce the Trimble Granite.

The other criterion of fertile granites, that uranium occur in labile phases, also developed as a function of progressive differentiation. The hornblende granodiorites of the Eolus batholith are infertile in that uranium appears to be tied up exclusively in refractory minerals. However, as uranium contents increase with differentiation, simple calculations show that the common accessory minerals can no longer contain all of the uranium in the rocks. In addition, the apparent unmixing of minimum melt and restite resulted in strong decreases in TiO_2, P_2O_5, and Zr, reducing the abundance of common accessory minerals and furthr limiting their ability to contain signifcant amounts of the rocks' uranium. As a result, more leachable uranium-rich minerals became more abundant with progressive differentiation. Because thorium became more enriched along with uranium, these high-uranium minerals were also rich in thorium. Thorium decreases the solubility of these minerals and probably results in rocks that are infertile with respect to cold surface or ground-water leaching. However, fission-track radiography indicates that uranium was leached during weak hydrothermal alteration.

The Role of Structure

Structural preparation played a significant role in mineralization of the Needle Mountains district. Not only did it provide an extensive plumbing system, but intense brecciation, particularly along the Bullion and Trimble Faults, allowed easy access of uranium-leaching fluids to the granites. Fractures in the Needle Mountains district developed over a long period of geologic time, beginning with the formation of rectilinear cooling joints following crystallization of the Precambrian granites and ending 10 m.y. ago with the intrusion of the Chicago Basin stock. Probably the most important structural event was the formation of the Bullion and Trimble Faults, probably during early Tertiary Laramide activity. Any genetic model for the uranium deposits must consider the close spatial association of most of the uranium in the area to these faults. The Bullion and Trimble Faults were probably less important as conduits for fluid movement than as the actual sources of uranium. The more extensive brecciation allowed greater permeation of fluids than other fractures, and hence more extensive alteration. Assuming an alteration zone 50 m wide and 500 m deep along the extent of the faults in the Trimble Granite, and assuming depletion of as much as 10 ppm uranium from the granite (containing an average of 15 ppm), the Bullion and Trimble Faults alone can account for all of the vein uranium occurrences in the study area.

The intrusion of the Chicago Basin stock and its postulated buried

equivalent in Vallecito Basin also played important roles in terms of structural development. The affinity of mineralization for north-south structures in the southern part of the area, and for east-west fractures in the east, as explained earlier, suggests that radial compression resulting from intrusion of the stock helped open pre-existing fractures.

Hydrothermal Mobilization and Concentration

The major mineralizing event in the Needle Mountains is believed to have coincided with the intrusion of the Chicago Basin stock. Although evidence from fission-track radiographs does not suggest that the Chicago Basin stock was a major source of uranium, it more than likely did contribute some metals such as molybdenum and also established the hydrothermal system, by which uranium was leached from the Trimble Granite and ultimately deposited in veins. Fission-track radiographs indicate that uranium was removed from primary high-uranium minerals such as uraninite during early propylitic wall-rock alteration. More advanced alteration also removed uranium from phases such as allanite, but these were probably only minor contributors. The extent of alteration in the study area, particularly about the Trimble and Bullion Faults, is sufficient to account for the amount of uranium found in the veins.

The chemistry of the ore-precipitating fluids can be estimated by the theoretical stability fields of the mineral assemblage occurring with pitchblende. In particular the assemblage pitchblende - barite - calcite - quartz - hematite - pyrite - sericite defines a fairly restricted range of pH - PO_2 conditions. These stability fields for 300°C, as roughly predicted by fluid inclusions, are shown on figure 26. However, using such a diagram to predict a mechanism of precipitation that can account for this assemblage presents a number of problems. The presence of early hematite and barite, the lack of later hematite and the abundance of sulfides, and the coprecipitation of pyrite and uraninite all point to reduction of initially oxidized fluids. Pyrite can only be effectively precipitated by reduction or by increases in iron or sulfur contents. Uraninite is also typically thought to form by reduction, but can also precipitate by changes in pH or temperature. Calcite becomes stable by increases in pH or activity of Ca^{2+} but becomes less stable with cooling. Barite may precipitate by increases in pH, PO_2, aBa^{2+}. or ΣS. Obviously changes in a single parameter cannot explain the presence of the entire assemblage. Reduction could account for the precipitation of pitchblende and pyrite, but would be inconsistent with the presence of barite.

Several factors must be kept in mind in evaluating a mechanism of precipitation. Principal among these are that the pitchblende-bearing fluids were high in CO_2, either boiled or effervesced CO_2, and were restricted in occurrence (at least the high-grade-producing fluids) to the Florida Mountains Fault block. Fluid inclusions seem to indicate that the ore-bearing fluids were similar to those that formed vein deposits in France in that they were rich in CO_2. Several French investigators believe that destruction of uranyl-carbonate complexes during boiling of the CO_2-rich solutions caused the deposition of pitchblende (Leroy, 1978). Rich and others (1977) presented strong arguments against such a mechanism. Loss of CO_2 during boiling would result in an increase in pH, unless sufficiently buffered by wall-rock alteration, and hence a decrease in pitchblende stability. However, Rich and

others (1977), as well as French investigators, assumed that uranium was transported as a uranyl-carbonate complex. If uranium was transported as a fluoride complex, which has been demonstrated thermodynamically to be more likely to occur than carbonate complexes at high temperatures (S. B. Romberger, oral commun., 1981), then an increase in pH as a result of CO_2 loss could actually precipitate pitchblende (see fig. 26). Massive fluorite veins in Vallecito Basin are evidence of high fluoride activity in the Florida Mountain area. An increase in pH as a result of CO_2 loss could explain the presence of calcite, barite, and pitchblende alone, but could not account for the coprecipitation of pitchblende and pyrite. According to Rich and others (1977), loss of CO_2 will cause a decrease in the oxidation state. This is usually offset in most boiling solutions by a simultaneous loss of CH_4, H_2, and H_2S, resulting in an overall increase in oxidation state. However, if a fluid were merely to effervesce CO_2 without accompanying general boiling, CO_2 loss might act as an effective reductant. Thus, one possible, but purely speculative, mechanism of uranium deposition could involve CO_2 loss by pressure reduction, particularly in the structurally and topographically high Florida Mountain structures, with accompanying breakdown of uranyl-fluoride complexes by increase in pH and drop in P_{O_2}.

Another equally viable mechanism would involve the mixing of oxidized and reduced fluids. An early stage of intrusion could thermally induce convecting, oxidizing waters to leach uranium from the granites. Further intrusion to shallower depths and the introduction of reducing magmatic fluids might then mix with the oxidizing fluids and cause pitchblende deposition. There is currently insufficient evidence to favor either mechanism, or to eliminate the possibility of other alternatives.

URANIUM OCCURRENCES OUTSIDE STUDY AREA

There are several uranium occurrences located immediately outside the study area. Although anomalies at Thunder Mountain, Grizzly Gulch, and Castilleja Lake are most likely related to those within the study area, difficulties in access prevented their study. The following discussion is a brief summary of investigations of these areas by Metzger (1978). Locations were shown on figure 21.

Grizzly Gulch

Grizzly Gulch lies in an extremely rugged area separated from the study area to the west by a range of mountains all in excess of 4000 m elevation. Uranium mineralization occurs in sills of Trimble Granite within Eolus Granite. Although there are numerous sills in the Grizzly Gulch area, most are not mineralized. One anomalous sill is 6-9 m thick and has a strike of N. 45° W. and a dip of 45° to the northeast. On the surface nearly the entire thickness of the sill is mineralized, as is 2-4 m of exposed Eolus Granite below the sill. Significant mineralization also occurs along much of the exposed strike extent of the sill. Uranium is located in thin (0.5-10 cm) jasperiod veinlets of very similar composition to those of the Cornucopia Vein. The jasperiod contains abundant pyrite and is associated with purple fluorite. The surrounding granite is strongly argillized. Surface grades vary from a few times background to 2.12 percent U_3O_8. In the subsurface the

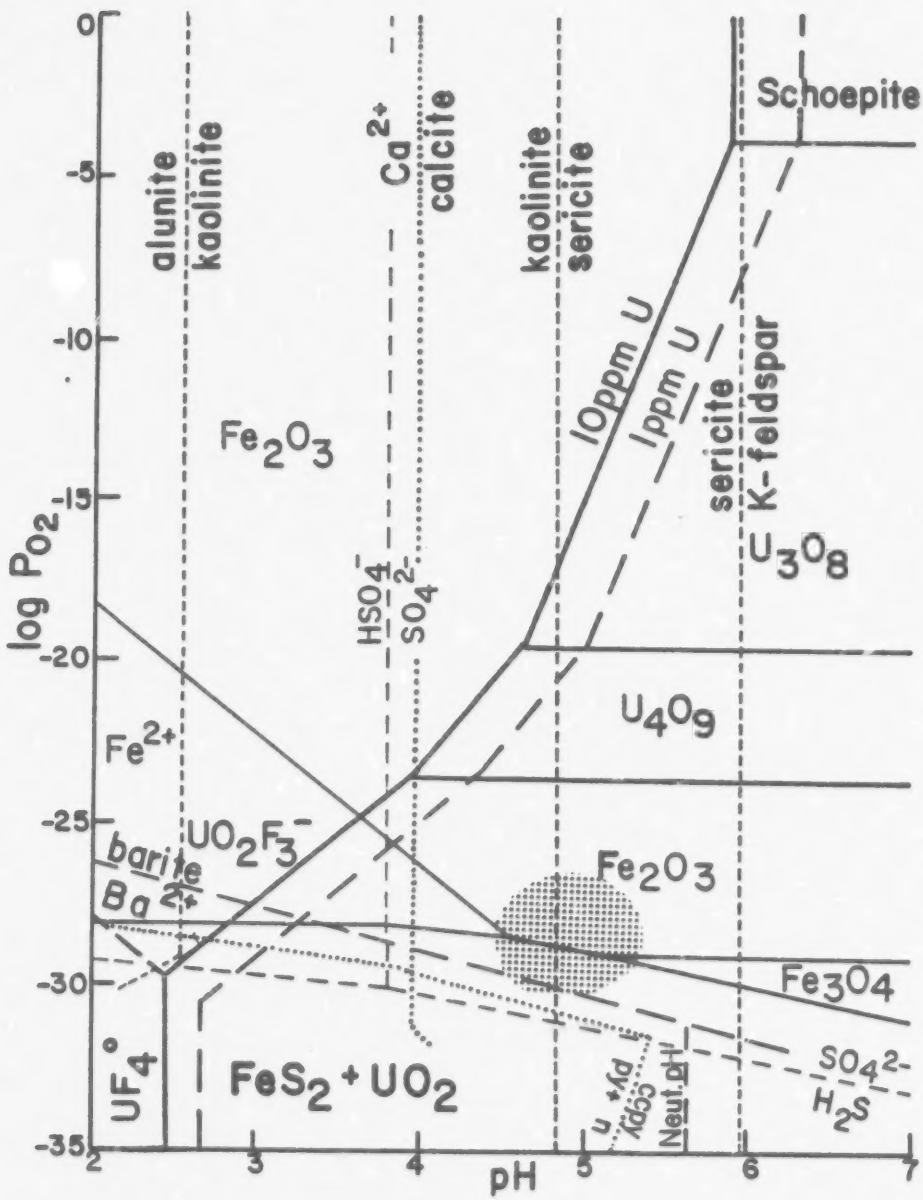

Figure 26. Log PO_2-pH diagram for the system U-Ba-K-Ca-Fe-F-S-CO_2-H_2O at 300°C. (Fe)=10 ppm, (F)=1000 ppm, (SO_4)=1000 ppm, P_{CO2}=1 atm. Modified from Romberger (unpublished data). Ba solubility calculated from data by Crerar and Barnes (1976) assuming (Ba^{2+})=0.001, ΣS=0.1. Stippled area represents approximate position of ore-depositing fluids.

uranium grade varies considerably, depending more on the vein thickness and stockwork density than on the uranium content of the jasperoid. Grades are very low, with highest values of about 0.045 percent U_3O_8.

Numerous other sills of various orientations are scattered about the Grizzly Gulch area. One sill about 15 m south of the main mineralized sill contains about 6 m of jasperoid stockwork exposed on the surface, but appears to be unaltered and barren at depth. Although occasional jasperoid veinlets are encountered in the other sills, most are barren of uranium mineralization.

Structure in the Grizzly Gulch area is complex. An abundance of slickensides and brecciation suggests that movement may have been more significant than at Florida Mountain. Slickensides along the main mineralized sill generally have striations with the same attitude as the sill itself, indicating dip-slip movement along the sill. The outcrop of the main sill is terminated at both its north and south ends by steeply dipping silicified faults. Mineralization also appears to decrease along strike extent, which Metzger (1978) interpreted to be due to control by an inferred underlying structural zone. Too little is known of the Grizzly Gulch area to accurately appraise the relations between structure and mineralization, or the relations to mineralization in the study area.

Thunder Mountain

The Thunder Mountain anomalies also occur in an extremely rugged area. Discontinuous, low-grade surface anomalies cover the slopes of Thunder Mountain for over 1500 m horizontally and 1200 m vertically. Associated with the anomalous uranium is a broad color anomaly resulting from limonite. Because of very low grades of uranium no drilling was done at Thunder Mountain. However, the surface geology suggests many similarities to Grizzly Gulch and the Cornucopia vein system.

Mineralization occurs principally within a fault zone located in a small pod of Trimble Granite surrounded by Eolus Granite. The fault zone, which is sympathetic in trend to the structures at Grizzly Gulch, consists of three fault planes striking about N. 40° W. and dipping 36° to the northeast. Slickensides indicate dip-slip movement of the faults. The faults pinch and swell in thickness (generally 10 cm-2 m), and are strongly silicified. Areas between the faults are propylitically to argillically altered and intensely fractured as a result of shearing. The fractures are commonly filled with fine-grained quartz and jasperoid veinlets.

Uranium occurs within red jasperoids similar to those of the Cornucopia vein. Grades are very low and range from 0.004 to 0.074 percent U_3O_8. Surface samples are strongly out of equilibrium in favor of radiometric uranium.

Other Occurrences

There are a few widely scattered, very low grade anomalies within the basin of Castilleja Lake. The anomalies, which occur mainly along the contact between the Trimble and Eolus granites, were considered too insignificant to

warrant study. A potentially interesting occurrence was discovered at the unconformity between the Eolus Granite and the Cambrian Ignacio Quartzite near West Virginia Gulch (pl. 1). A strong radiometric anomaly of less than a meter in extent was picked up by scintillometer. Unfortunately, the discovery was made at night and nothing could be ascertained about the nature of mineralization.

ECONOMIC POTENTIAL

The history of mining and exploration in the Needle Mountains district is a testimony to the potential for economic development of the area. Despite discouraging results from past efforts, the district still possesses good potential for uranium and molybdenum, and a smaller potential for precious metals. However, such prospects are mitigated by a variety of factors, foremost of which are the remoteness of the area coupled with the politico-economic climate of the nation.

Assay data presented in table 1 show that silver is present in moderately high grades in quartz-sulfide veins of the study area. Records of past production indicate that gold was also found in significant concentrations within small oxidized pods. Although there is little direct evidence to predict the nature of precious-metal mineralization at depth, the past history of mining indicates that ore-grade concentrations of precious metals are widely scattered and of very small volume. It is doubtful that there is sufficient volume of precious metals to support a large operation. Small pockets of quartz-pyrite veins, such as at the Pittsburg Shaft, are probably sufficiently rich in silver to support small-scale mining operations, but profits would be severely limited by costs of removing ore by pack animals or helicopters.

Geochemical anomalies as well as the nature and chemistry of the Chicago Basin stock presented a good target for molybdenum exploration. In response, AMAX drilled a number of holes into the stock. Results were discouraging and the efforts abandoned. However, the surface geochemical evidence discussed earlier suggests that Vallecito Basin was also a mineralizing center and probably contains an intrusive cupola at depth. Known granite molybdenite systems are commonly flanked and overlain by late-barren stages consisting of base-metal sulfides, fluorite, and rhodochrosite (Mutschler and others, 1981; Westra and Keith, 1981). Veins of such mineralogy are missing from the vicinity of the Chicago Basin stock, but are present in great abundance in Vallecito Basin. Thus, Vallecito Basin is a more attractive molybdenite target than was Chicago Basin and remains an untested molybdenum exploration target in the area.

Excellent potential for uranium deposits within and immediately outside the study area is quite evident by the abundance of surface anomalies. Of the many uranium-bearing structures in the region, only the Cornucopia vein has been sufficiently "blocked out" by drilling to allow reserve calculations. Metzger (1978) calculated reserves for the Cornucopia vein alone to be 576 metric tons, using a cut-off at 0.05 percent U_3O_8 and a mining height of 2.44 m. Considering ancillary structures not included in the calculations, he felt the probable reserves for the Cornucopia system to be closer to 1,000

metric tons. The UJC and LJC veins were not sufficiently drilled to allow calculations, but the similarity in strike length and mineralogy to the Cornucopia vein suggests at least equal potential for each structure. Because the Cornucopia vein is structurally higher, it is quite possible that its thickest and highest grade portions have been eroded. If these portions are preserved in the UJC and LJC veins, their reserves could be larger. It is also possible that stacked structures exist below the LJC Vein, which do not intersect the surface. Thus, the Florida Mountain block alone appears to contain a potential of at least 3,000 metric tons of U_3O_8, and has the potential for considerably more. Including speculative reserve estimates for Grizzly Gulch and Thunder Mountain, as well as additional uranium which might be discovered by more drilling or during mining, the study area and its immediate surroundings may contain as much as 10,000 metric tons of U_3O_8. Although small by some world standards, this tonnage is comparable to the hard rock uranium deposits currently being mined in the United States at the Midnite Mine, Washington, and Schwartzwalder Mine, Colorado. Present uranium prices and politics, as well as the costs and environmental implications of operating in a remote wilderness area, make it unlikely that the deposits will be mined in the near future. However, the area will remain a significant resource of uranium, as well as an exploration model for potential intragranitic uranium deposits elsewhere in the United States.

REFERENCES CITED

Arth, J. G., 1976, Behavior of trace elements during magmatic processes--a summary of theoretical models and their applications: Journal of Research of the U.S. Geological Survey, v. 4, p. 41-47.

Barker, Fred, 1969, Precambrian geology of the Needle Mountains, southwestern Colorado: U.S. Geological Survey Professional Paper 644-A, 35 p.

Basham, I. R., 1981, Some applications of autoradiographs in textural analysis of uranium-bearing samples - a discussion: Economic Geology, v. 76, p. 974-976.

Basham, I. R., Vairinho, M. N. B., and Bowles, J. F. W., 1979, Uranium-bearing accessory minerals in the Sao Pedro do Sul granite, Portugal: unpublished paper presented to International Atomic Energy Agency Technical Committee Meeting on the Geology of Vein and Similar Type Uranium Deposits, Lisbon, Portugal.

Bickford, M. E., Barker, Fred, Wetherill, G. W., and Lee-Hu, Chin-Nan, 1968, Precambrian chronology in the Needle Mountains, southwestern Colorado - Pt. 2, Rb-Sr results [abs.]: Geological Society of America Special Paper 115, p. 14.

Brown, G. C., and Hennessy, J., 1978, The initiation and thermal diversity of granite magmatism: Philosophical Transactions of the Royal Society of London, A, v. 288, p. 631-643.

Burnham, C. W., 1979, Magmas and hydrothermal fluids, in Barnes, H. L., ed., Geochemistry of hydrothermal ore deposits: New York, Wiley, 798 p.

Carrat, H. G., 1974, Le magmatisme basique comme quide de la distribution des gisements d'uranium des granitoids francais: Comptes rendus de l'academie des sciences, t. 279, serie D, p. 115-118.

_____1975, Le role de la geochimie de l'uranium et du thorium dans le recherche des gisements uraniferes intragranitiques: Sciences de la Terre, t. 20, p. 129-164.

Cawthorn, R. G., Strong, D. F., and Brown, P. A., 1976, Origin of corundum-normative intrusive and extrusive magmas: Nature, v. 259, p. 102-104.
Chappell, B. W., and White, A. J. R., 1974, Two contrasting granite types: Pacific Geology, v. 8, p. 173-174.
Collier, J. D., 1982, Geology and uranium mineralization of the Florida Mountain area, Needle Mountains, southwestern Colorado: Colorado School of Mines, Ph.D. thesis, 235 p.
Comstock, T. B., 1883, Notes on the geology and mineralogy of San Juan County, Colorado: Transactions of the American Institute Mining and Metallurgical Engineers, v. 11, p. 165-191.
Crerar, D. A., and Barnes, H. L., 1976, Ore solution chemistry V. Solubilities of chalcopyrite and chalcocite assemblages in hydrothermal solutions at 200° to 350°C: Economic Geology, v. 71, p. 772-794.
Cross, Whitman, and Larsen, E. S., 1935, A brief review of the geology of the San Juan region of southwestern Colorado: U.S. Geological Survey Bulletin 843, 138 p.
Cross, Whitman, Howe, Ernest, Irving, J. D., and Emmons, W. H., 1905, Description of the Needle Mountains quadrangle, Colorado: U.S. Geological Survey Atlas, Folio 131, 14 p.
Cuney, Michel, 1978, Geologic environment, mineralogy, and fluid inclusions of the Bois Noirs - Limouzat uranium vein, Forez, France: Economic Geology, v. 73, p. 1567-1610.
Cunningham, C. G., and Carollo, C., 1980, Modification of a fluid-inclusion heating/freezing stage: Economic Geology, v. 75, p. 335-337.
Deer, W. A., Howie, R. A., and Zussman, J., 1966, An introduction to the rock forming minerals: London, Longman, 528 p.
Dooley, J. R., 1958, The radioluxograph: a fast simple type of autoradiograph, in Second United Nations International Conference on the Peaceful Uses of Atomic Energy, v. 3, Paper 1762, p. 550-553.
Ellingson, J. A., 1982, The Irving Formation and the Proterozoic sequence in the Needle Mountains, southwestern Colorado: Geological Society of America Abstracts with Programs, v. 14, no. 6, p. 311.
Emmons, S. F., 1890, Orographic movements in the Rocky Mountains: Geological Society of America Bulletin, v. 1, p. 245-286.
Endlich, F. M., 1876, Report on the San Juan district, Colorado: U.S. Geological and Geographical Survey (Hayden), 8th Annual Report, p. 181-240.
Frondel, Clifford, 1958, Systematic mineralogy of uranium and thorium: U.S. Geological Survey Bulletin 1064, 400 p.
Frondel, J. W., Fleischer, Michael, and Jones, R. S., 1967, Glossary of uranium- and thorium-bearing minerals: U.S. Geological Survey Bulletin 1250, 69 p.
Grandstaff, D. E., 1976, A kinetic study of the dissolution of uraninite: Economic Geology, v. 71, p. 1493-1506.
Haas, J. L., Jr., 1971, The effect of salinity on the maximum thermal gradient of a hydrothermal system at hydrostatic pressure: Economic Geology, v. 66, p. 940-946.
Hanson, G. N., 1978, The application of trace elements to the petrogenesis of igneous rocks of granitic composition: Earth and Planetary Science Letters, v. 38, p. 26-43.

Heinrich, E. W., 1958, Mineralogy and geology of radioactive raw materials: New York, McGraw-Hill, 654 p.
Hyndman, D. W., 1972, Petrology of igneous and metamorphic rocks: New York, McGraw-Hill, 533 p.
Ishihara, Shunso, 1977, The magnetite-series and ilmenite-series granitic rocks: Mining Geology, v. 27, p. 293-305.
Larsen, E. S., and Cross, Whitman, 1956, Geology and petrology of the San Juan region, southwestern Colorado: U.S. Geological Survey Professional Paper 258, 303 p.
Leroy, Jacques, 1978, The Margnac and Fanay uranium deposits of the La Crouzille district (western Massif Central, France): geologic and fluid inclusion studies: Economic Geology, v. 73, p. 1611-1634.
Leroy, Jacques, and Poty, Bernard, 1969, Recherches preliminaires sur les fluids associes a la genese des mineralisations en uranium du Limousin (France): Mineralium Deposita, v. 4, p. 395-400.
Lipman, P. W., Steven, T. A., and Mehnert, H. H., 1970, Volcanic history of the San Juan Mountains, Colorado, as indicated by potassium-argon dating: Geological Society of America Bulletin, v. 81, p. 2329-2352.
Metzger, C. W., 1977, Thunder Mountain project: report of operations through 1977, La Plata County, Colorado: unpublished report prepared for Public Service Company of Oklahoma.
Metzger, C. W., 1978, Thunder Mountain project: report of operations through 1978, La Plata County, Colorado, Volume I: unpublished report prepared for Central and South West Fuels, Inc.
Miyoshiro, A., 1961, Evolution of metamorphic belts: Journal of Petrology, v. 2, p. 277-311.
Moreau, Marcel, Poughon, A., Puybaraud, Y., and Sanselme, H., 1966, L'uranium et les granites: Chronique des Mines et de la Recherche miniere, v. 350, p. 47-50.
Moreau, Marcel, and Ranchin, G., 1973, Alterations hydrothermales et controles techtoniques dans les gites filoniens d'uranium intragranitiques du Massif Central francais, en Les roches plutoniques dans leur rapport avec les gites mineraux: Paris, Masson et Cie, 403 p.
Mutschler, F. E., Wright, E. G., Ludington, S., and Abbott, J. T., 1981, Granite molybdenite systems: Economic Geology, v. 76, p. 874-897.
Nash, J. T., 1972, Fluid-inclusion studies of some gold deposits in Nevada: U.S. Geological Survey Professional Paper 800-C, p. 15-19.
Naumov, G. B., Motorina, Z. M., and Naumov, V. B., 1971, Conditions of formation of carbonates in veins of the Pb-Co-Ni-Ag-U type: Geochemistry International, v. 6, p. 590-598.
Pitcher, W. S., 1979a, Comments on the geological environments of granites, in Atherton, M. P., and Tarney, J., eds., Origin of granite batholiths - geochemical evidence: Orpington, Kent, Shiva Publishing, p. 1-8.
_____1979b, The nature, ascent and emplacement of granitic magmas: Journal of the Geological Society of London, v. 136, p. 627-662.
Potter, R. W., 1977, Pressure corrections for fluid-inclusion homogenization temperatures based on the volumetric properties of the system NaCl-H_2O: Journal of Research of the U.S. Geological Survey, v. 5, p. 603-607.
Potter, R. W., Clynne, M. A., and Brown, D. L., 1978, Freezing point depression of aqueous sodium chloride solutions: Economic Geology, v. 73, p. 284-285.

Poty, Bernard, Leroy, Jacques, and Cuney, Michel, 1974, Les inclusions fluides dans les minerais des gisements d'uranium intragrnitiques du Limousin et du Forez (Massif Central francais), in Formation of uranium ore deposits: Vienna, International Atomic Energy Agency, p. 569-582.

Poty, Bernard, Leroy, Jacques, and Jachimowicz, L., 1976, Un nouvel appareil pur la mesure des temperatures sous le microscope: l'installation de microthermometrie Chaixmeca: Bulletin de la societe francaise de mineralogie et de crystallographie, v. 99, p. 182-186.

Rich, R. A., Holland, H. D., and Petersen, Ulrich, 1977, Hydrothermal uranium deposits: Amsterdam, Elsevier, 264 p.

Rogers, J. J., and Adams, J. A., 1967, Uranium, in Wedepohl, K. H., ed., Handbook of geochemistry, v. 2, pt. 1: Berlin, Springer-Verlag, 50 p.

Roedder, Edwin, 1970, Application of an improved crushing microscope stage to studies of the gases in fluid inclusions: Schweizerischen mineralogische und petrographische Mitteilungen, v. 50, pt. 1, p. 41-58.

_____1979, Fluid inclusions as samples of ore fluids, in Barnes, H. L., ed., Geochemistry of hydrothermal ore deposits: New York, Wiley, 798 p.

Schmitt, L. J., and Raymond, W. H., 1977, Geology and mineral deposits of the Needle Mountains district, southwestern Colorado: U.S. Geological Survey Bulletin 1434, 40 p.

Shand, S. J., 1927, The eruptive rocks: New York, John Wiley.

Shaw, D. M., 1970, Trace elem ent fractionation during anatexis: Geochimica et Cosmochimica Acta, v. 34, p. 237-243.

Silver, L. T., and Barker, Fred, 1968, Geochronology of Precambrian rocks of the Needle Mountains, southwestern Colorado - Pt. 1, U-Pb zircon results [abs.]: Geological Society of America Special Paper 115, . 204-205.

Steven, T. A., Schmitt, L. J., Sheridan, M. J., and Williams, F. E., 1969, Mineral resources of the San Juan primitive area, Colorado: U.S. Geological Survey Bulletin 1261-F, 187 p.

Steven, T. A., Lipman, P. W., Hail, W. J., Jr., Barker, Fred, and Luedke, R. G., 1974, Geologic map of the Durango quadrngle, southwestern Colorado: U.S. Geological Survey Miscellaneous Investigations Map I-764, scale 1:250,000.

Streckeisen, A., 1976, To each plutonic rock its proper name: Earth Science Review, v. 12, p. 1-33.

Strong, D. F., 1980, Granitoid rocks and associated mineral deposits of eastern Canada and western Europe, in Strangway, D. W., ed., The continental crust and its mineral deposits: Geological Association of Canada Special Paper 20, p. 741-769.

Takenouchi, S., and Kennedy, G. C., 1964, The binary system H_2O - CO_2 at high temperatures and pressures: American Journal of Science, v. 262, p. 1055-1074.

Tewksbury, B. J., 1982, Polyphase deformation in allochthonous rocks of the Precambrian Uncompahgre Formation, Needle Mountains, southwestern Colorado [abs.]: Geological Society of America Abstracts with Programs, v. 14, no. 6, p. 351.

Turgarinov, A. I., and Naumov, V. B., 1969, Thermobaric conditions of formation of hydrothermal uranium deposits: Geochem. International, v. 6, p. 89-103.

Westra, Gerhard, and Keith, S. B., 1981, Classification and genesis of stockwork molybdenum deposits: Economic Geology, v. 76, p. 844-873.

White, A. J. R., 1979, Source rocks of granite magmas: unpublished lecture notes prepared for symposium on the origin of granites, Geological Society of America Annual Meeting, San Diego, California.
White, A. J. R., and Chappell, B. W., 1977, Ultrametamorphism and granitoid genesis: Tectonophysics, v. 43, p. 7-22.
Yoder, H. S., Stewart, D. B., and Smith, J. R., 1957, Ternary feldspars, in Annual report of the director of the geophysical laboratory: Carnegie Institute of Washington Year Book 56, p. 206-214.
Zwart, H. J., 1967, The duality of orogenic belts: Geol. Mijnbouw, v. 46, p. 283-309.
Zwart, H. T., 1969, Metamorphic facies in the European orogenic belts and their bearing on the causes of orogeny: Geological Association of Canada Special Paper 5, p. 7-16.

DEPARTMENT OF THE INTERIOR
U. S. GEOLOGICAL SURVEY

OPEN-FILE REPORT 84-336
PLATE 1 OF 2

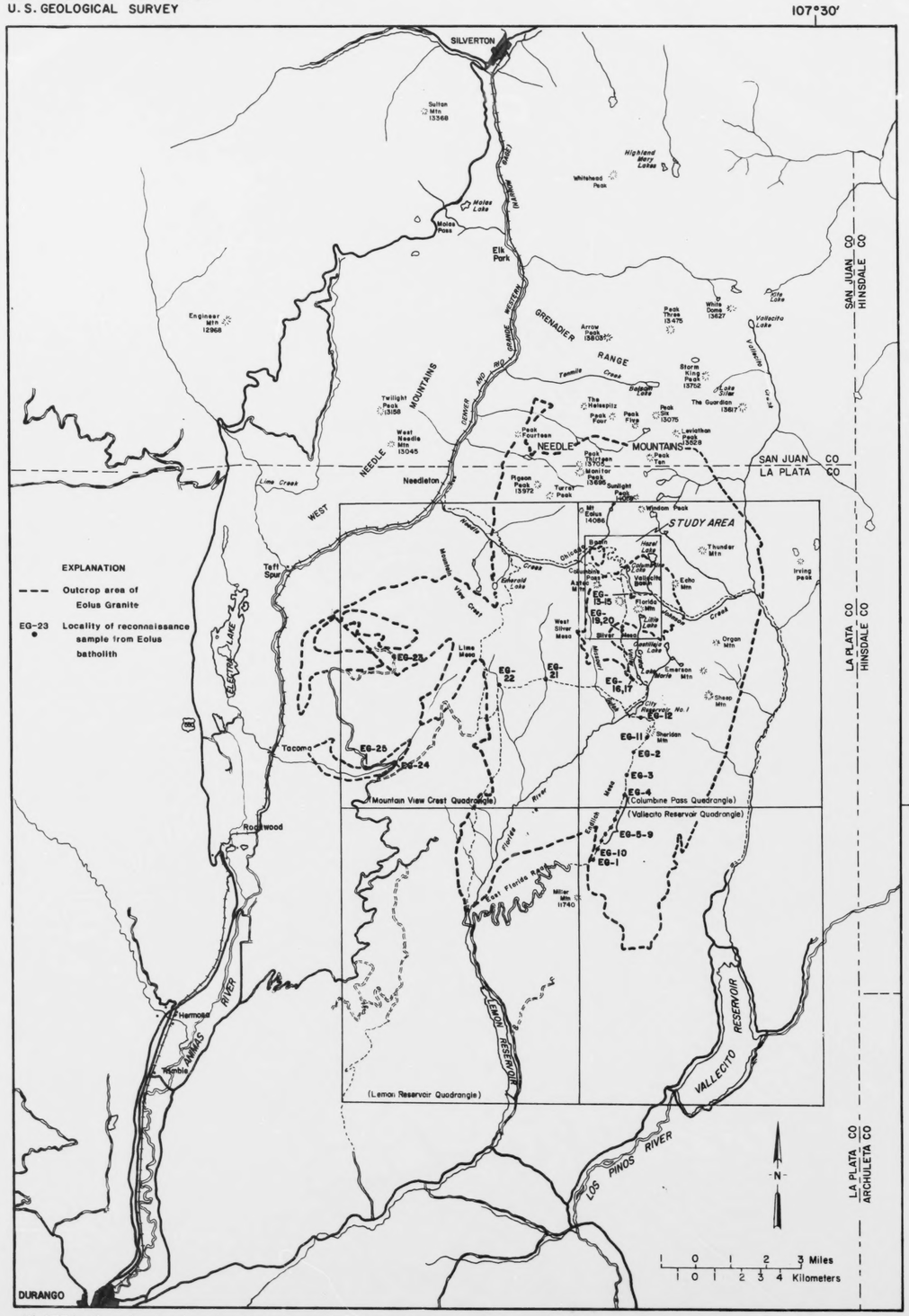

PLATE I. Map showing location of study area in relation to prominent geographic features of Needle Mountains region. Outcrop area of Eolus Granite shown by bold dashed lines. Also shown are locations of reconnaissance samples from the Eolus batholith (EG- series samples). **Compiled by James D. Collier, 1979.**

This map is preliminary and has not been reviewed for conformity with U.S. Geological Survey editorial standards and stratigraphic nomenclature.

Jupiter Mountain
13630
Hazel Lake
12435
Hope Mountain
13012
Columbine Lake
Columbine Pass
USLM
20132
VALLECITO
×12170
BASIN
Aztec Mountain
×13190
Bullion Mountain
×13132
USLM
Florida Mountain
13076
Mines
Mine
TRAIL
FOOT
PACK
AZTEC VEIN
BULLION
FAULT
VALLECITO
Needle
Chicago Creek
12926
12600
12400
12800
11400
pCe
pCtr
Tio
Tiy
Tid
Tim
CB-1
CB-2
CB-3
CB-4
CB-5
CB-6
CB-7
CB-8
CB-9
CB-10
CB-11
CB-12
CB-13
CB-14
VB-1
VB-2
VB-3
VB-4
VB-5
VB-6
VB-7,8,9
VB-10
VB-11
VB-12,13
VB-14
VB-15
VB-16
VB-17
VB-18
VB-19
VB-20
VB-21
VB-22
VB-23
VB-24
VB-25
VB-26
VB-27
VB-28
VB-29
VB-30
VB-31
VB-32
VB-33
VB-34
VB-35
VB-36
VB-37
VB-38
VB-39
VB-40
VB-41
VB-42
VB-43
VB-44,47
VB-45
VB-46
VB-48,49
VB-50
VB-51
VB-52
VB-53
VB-54
VB-55
VB-56
SM-18
SM-20
SM-21
SM-22
FM-9
FM-10
FM-35
FM-36
FM-37
FM-38
LOWER JOHNSON CREEK VEIN
UPPER JOHNSON CREEK VEIN

Base from U.S. Geological Survey, Columbine Pass 7.5'
Topographic Quadrangle, La Plata Co., Colorado, 1973.

GEOLOGIC MAP OF THE FLORIDA MOUNTAIN AREA, NEEDLE MOUNTAINS, SOUTHWESTERN COLORADO

SCALE 1:4 800

100 0 100 200 300
METERS

500 0 500 1000
FEET

JAMES D. COLLIER
1979
(REVISED 1980)

MN
13.5°
N

EXPLANATION

- Tld — TERTIARY LATE DIKE - Dark green altered mafic porphyry
- Tly — TERTIARY INTRUSION, YOUNGER BODY - Rhyolite porphyry
- Tio — TERTIARY INTRUSION, OLDER BODY - Granite porphyry and related dikes
- md — MAFIC DIKES (PRECAMBRIAN?) - Dark green lamprophyre dikes. Younger than Eolus Granite
- pCtr — TRIMBLE GRANITE (PRECAMBRIAN) - Homogeneous, light red to pink, fine- to medium-grained biotite granite. Intrudes Eolus Granite
- pCe — EOLUS GRANITE (PRECAMBRIAN) - Heterogeneous body ranging in composition from hornblende qtz diorite to biotite granite. Aplitic to coarse-grained porphyritic
- CONTACT - Dashed where covered
- 85 — VEINS - Fractures showing evidence of passage of mineralizing fluids. Arrow indicates direction of dip. Dashed where covered.
- FM-21 — SAMPLE LOCALITY AND NUMBER - Prefix indicates physiographic locality: FM-Florida Mtn.; SM-East Silver Mesa; VB-Vallecito Basin; CS-Chicago Basin; CV-Crystal Valley
- 800/100 cps — SURFACE RADIOMETRY - Local radiometry and average background radiometry of adjacent vicinity in counts per second

This map is preliminary and has not been reviewed for conformity with U.S. Geological Survey editorial standards and stratigraphic nomenclature.